MÖSSBAUER SPECTROSCOPIC STUDIES OF TIN IN GLASS

Thesis submitted in accordance with the requirements of the

University of Liverpool for the degree of Doctor in Philosophy by

Kyle Fiona Eirwen Williams.

September 1995

Oliver Lodge Laboratory

University of Liverpool

To my parents

&

in memory of my grandparents

Contents

Page

Acknowledgements

I would like to thank Professor P.J. Twin for the use of the facilities available in the Department of Physics. The work was made possible through the financial support of an EPSRC CASE award supported by Pilkington.

I am very grateful for the help and patience of my supervisor Professor C.E. Johnson, over the last three years. His experience and such considerable knowledge has been invaluable. The additional help and assistance from Dr. Jackie Johnson, especially for taking time to listen and to read and check written work, was also much appreciated.

I would like to thank Dr. B.P. Tilley of Pilkington Technology Management for his supervision and help throughout. Thanks also to many other people from Pilkington Technology Centre, notably Dr. J. Brettle, Mr. D. Gelder, Mrs. J. Kells and Mr. R.A. Chappell. I am especially extremely grateful to Miss Jane Greengrass, for so much help and for her consideration. Thank you for being so nice!

I am grateful to Dr. D. Holland of Warwick University for the useful discussions about glass, and Dr. M.M. Karim for the preparation of several glass samples and the analysis of their physical properties.

Thank you also to Dr. M.F. Thomas, especially for help with the detector, and Dr.'s D.P.E. Dickson, I. Hall, Q.A. Pankhurst and M.A. Houlden for their assistance at different times.

Thank you to Keith Williams for his "technical" help, and for lifting detectors and opening my mail, and to Dave Muskett for his help and for making it possible for me to go home, (by changing one very flat tyre), and also for some entertainment in the lab. Also to the Mössbauer group over three years, Colette, Kay, Steve, Ahmed, Sankar, Guy, (Jason), Doğan (& Steven) at the start (when it was all new and confusing) and more recently Michael, Sarah and John (when it can still be ....).

I have always appreciated such a lot of help from my parents in many things over all the years. Finally, thank you to Steven, my fiancé, for helping in many ways and for 'being there' when necessary.

Abstract

Glasses of variable composition containing tin have been studied using ^{119}Sn Mössbauer spectroscopy. The glass samples consisted of three different systems; binary tin oxide-silicate glasses, re-melted tin-doped float-composition glass and commercially produced float glass.

Mössbauer spectra of tin in the binary glasses were recorded for various compositions, between 16.8 and 71.5 mol.% SnO in SiO_2. The tin was shown to exist predominantly as Sn^{2+} and the Mössbauer hyperfine parameters, chemical shift and quadrupole splitting, were found to be significantly greater than those of Sn^{2+} in crystalline tin oxide. Variable temperature measurements of two of the glass samples obtained between 10 K and 300 K, showed a decrease in shift with increasing temperature which was accounted for partly by the second order Doppler shift and also by the temperature dependence of the chemical shift. Data obtained separately on the expansivity and density was used to correct the shift for the effect of volume changes. The results showed that the volume corrected chemical shift increased with increasing tin concentration. From measurements of the change in absorption area with temperature and hence in the tin recoil-free fraction, the Debye temperature of the tin was calculated for two glasses and found to be 181 K and 191 K, i.e. lower than that of crystalline SnO. The results suggested that the Sn-O bonds became less covalent as the tin oxide concentration increased. Three series of Mössbauer spectra were also recorded for three of the binary glass samples after they had undergone a range of heat treatments. These showed that the tin oxidation state changed and was dependent on the heating conditions, and also the possible presence of two different crystalline tin species.

Mössbauer spectra of tin-doped float-composition glasses, which were prepared from commercial float glass and tin oxalate, were also recorded. High temperatures (~1500°C) were used in their preparation and up to 15 percent of tin oxide by weight was found to be present by chemical analysis. The Mössbauer spectra showed that both oxidation states of tin were present and that the chemical shift and quadrupole splitting were sensitive to differences in the composition of the constituent compounds, e.g. the presence of increased alumina concentrations. Variable temperature measurements up to

900 K showed that temperature had a smaller effect on the recoil-free fraction of Sn^{4+} than on that of Sn^{2+}, and a corresponding difference in Debye temperature of about 320 K compared with 190 K. This suggests that Sn^{4+} may act as a network former (NWF) when melted together with the glass constituents.

Tin is found in commercially produced float glass as small quantities diffuse into the bottom surface of the glass ribbon during manufacture. Mössbauer spectra of the tin in this region were obtained by using specially prepared ground glass, just 0.1mm in thickness, and by recording the spectra at low temperatures (~78 K). The glass samples were taken from several manufacturing plants where the glass is produced by floating it on molten tin, and also from different regions of the same glass ribbon. Both Sn^{4+} and Sn^{2+} were found to be present in the glass, and it was shown to contain between 16 and 43% stannic ions. Bloom tested glass (i.e. that which has undergone heat treatment for several minutes) has also been analysed and results showed that oxidation had occurred. The change in oxidation of Sn^{2+} to Sn^{4+} was also investigated in float glass samples heated for up to 345 hours and at temperatures between 500°C and 1050°C. The oxygen diffusion coefficients were found to be 1.285×10^{-18} m^2s^{-1} at 500°C, 9.598×10^{-18} m^2s^{-1} at 600°C and 1.92×10^{-16} m^2s^{-1} at 730°C. The Mössbauer spectra were used in conjunction with other techniques, such as x-ray photoelectron spectroscopy, to obtain information on the processes occurring when float glass is heated and how the tin affects the glass surface. Depth profiles of the tin oxidation states were measured and showed that the ratio of stannic to stannous tin changes with depth into the glass. Tin Debye temperatures were also calculated for several samples and the results obtained were significantly lower than those of Sn^{4+} in the re-melted tin-doped float-composition glasses; ~180 K for Sn^{2+} and ~260 K for Sn^{4+}. The measured chemical shift and low Debye temperatures imply that the tin is ionically bonded in float glass and is present in interstitial sites in the glass network, i.e. that it is acting as a network modifier (NWM).

Chapter 1 Introduction; Glass Structure and Sample Production

1.1 Introduction

Glass is an unusual material unlike the crystalline solids that its constituent compounds usually form. It is a material with the viscosity of a solid, although from thermodynamical considerations it should not exist. The fact that it does, both as a naturally occurring substance and as a product manufactured for many purposes, results from certain conditions for formation whereby it attains a metastable state. The strong covalent bonds, characteristic in a glass, need to be overcome to achieve the thermodynamically stable state. One such method of partially reaching this state is by a controlled crystallisation process in the formation of glass ceramics. These materials have increasingly widespread uses, however the more obvious uses of glass are in windows and everyday products such as bottles and glasses.

Several models of glass structure now exist and were proposed and updated as further information was obtained from different experimental techniques. X-ray diffraction measurements showed that no long range order was present in glass and that it was therefore an amorphous material without a unique structure like that of a crystalline solid. Models were modified by techniques such as EXAFS, (extended x-ray absorption fine structure).

Information about glass and the effect of different elements on glass properties can be useful in industry. Nuclear magnetic resonance (NMR) may be employed in investigating the structural role of glass constituents and Mössbauer spectroscopy may also be used when a suitable Mössbauer isotope is present in the glass.

Oxides of tin are rarely constituent compounds of glasses, but may be used for glazes, as window glass coatings and in the toughening of glass products by the

application of thin films of stannic oxide. [1] Small quantities of tin are also found to be present in glass produced by the float process and it is therefore convenient that an isotope of tin exists which exhibits the nuclear resonance fluorescence effect known as the Mössbauer effect.

A considerable number of investigations of tin-containing glasses have been reported previously and those that are most significant to this current study will be referred to later throughout this thesis. Mössbauer spectroscopy is particularly useful in analysing the environment of tin in different types of glasses and it is the principal technique used throughout this work.

The aim of this study has been to obtain information specifically about tin that has diffused into the bottom surface of float glass during manufacture. Results have been obtained in collaboration with Pilkington and these are presented together with results for tin doped samples prepared at the University of Warwick.

The structure of glass will briefly be discussed as an introduction to the glass samples studied. The float process, which revolutionised flat glass production in the late 1950's, will also be described to illustrate why tin is significant to commercial glasses.

1.2 Composition and Structure of Glass

The most widely accepted definition of a glass was proposed by the American Society for Testing Materials in 1945. This states that 'glass is an inorganic product of fusion which has cooled to a rigid condition without crystallising'. It is often considered

to be a transparent material which is rigid and brittle but softens slowly when heated.

Many glasses, especially commercial glasses, are mixtures of inorganic oxides. Some oxides will form a glass when cooled from the molten state, and in these cases as the temperature decreases their viscosity increases gradually until it attains values consistent with those of a rigid solid. As there is no discontinuous volume change, the structure resembles a liquid, and this similarity is shown in their x-ray diffraction patterns (a diffuse halo). A glass may therefore be considered to possess short range order but no long range order like that found in periodic arrays of crystalline solids. It is also isotropic.

The continuous state of glass with liquid is illustrated for a possible glass forming substance by the variation of volume with temperature [2] in figure 1.1.

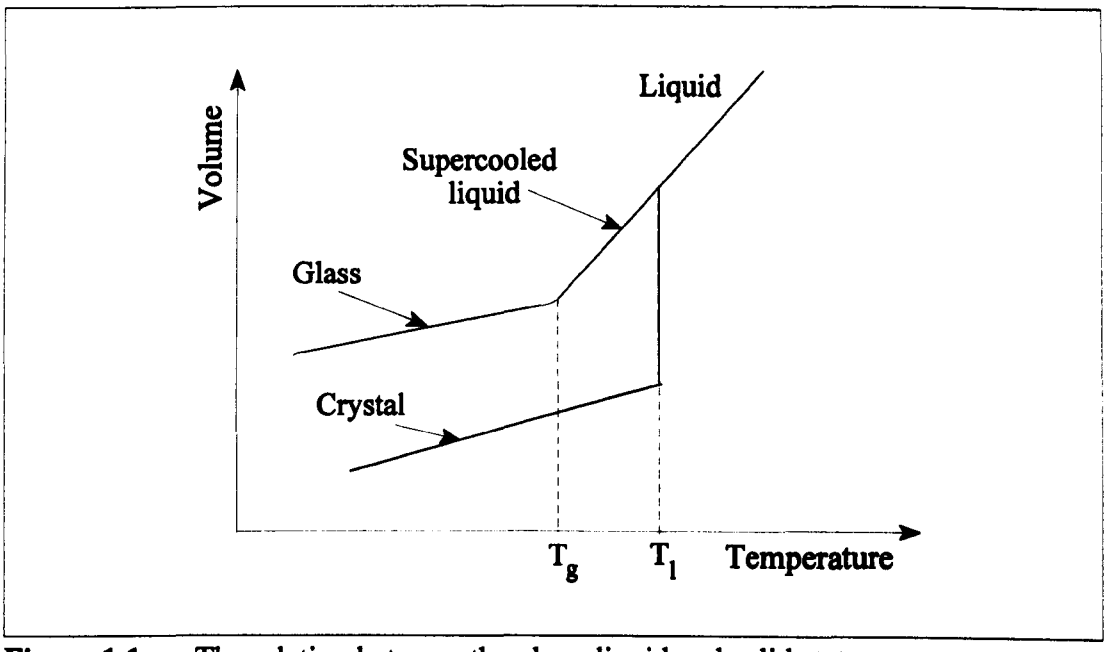

Figure 1.1 The relation between the glass, liquid and solid states.
T_g = glass transition temperature, T_l = liquidus temperature.

Silicate glasses are the most useful and most commonly formed oxide glasses. Tin-containing silicate glasses have been studied by Mössbauer spectroscopy, therefore structure and glass forming ability will be discussed in relation to these particular glasses.

1.2.1 Conditions for Glass Formation

Silica is one oxide which readily forms a glass; however it does not have much practical application because of the high temperatures required in melting. Addition of sodium oxide (Na_2O) lowers the melting temperature and calcium oxide (CaO) is added to increase the glass's durability. This mixture forms the basis of commercial flat glasses.

The first suggestions about the ability of an oxide to form a glass were related to the arrangement of the oxygen ions around the cation. The idea was expanded later by Zachariasen in 1932 [3]. He developed the random network theory which is still essentially accepted with certain modifications based on more recent experimental data.

The theory was developed from the assumption that interatomic forces in glasses should not be dissimilar to those in crystals and therefore that the atoms should form a non-periodic three-dimensional network. This structure would arise from distortion of the M-O-M bond angles and is illustrated in figure 1.2.

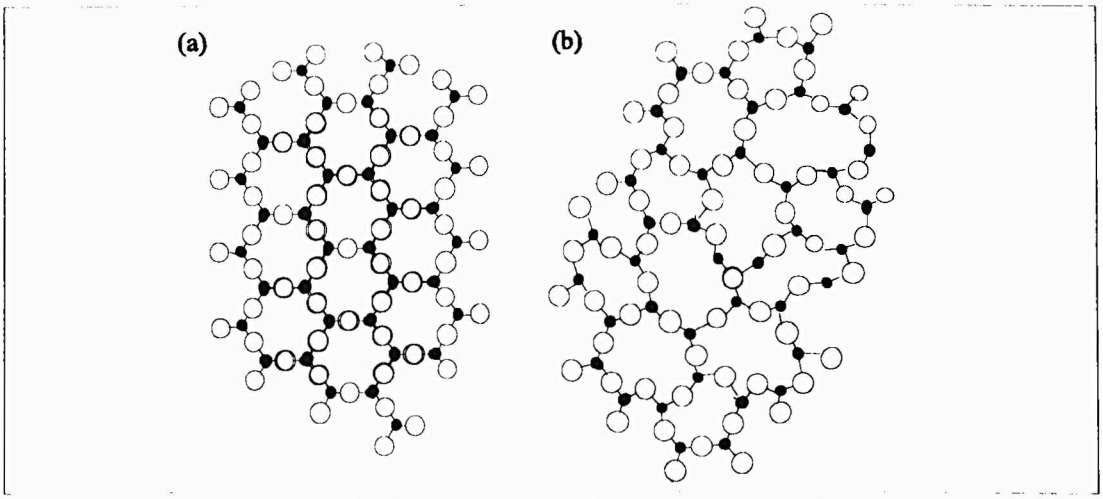

Figure 1.2 Two dimensional comparison of the crystal and glass structure proposed by Warren & Zachiarasen (a) the regular crystalline lattice, (b) the random network for an oxide glass M_2O_3.

The stated glass formation conditions for an oxide of the form M_xO_y were mainly as follows:-

(a) An oxygen atom must not be linked to more than two 'M' atoms.

(b) The number of oxygen atoms surrounding 'M' must be small.

(c) The oxygen polyhedra must share corners only and not edges or faces.

Therefore those that are suitable have the form M_2O_3, MO_2 or M_2O_5, and examples are boric oxide (B_2O_3), silica (SiO_2) and phosphorus pentoxide (P_2O_5). [4]

1.2.2 Components of Glass Systems

Individual oxides may be further categorised into one of a network forming oxide (network former, NWF), a modifying oxide (NWM), or an intermediate oxide. A NWF is able to form a continuous three-dimensional network when it is melted and cooled, whereas a NWM is not. Predominantly covalent bonding exists in the network of a glass, but more ionic bonding occurs when a NWM is incorporated into it. When a NWM is

present it may be considered to weaken the glass network. An intermediate oxide does not form a glass on its own, but it can become part of the glass network. Examples of the above are silica, sodium oxide (Na_2O) and aluminium oxide (Al_2O_3) respectively.

If a modifying oxide such as sodium oxide is introduced into a glass melt then two non-bridging oxygen ions per Na_2O molecule result, which cause a break in the continuous glass structure. The sodium ions fit into the interstitial sites between the random structure. Increasing their concentration further would create individual silica tetrahedra (i.e. four non-bridging oxygen ions), which would preclude glass formation. This is the orthosilicate composition, $2Na_2O.SiO_2$, when all oxygen ions are non-bridging.

Aluminium oxide may occur as tetrahedral AlO_4 or as octahedral AlO_6. In the former case the alumina tetrahedra may replace the silica units. Lead oxide, although not itself a NWF, may be incorporated to very high levels in silicate (and borate) glasses. The high levels of lead oxide suggest that it bridges silica tetrahedra.

1.2.3 Other Glass Models

The more recent modifications to the random network model are designed to incorporate the possibilities that glasses are not entirely homogeneous on a small scale. This is suggested by electron microscopy results. [4] Other models are discussed in several references, for example Greaves, 1985. [5]

1.2.4 Features of a Glass

Glass, although it does not undergo crystallisation, forms by passing through a range of temperatures where crystal growth can occur. If the cooling process is not carried out at the correct rate but is too slow, then crystal growth may begin which may cause the glass to become opaque. This crystallisation is known as devitrification and may occur between T_g and T_l. The glass transition temperature, T_g, is the temperature below which the material may be described as a glass. The temperature is shown in figure 1.1 on the volume-temperature curve, in the region where the gradient changes sharply. This transformation temperature depends on the rate of cooling. The viscosity at T_g is about 10^{13} Poise or 10^{12} Nsm^{-2}. Properties of the glass, such as the volume, may change with time near T_g as the glass stabilizes.

In the case of silicate glasses, devitrification would usually lead to the formation of cristobalite rather than the other crystal phases of silica, namely quartz and tridymite. These phases are identified from their x-ray diffraction spectra. Commercial soda-lime-silicate glasses would produce devitrite ($Na_2O.CaO.6SiO_2$) as the major phase.

1.3 Glass Production

All commercial glass samples to have been analysed were those of flat glass. The brief description to follow will therefore refer to the method of producing flat glass such as that used in windows. Glass is formed after melting the 'batch', i.e. the constituent inorganic oxides.

1.3.1 The Float Process [6]

Prior to the invention and development of the float process, flat glass had been successfully produced to a good quality by the polished plate process. This technique of continuous melting and rolling of the glass ribbon with grinding taking place on both sides of the glass provided high quality plates. However, it was expensive to produce.

The process which superseded this was invented in 1952 by Sir Alistair Pilkington, and was developed over seven years. It is now almost the only flat glass manufacturing technique used worldwide.

The float process involves floating glass on the surface of molten tin, held in an enclosed bath, to produce a ribbon. A continuous stream of glass is supplied from the furnace where the batch is melted and the glass is passed into the bath where the atmosphere is chemically controlled. The temperature regime is maintained whilst the glass is in the bath, so that irregularities disappear and the surfaces of the glass become flat and parallel under the forces of gravity and surface tension. The glass moves along the tin bath and is progressively cooled so that it may be removed from the bath by rollers when the surface is hard enough for no damage to occur. Tin metal is the most suitable support material to use due to its appropriate density, low vapour pressure, small interaction with glass and also its availability. A diagram of the process is shown in figure 1.3.

The bath atmosphere is chemically controlled to reduce oxygen and other impurities from entering the tin as this causes damage to the ribbon. However, it is not possible to eliminate all oxygen from the tin therefore some tin ions do diffuse into the glass.

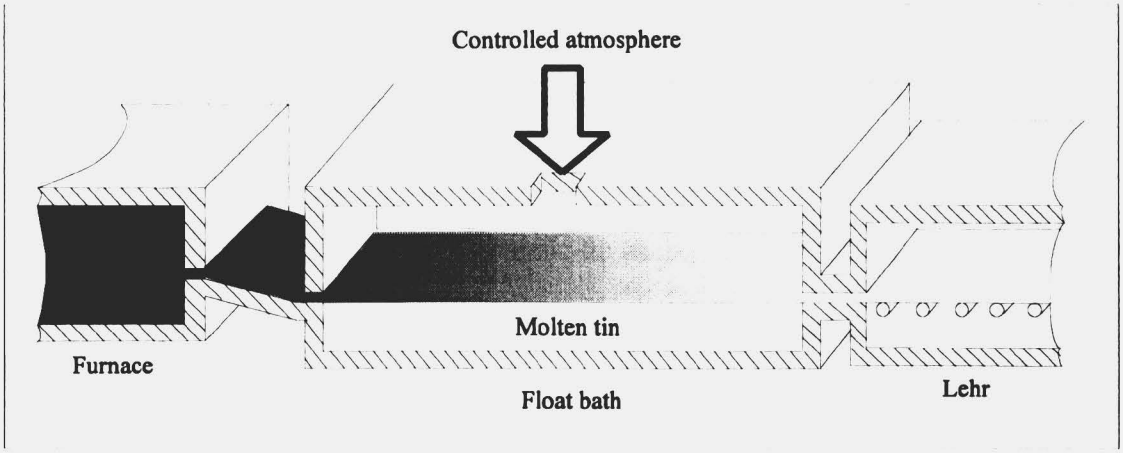

Figure 1.3 Schematic diagram of the float process.

1.3.2 Modifications to the Process and Glass Treatments

Under the natural forces present in the bath the glass ribbon reaches an equilibrium thickness of about 6.5 mm. This may be made thinner or thicker by different techniques and the float glass may be manufactured to thicknesses of between about 0.5 mm and 25 mm.

The electrofloat process may be carried out during the time that the glass is floating on the tin. In this treatment a voltage is passed between an electrode and metal pool on the top surface and the molten tin below, allowing metals to be 'driven into' the surface. Such modifications can produce glass which is opaque to certain radiation. [7]

Low emissivity glass, e.g. Pilkington 'K' glass, is produced by coating the float glass with tin oxide (SnO_2). The coating is applied by chemical vapour deposition, either while the ribbon is in the bath or just after it emerges. The product, used in double glazing, is claimed to be as effective as triple glazing.

Float glass may also be tempered. This is carried out as a toughening process, and

also to produce curved sheets in, for example, car windscreens. The glass is heated at 600°C or above, and is then quenched, placing the surfaces under compressive stress and the internal region under tension. Glass is strong under compression. It is important for the glass to contain as small an amount of tin as possible. During heating, the stannous tin at the surface becomes oxidised to stannic tin as oxygen is absorbed, and this impairs the optical quality of the glass. The haze which appears in these cases is caused by the surface wrinkling, and this is known as 'bloom'. To check if the tin concentration is too high for thermal treatment to be successful, a bloom test is performed. A sample is heated at the toughening temperature for a few minutes, and then the surface is viewed to check for any signs of the microscopic wrinkling.

1.4 Glass Sample Preparation

Several glass samples studied were prepared by Dr. M.M. Karim at the University of Warwick. A fuller description may be found in Dr. Karim's Ph.D thesis [8]. The methods were based on previous work. [9] [10] [11]

1.4.1 Binary SnO-SiO_2 Glasses

A series of binary tin-silicate glasses was prepared by a conventional melting technique to different tin oxide concentrations. The resulting glasses contained between about 17 and 70 mole percent of tin oxide, SnO, and varied in colour from pale yellow to deep reddish brown. Compressed pellets of Wacomsil quartz and stannous oxalate

were melted in alumina crucibles at temperatures ranging between 1100°C and 1600°C, i.e. about 100°C above the liquidus temperature, T_L. The mixture was quenched in air and then annealed at 400°C before being cooled to room temperature.

The main problem encountered when trying to obtain glass containing stannous oxide is the disproportionation of SnO to SnO_2 and Sn^0. As a result of the formation of stannic oxide and tin metal the outer region containing these materials was ground away to obtain the glass.

The glasses were analysed by titration at Warwick University and also at Pilkington Technology Centre. They were found to contain small amounts of aluminium oxide, Al_2O_3, from the crucibles. The compositions are discussed in chapter 5, which describes the results of Mössbauer measurements on these binary glasses.

1.4.2 Tin-doped Float Composition Glass

Two sets of float glass doped with different quantities of tin were prepared from powdered float glass and stannous oxalate. The intention was to study the behaviour of tin in a glass with the composition of industrial float glass. The float glass was provided by Pilkington and after removing the surfaces, which may have already contained a small quantity of tin, the glass was broken up and melted at 1400°C. After one hour it was transferred into deionized water. It was then further treated by milling for two days before it was dried to a powder and sieved. The powdered float glass was analysed and then measured quantities were mixed with stannous oxalate to prepare glasses containing nominally 2.5, 5, 7.5, 10, 12.5 and 15 weight percent of SnO. Stannous oxide is produced

from the decomposition of the stannous oxalate, SnC_2O_4, and stannic oxide is formed as a result of oxidation. The solubility of the stannic oxide in the glass is increased by the presence of alkali oxides.

The mixture was melted in alumina crucibles above 1500°C. Analysis showed a high concentration of Al_2O_3 to be present.

A further set of samples were prepared to eliminate the effect of the aluminium oxide. These were melted in silica crucibles at 1400°C and then at 1500°C. They were then annealed at 600°C and cooled to room temperature.

Each set of samples were analysed at Pilkington Technology Centre to obtain their full compositions. The chemical analysis is related to their Mössbauer parameters in chapter 6, which deals with the results for these glasses.

1.5 Sample Preparation for Analysis by Mössbauer Spectroscopy

The glass samples varied between having a high concentration of tin in those that were doped with tin and very low concentrations in all commercial float glass. It was therefore necessary to use different quantities of each glass when making the samples to be used for recording their Mössbauer spectra.

1.5.1 High Concentration Tin-Containing Glasses

All binary glass and tin doped float composition glass samples were powdered and therefore suitable to be held in the small cylindrical plastic sample holders described

later. As with crystalline solids such as tin oxide, the atomic mass, atomic absorption coefficient and the mole percentage of each element were included when calculating the optimum sample thickness. This is discussed later in chapter 4.

1.5.2 Commercial Float Glass Samples

The bottom few microns of the surface of float glass contain tin after it has been in contact with the molten metal. Initial attempts to obtain a Mössbauer spectrum produced no signal at all, which was an indication of how small the quantities of tin were in a single piece of glass. It was necessary to increase the concentration of tin in the sample by using more of the glass without having a considerable reduction in γ-ray intensity due to a large amount of non tin-containing glass. The solution was to remove the bulk of the glass, leaving about 0.1 mm of the bottom surface. The bulk was therefore ground away and the surface was held together on a paper backing.

A further improvement in the Mössbauer signal was found by removing the paper backing with chloroform and grinding the glass to a powder to be held in a sample holder. It was then possible to make low temperature measurements down to 4.2 K in a cryostat.

Chapter 2 A Review of Tin Compounds and Tin-Containing Glasses

2.1 Introduction

The element tin is one of the earliest recorded metals used in the formation of alloys. It occurs, however, most commonly as cassiterite, SnO_2, and the metal may be obtained by a reduction process. [1] Apart from its major uses in several alloys, e.g. in solder and bronze, and as a coating, e.g. in food packaging, tin is the molten metal used in the manufacture of float glass as discussed previously.

Several compounds of tin also have specific uses in industry. One relevant example of this is the application of a thin film of tin IV oxide to glass in the production of low emissivity windows.

Much discussion of tin and its compounds has been reported with emphasis over a wide range of subjects. The following sections are intended to contain just a brief review of some relevant information about tin.

2.2 Tin and Tin Compounds

Tin compounds have been studied by many techniques including infra-red spectroscopy, N.M.R. spectroscopy, Mössbauer spectroscopy and chemistry. The tin atom has an electronic structure of $(4d)^{10}(5s)^2(5p)^2$ outside the Krypton core structure. It forms predominantly two ions, Sn^{4+} (stannic ions), and Sn^{2+} (stannous ions) with the consequent electronic structure of [Kr] $(4d)^{10}$ and [Kr] $(4d)^{10}$ $(5s)^2$ respectively. This is significant in the resulting structure of the oxides.

2.2.1 Structure of Tin

Tin metal exists in two different forms at low and high temperatures. Above 13.2°C the form is white or β-tin and it possesses distorted octahedral coordination geometry. If exposed to low temperatures over a period of time, β-tin transforms into grey or α-tin which has a structure like that of diamond. The high temperature β-tin has a greater density. A change in the distribution of valence electrons between the two forms can be seen from the difference in their Mössbauer chemical shifts, i.e. for α-Sn δ=2.10 mms^{-1} and for β-Sn δ=2.65 mms^{-1}. [12]

2.2.2 Stannous Oxide

Bonding in tin compounds is often covalent but ionic bonding does occur. The effect of the 'lone-pair' of electrons associated with stannous tin in a molecule is to lower the electronegativity (the power of an atom to attract electrons to itself) relative to tin 4+ ions. The tin 2+ ion has a larger ionic radius than the tin 4+ ion, 93 pm compared with 74 pm respectively. [59]

Tin II oxide or stannous oxide, SnO, exists mainly as a black tetragonal crystalline solid, but it may also be found in metastable red form. Both modifications are amphoteric oxides (i.e. they are soluble in both acids and alkalis). Tetragonal SnO has a structure of square pyramids with the Sn^{2+} at the apex as shown in figure 2.1(a). [1] Each of these pyramids is arranged in layers; the unit cell of SnO is shown

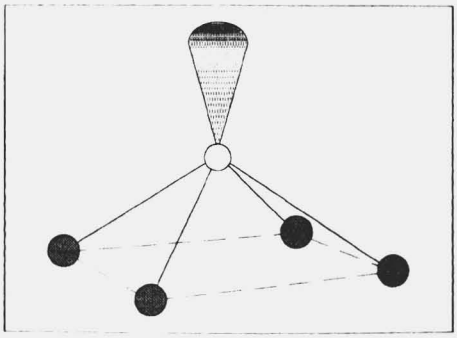

Figure 2.1(a) Tetragonal SnO.

in figure 2.1(b). [60] Both forms will oxidize to SnO_2 on heating, or will disproportionate in the absence of oxygen.

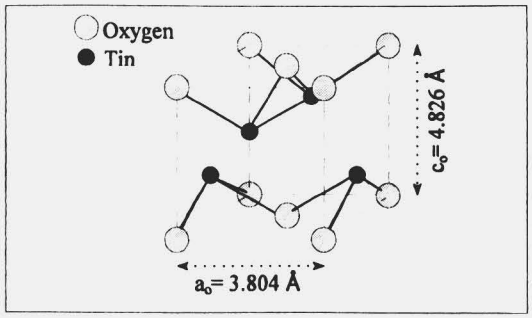

Figure 2.1(b) Tetragonal unit cell of SnO.

2.2.3 Stannic Oxide

Tin IV oxide or stannic oxide SnO_2 exists in a rutile structure. It is a hexagonal close packed structure of oxygen atoms which is slightly distorted. The tin atoms possess octahedral coordination and the unit cell is shown in figure 2.2. [1] SnO_2 is not soluble in water or dilute acids or alkalis and also has a low solubility in many glasses.

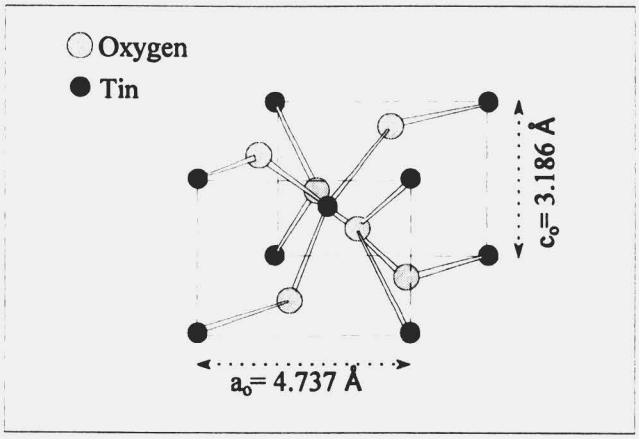

Figure 2.2 Tetragonal unit cell of SnO_2.

2.2.4 Review of ^{119}Sn Mössbauer Hyperfine Parameters

The origin of the Mössbauer hyperfine parameters is discussed in chapter 3, however some features are especially significant to tin compounds. Changes in the valence s electron density essentially give rise to changes in the chemical shift, but it is also necessary to consider other valence electrons because of the effect they may have in screening the nucleus from the s electrons.

As the difference between the radii of the excited and ground states of the tin nucleus is positive (fractional difference ~ $+10^{-4}$, Parish, 1972 [13]), then the chemical shift is greater (more positive) as the electron density at the nucleus, $\psi^2(0)$, increases.

The effective s electron density that contributes to changes in the chemical shift will depend on the covalent nature of the bond under consideration. In the case of tin IV compounds the shift increases as the covalent character of the bonding increases. This may be seen especially in the halide compounds where the shift decreases from SnI_4 to SnF_4, [13] [14] i.e. as the ionic nature of the bonding increases. The chemical shift is therefore related to the difference in the electronegativities of the atoms involved. Few inorganic tin IV compounds show a resolved quadrupole splitting of the absorption peak. Tin may be found in tetrahedral coordination in molecular tetravalent compounds (e.g. halides) but more often occurs in octahedral coordination in solids, for example in SnO_2.

Another factor which may influence the chemical shift of Sn^{4+} is the coordination number of the tin atom. Generally if the coordination number increases, there is a corresponding decrease in the chemical shift. This may be caused by an increase in the bond length as the coordination number increases or an increase in the shielding of the s electrons by increased d orbital population [13].

Tin II compounds have more positive chemical shifts than the stannic compounds, and also larger quadrupole splittings. In these compounds, an increase in the chemical shift occurs as a result of an increase in the ionic nature of the tin 2+ bonds, (i.e. the reverse situation to that in the tin 4+ bonding). A $(5s)^2$ $(5p)^2$ configuration occurs in the covalent bonding and this causes shielding of the nucleus from the s electron density, hence in the ionic (5s) configuration the s electron density will increase at the nucleus.

Unlike many tin IV compounds no relationship exists between the tin 2+ chemical shifts and the electronegativities of the surrounding ions. This may be explained by the fact that the hybridized nature of the bonding in the compounds varies considerably, thus masking ionic changes.

The observed quadrupole splittings are mainly caused by the valence p electrons which create large electric field gradients at the nucleus. This will occur in covalently bonded compounds when there is an unequal population of the p orbitals. The relation between the chemical shift and quadrupole splitting was described by Lees and Flinn [15]. A decrease in the 5p bond character (i.e. greater ionic $(5s)^2$ configuration) results in a decrease in the quadrupole splitting as the chemical shift increases.

Chemical shift data for some tin compounds is given in table 2.1. The values have been corrected to quote the shifts relative to calcium stannate, $CaSnO_3$, as this is the standard used later and the temperature of measurement is indicated where known.

Table 2.1 (a) Tin IV Compounds

Absorber	Temp (K)	Chemical Shift (mms^{-1}) w.r.t. stated source	Shift (mms^{-1}) w.r.t. $CaSnO_3$	Quadrupole Splitting (mms^{-1})
$CaSnO_3$		+0.031 ($BaSnO_3$) [a]	0	-
$BaSnO_3$	80	-2.10 (α-Sn) [e]	-0.126	-
SnO_2		-2.10 (α-Sn) [e]	-0.126	-
α-Sn		+2.10 ($BaSnO_3$) [d]	+2.057	-
β-Sn	295	+2.6 ($CaSnO_3$) [e]	+2.600	-
SnF_4	80	-0.47 (SnO_2) [c]	-0.474	1.66
	80	-2.35 (α-Sn) [b]	-0.376	1.75
$SnCl_4$	80	+0.85 (SnO_2) [c]	+0.846	-
	80	-1.25 (α-Sn) [b]	+0.724	-
	80	+0.8 ($CaSnO_3$) [d]	+0.769	-
$SnBr_4$	80	+1.15 (SnO_2) [c]	+1.154	-
	80	-0.96 (α-Sn) [b]	+1.014	-
	80	+1.10 ($CaSnO_3$) [d]	+1.057	-
SnI_4	80	+1.55 (SnO_2) [c]	+1.554	-
	80	-0.65 (α-Sn) [b]	+1.324	-
	80	+1.45 ($CaSnO_3$) [d]	+1.407	-

Table 2.1 (b) Tin II Compounds

Absorber	Temp (K)	Chemical Shift (mms^{-1}) w.r.t. stated source	Shift (mms^{-1}) w.r.t. $CaSnO_3$	Quadrupole Splitting (mms^{-1})
SnO- black		+2.71 (SnO_2) [c]	+2.706	1.45
- red		+2.6 (SnO_2) [c]	+2.596	2.2
	80	+0.67 (α-Sn) [b]	+2.687	1.5
SnC_2O_4	80	+1.6 (α-Sn) [b]	+3.617	1.45
	295	+3.47 ($BaSnO_3$) [e]	+3.513	1.59
SnF_2 *		+3.6 / 3.2 (SnO_2) [c]	+3.596 / 3.196	1.8 / 2.2
* 2 forms	80	+1.55 (α-Sn) [b]	+3.567	1.67
	80	+3.6 ($CaSnO_3$) [d]	+3.557	2.2
$SnCl_2$	80	+4.07 (SnO_2) [c]	+4.066	-
	80	+2.14 (α-Sn) [b]	+4.114	-
	80	+4.15 ($CaSnO_3$) [d]	+4.15	0.3
$SnCl_2 \cdot 2H_2O$	80	+3.55 (SnO_2) [c]	+3.546	-
	80	+1.57 (α-Sn) [b]	+3.544	1.10
$SnBr_2$	80	+3.93 (SnO_2) [c]	+3.926	-
	80	+1.85 (α-Sn) [b]	+3.824	0.055
	80	+4.06 ($CaSnO_3$) [d]	+4.06	0.2
SnI_2	80	+3.85 (SnO_2) [c]	+3.846	-
	80	+3.98 ($CaSnO_3$) [d]	+3.98	0.2

References (a) - [16] page 903 (d) - [13]

(b) - [14] (e) - [17]

(c) - [21]

2.2.5 Review of ^{119}Sn Mössbauer f-factor Measurements

The recoil-free fraction of γ-rays is discussed in chapter 3, which includes an expression derived on the basis of the Debye model. The values of the recoil-free fraction are proportional to the mean square atomic displacements. Measurements of the f-factor for tin in a number of materials have been made. [18] [19] [20] At low temperatures, in-phase atomic vibrations (acoustic modes) are most significant, but at higher temperatures out of phase atomic vibrations (optical modes) are important.

The second order Doppler shift is proportional to the mean square velocity. It may be estimated on the Debye model, using the Debye temperature determined from measurements of the recoil-free fraction. A few results [14] [15] are listed in table 2.2.

Table 2.2

Absorber	f (4.2 K)	f (77 K)	f (300 K)	S.O.D.S calc.	S.O.D.S expt.
β-Sn [18]	0.72 (1)	0.455 (10)	0.039 (10)	-	-
β-Sn [16]	-	-	0.04	0.07	0.07
$CaSnO_3$ [14]	-	0.25	0.27	-	-
SnO_2 [14]	-	0.55	0.44	-	-
SnO [14]	-	0.40	0.14	-	-
$SnCl_2 \cdot 2H_2O$ [14]	-	0.15	0.02	-	-
$BaSnO_3$ [14]	-	0.56	-	0.06	0.05

2.3 Tin-Containing Inorganic Oxide Glasses

Tin oxide has been added to soda-lime silica glasses specifically to produce coloured glasses (ruby glass). [22] This procedure dates back many years but there was then no knowledge as to the role that the tin oxides played in these glasses.

Many silicate glasses are colourless as they transmit all electromagnetic radiation in the visible region. Ultra-violet radiation however, is absorbed as it has enough energy to promote electrons to a higher energy state. The presence of tin in the glass must introduce a lower energy level in the energy band gap, which results in the absorption of radiation with a wavelength in the visible region. Absorption at the violet-blue end of the visible spectrum would cause the glass to appear coloured yellow-red.

There are a number of mechanisms which can give rise to coloration in solids and the particular mechanism that occurs in the case of the tin oxide-silicate glasses is not obvious. In ruby glasses containing gold and tin oxide, the presence of the tin oxide increases the formation of regions of small metallic gold particles.[61] It is these particles which absorb light and create the coloured glass. However, in coloured binary tin oxide-silicate glasses, no metallic tin has been identified thus this mechanism does not account for the colour in these glasses. Another possible mechanism seen in some glasses is the formation of colour centres, where faults in the network allow bound electron states to absorb visible radiation. To clarify the cause of the colour in these glasses would require studies of conductivity, absorption and X.P.S. measurements.

Several glass systems containing tin have been studied previously, for example, borate, germanate, phosphate and silicate glasses. In both $SnO\text{-}B_2O_3$ and the alkali borate glasses it was concluded that the Sn-O bonding was more strongly ionic than in the oxides. [23] [24] Differences in the Mössbauer parameters between the glasses and crystal were also observed. Binary $SnO\text{-}GeO_2$ glasses have been reported to contain tin in only the divalent state. [25] Larger Mössbauer chemical shifts and quadrupole splittings in the glass indicated greater ionicity and distortion than in crystalline SnO. Results obtained for the $SnO\text{-}SnF_2\text{-}P_2O_5$ glass systems [26] implied that the tin ions were acting as network formers.

2.3.1 The Role of Tin in Silicate Glasses

Binary tin oxide-silica glasses have been prepared and studied by Carbó-Nóver and Williamson. [10] Their methods of production were based on previous work, but they

also chemically analysed the glasses and studied the effect of heat treatments in air. More than 99% of the tin ions were found to exist in the divalent state and the total weight percent varied between 46% and 76%. After heating at approximately 550°C a crystalline phase (stannous metasilicate, $SnO{\cdot}SiO_2$) was found to be present. The x-ray diffraction pattern was found to be similar to that of SnO. At higher temperatures, the crystalline phase was found to decompose, predominantly to SnO and SiO_2, but SnO_2 was also produced. Similar results were obtained by Ishikawa and Akagi [11] whose methods of analysis included infra-red spectroscopy.

Information about the sites occupied by tin in silicate and other inorganic oxide glasses has been obtained. [27] Nishida suggested that tin occupies a network former site when the measured Debye temperature is greater than about 280 K, and a network modifier site when θ_D is below 270 K.

Several reports [28] [29] suggest that tin in the quadrivalent state has a stronger ionic Sn-O bond in glass than in the crystal, and that it has octahedral coordination with respect to oxygen, i.e. a coordination number of 6. Divalent tin, however, frequently has a coordination number of 4, as in SnO.

2.3.2 ^{119}Sn Mössbauer Results

Much of the analysis of tin in silicate glasses has involved Mössbauer spectroscopy. Reviews have been reported by Kurkjian [30] and Coey [31] of the Mössbauer effect in glasses and amorphous materials. Collins et al [32] compared two sets of amorphous samples of tin oxide with the crystalline SnO_2 and SnO. The samples were prepared from metallic tin and oxygen and variable temperature Mössbauer spectra were

recorded for the amorphous oxides. Sn^{2+} and Sn^{4+} were found to be present, and the chemical shift and the quadrupole splitting were greater in the amorphous material than in the crystalline oxides. From measurements of the recoil-free fraction between 100 K and 500 K, the Debye temperature was found to be significantly lower in the amorphous oxides than in the crystalline oxides.

Conversion electron Mössbauer spectroscopy has been used by Principi et al [33] to study the oxidation state of tin in industrially produced float glass. Both Sn^{2+} and Sn^{4+} were found to be present, there being more Sn^{2+}, with a chemical shift and quadrupole splitting larger than those of the corresponding crystalline oxides.

Chapter 3 The Mössbauer Effect and Mössbauer Spectroscopy

3.1 Introduction

The Mössbauer Effect was discovered in 1957 by R. Mössbauer and is the emission and absorption of γ-rays without energy loss in nuclear recoil. Previous attempts to obtain nuclear resonance fluorescence involved compensating for the energy of recoil using the Doppler effect with very large velocities. Recoil free emission and absorption may be obtained if the atoms are bound in a solid, there is a low energy nuclear transition to the ground state and the lowest vibrational excitation energy of the solid is greater than the recoil energy.

Since its discovery, a number of isotopes have been found to exhibit the above properties. Those which are most commonly investigated are ^{57}Fe and ^{119}Sn, for example in the study of magnetic materials and in chemistry. A Mössbauer spectrum can provide information about the interactions between the nucleus and the surrounding atomic electrons, as very small energy differences may be resolved. This is discussed in several references [21] and briefly later in this chapter.

3.2 The Mössbauer Effect

The initial attempts to produce resonant absorption of γ-rays involved using the Doppler energy by moving the emitter towards the absorber at high velocities to overcome the energy lost in recoil. From the conservation of energy and momentum, this recoil energy can be shown [21] to depend on the mass of the nucleus and the energy of the γ-ray according to $E_R = \frac{E_\gamma^2}{2Mc^2}$.

The mean Doppler broadening, E_D, depends on the thermal motion of the nucleus

and will have a temperature dependent distribution of values. The resulting statistical energy distributions of the emitted and absorbed γ-rays are thus as shown in figure 3.1, broadened by an amount dependent upon the recoil energy and the absolute temperature. In this case little nuclear resonance occurs.

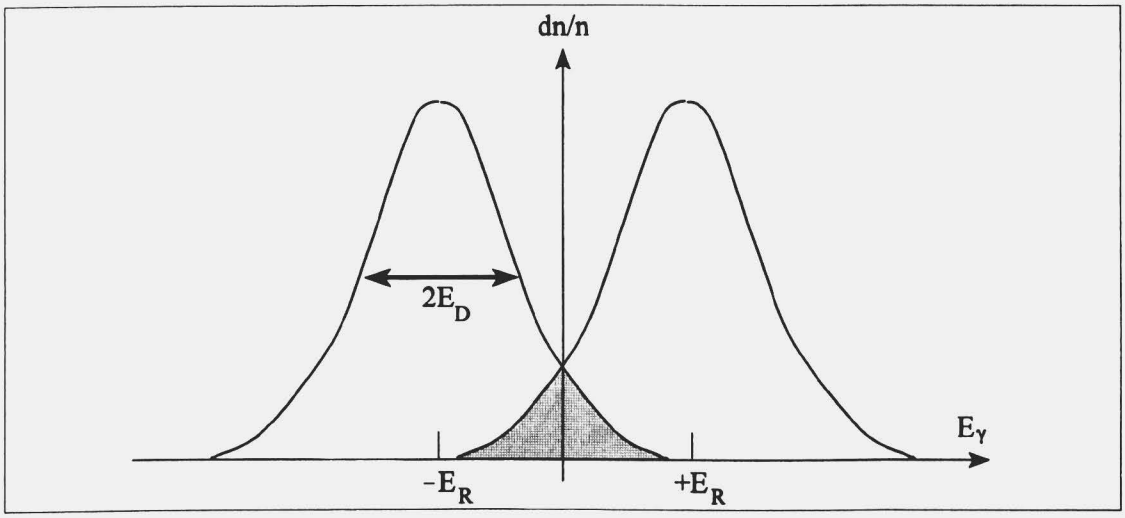

Figure 3.1 Statistical energy distributions of the emitted and absorbed γ-rays showing the small resonance overlap (shaded).

If however the emitting and absorbing nuclei are bound in a solid lattice, then the recoil energy will be taken up by the whole solid. As the mass, M, is now much larger (the lattice mass rather than the nuclear mass), then E_R is effectively zero and resonant absorption may occur.

Although the nuclei are bound in the lattice, they are still able to vibrate about their mean position. If lattice phonons are excited, then recoil energy may be transferred to the solid, resulting in a reduction of the energy of the γ-ray from the emitting nucleus. Consequently, the γ-ray energy distribution (dependent upon E_R) will be broadened as above. However, as lattice vibrations are quantised (as 0, $\hbar\omega$, $2\hbar\omega$... in the Einstein model), then if only low energy transitions are involved, there is a probability of zero

phonon events occurring and hence there is no recoil and no broadening. The fraction of recoil-free events is discussed later. The Mössbauer effect may therefore be found to occur if the nuclei;-

(i) have an excited state of moderately low energy

(ii) are bound in solid lattices whose lowest vibrational excitation energy, $E > E_R$.

The isotope used in this work is ^{119}Sn, and the decay scheme which leads to the Mössbauer transition is shown in figure 3.2.

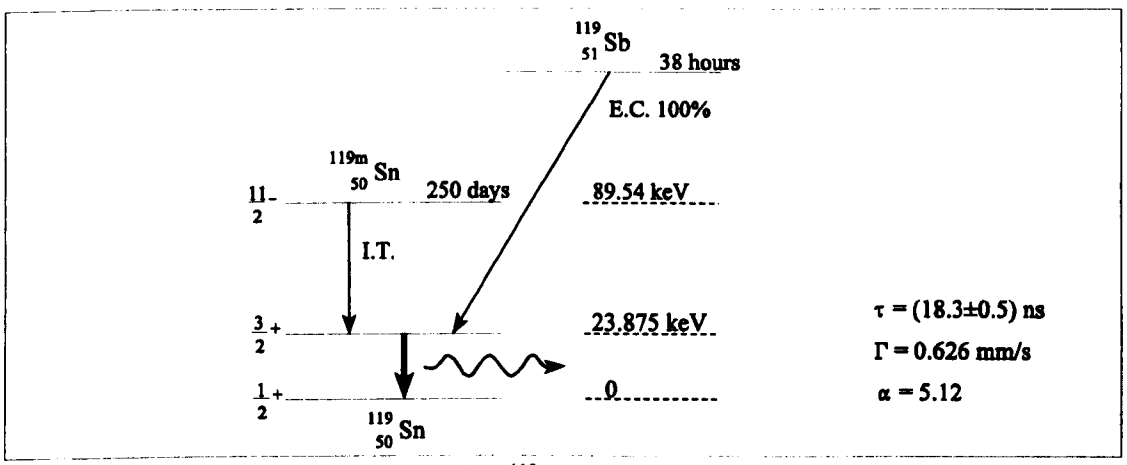

Figure 3.2 The decay scheme for ^{119}Sn. (I.T.=Isomeric transition, E.C.=Electron capture).

3.2.1 Linewidth

Thermal broadening of the γ-ray energy distribution is eliminated, as discussed above, in the recoil-free emission and absorption obtained from the Mössbauer transition. The width of the distribution is therefore defined by the energy width of the excited state nuclear level. According to the Heisenberg uncertainty principle which relates the uncertainties in energy and time, $\Delta E \Delta t \geq \hbar$, the mean lifetime of the excited state, τ, and

the energy width, Γ_s, are related by $\Gamma_s\tau=\hbar$. As the stable ground state level has an infinite lifetime, then $\Delta E_{GS} = 0$. The width, Γ_s, is of the order of 10^{-7} eV - 10^{-8} eV and hence hyperfine interactions (with similar energies) may be studied. Another contribution to the linewidth, for example in glasses or alloys, arises from disorder.

3.2.2 The Recoil-Free Fraction

If the fraction of γ-ray emissions occurring without causing vibrational excitation of the lattice is *f*, then, for a simple model, the fraction (1-*f*) transfers energy $\hbar\omega$ to the lattice. The mean energy transferred in each event has been found to be equal to the recoil energy, E_R, [34], hence

$$f = 1 - \frac{E_R}{\hbar\omega} \qquad (3.1)$$

The Debye model which considers a range of frequencies is more realistic, and the Mössbauer effect is still possible as low frequencies are not easy to excite. The recoil-free fraction, *f*, increases when;-

(i) the γ-ray energy is low (there is a smaller probability of exciting phonons),

(ii) the atomic binding in the lattice is strong,

(iii) the temperature is lower.

Quantitatively, the recoil-free fraction has been calculated (using dispersion theory)[34] [35] and this gives

$$f = \exp(-\kappa^2\langle x^2\rangle) \qquad (3.2)$$

where κ is the γ-ray wave vector, and $\langle x^2\rangle$ is the component of the mean square

vibrational amplitude of the emitting atom in the direction of the γ-ray.

Using the Debye model for lattice vibrations, the expression for the fraction, f may be written as

$$\ln f = \frac{-6E_R}{k\theta_D}\left[\frac{1}{4} + \left(\frac{T}{\theta_D}\right)^2 \int_0^{\frac{\theta_D}{T}} \frac{x\,dx}{e^x - 1}\right] \qquad (3.3)$$

where k is Boltzmann's constant. This expression is used later to calculate the Debye temperature and therefore to compare the strength of binding of tin in several glass samples. The Debye model is not strictly applicable to glasses as it refers to monatomic lattices. However, it is useful as a means of comparing different samples.

3.2.3 Absorption Cross-Section and Mössbauer Lineshape

The probability of resonant absorption, independent of the recoilless fraction, or cross-section for absorption for the resonant isotope (σ_0), depends on the γ-ray wavelength, the nuclear spins of the excited state and ground state, and also on the internal conversion coefficient of the γ-transition, i.e. $\sigma_0 = \frac{\lambda^2}{2\pi}\left(\frac{2I_e + 1}{2I_g + 1}\right)\frac{1}{1+\alpha}$. The energy distribution of the emission or absorption cross-section for a nuclear transition between a single excited state and the ground state is given by the Breit-Wigner formula [36];

$$\sigma(E) = \sigma_0 \frac{\left(\frac{\Gamma_a}{2}\right)^2}{(E - E_\gamma)^2 + \left(\frac{\Gamma_a}{2}\right)^2} \qquad (3.4)$$

which is a Lorentzian distribution where Γ_a is the Heisenberg width at the half height of the absorption profile.

In a standard Mössbauer transmission experiment, the γ-rays are detected after passing through the sample. A spectrum is produced which is a combination of a single Lorentzian lineshape from the source and the Lorentzian lineshapes from the absorber, as defined by the hyperfine interactions in the sample. The lineshape may also be influenced by, for example, vibrations of the apparatus and thickness effects. The latter is described quantitatively by Margulies and Ehrman.[37]

3.2.4 Absorber Thickness

Generally a thick absorber attenuates the γ-rays passing through and this is especially so near the resonant frequency. This results in a non-Lorentzian lineshape where the effective linewidth is increased. In order to calculate the optimum thickness, samples were initially prepared as described in "The Ideal Mössbauer Effect Absorber Thickness", by G. Long et al.,[38] but some modifications were necessary as described later.

3.3 Mössbauer Spectroscopy

To obtain a Mössbauer spectrum, the γ-rays from a source (which is usually a single line source) are passed through the absorber (the sample to be investigated), and the transmission over a range of energies is detected. The transmission of γ-rays

decreases at energies corresponding to the energy of resonant absorption. The γ-rays are re-emitted from the absorber in all directions as the nucleus returns to the ground state. This leads to a drop in intensity along the direction of the γ-ray beam, hence an absorption dip occurs in the spectrum.

Conversion electron Mössbauer spectroscopy may also be used, where the conversion electrons produced during the decay of the Mössbauer nucleus are detected instead of the γ-rays. The internal conversion coefficient (the number of electrons to the number of photons emitted in a given time) of ^{119}Sn is ~5. This technique is especially applied when studying surfaces (~ a few hundred nanometres) as only the electrons emitted from this depth will escape before losing their energy in the material.

The variation in the γ-ray energy is achieved by moving the source relative to the absorber, causing the energy to be Doppler shifted. The velocity is measured in mms^{-1} and in the case of the 23.87 keV γ-ray of ^{119}Sn, 1 mms^{-1}≡7.9624×10^{-8} eV. The energy at velocity, v is thus

$$E = E_{\gamma}\left(1 + \frac{v}{c}\right) \tag{3.5}$$

where c is the velocity of light. The percentage absorption is recorded as the velocity range is scanned.

As mentioned earlier, the small experimental linewidth enables the shifts and splittings of the nuclear energy levels, caused by the hyperfine interactions with the surroundings, to be measured. Discussions of these interactions follow.

3.4 Hyperfine Interactions

The nuclear energy levels are shifted by interactions of the nucleus with its surrounding electrons, i.e. the chemical environment. The separate terms in the interaction may be split up into the electric monopole (Coulomb) interaction, the electric quadrupole interaction and the magnetic hyperfine interaction. As a result of these hyperfine interactions, the absorption peaks are shifted and split and these will each be discussed.

3.4.1 The Centre Shift

The centre shift consists of the chemical isomer shift and a temperature shift. It is the shift of the maximum of the absorption peak from some calibration point. The chemical shift arises from the Coulomb interaction.

During the nuclear transition, the size of the nucleus alters and the resulting difference in the interaction energy means that there is a change in the energy separation between the ground state and the excited state of the nucleus. Different materials will have different chemical environments, therefore the electron charge density in the nuclear volume will vary. For example, between the source and the absorber $|\psi_a(0)|^2 \neq |\psi_s(0)|^2$. Both these effects will result in a shift in the position of the observed absorption line as shown in figure 3.3. The energy is given by [39] [40]

$$\delta = \frac{Ze^2}{6\varepsilon_0}\left\{|\psi_a(0)|^2 - |\psi_s(0)|^2\right\}\left[\langle R_e^2\rangle - \langle R_g^2\rangle\right] \qquad (3.6)$$

where $|\psi_s(0)|^2$ and $|\psi_a(0)|^2$ are the electron densities at the nucleus for the source and the

absorber, and $\langle R_e^2 \rangle$ and $\langle R_g^2 \rangle$ are the mean-square radii of the nucleus in the excited and the ground states, (ε_0 is the permittivity of free space). The term involving the change in nuclear radius will be constant for a given nuclide. The nuclear radius of ^{119}Sn in the excited state is greater than in the ground state, hence a shift to the right in the spectrum (positive) is indicative of a greater electron density in the absorber nuclei than in the source. In equation (3.6), relativistic wave functions should be used, otherwise a correction should be made for relativistic effects as described by Shirley, 1964.[41]

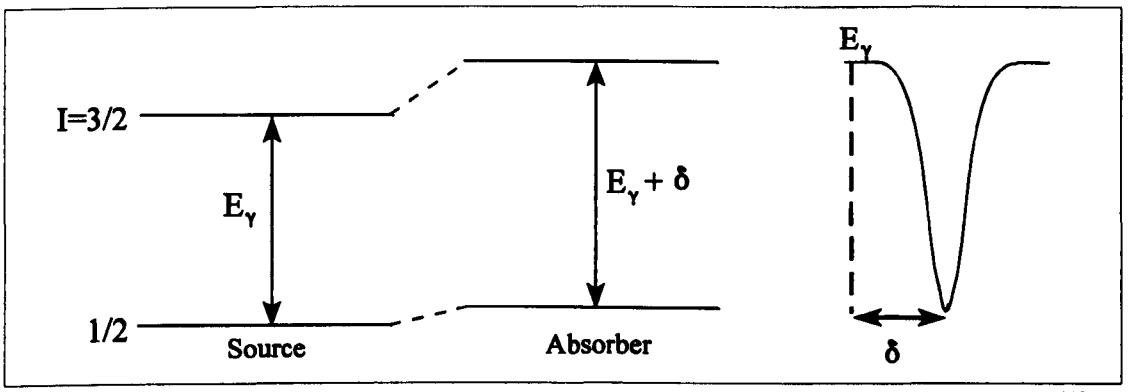

Figure 3.3 Energy level diagram and corresponding Mössbauer spectrum for ^{119}Sn in the presence of the centre shift.

Changes in the chemical shift are usually attributed to changes in the valence s-electrons, and the contribution of the inner s-electrons is constant[39]. There is a small shielding effect by the p and d-electrons on the electron density at the nucleus.

The expression (3.7) for the chemical isomer shift may be re-written so that it is quoted relative to some standard absorber. Spectra recorded in this work were calibrated with an iron source and α-iron absorber (see section 3.4.3 and chapter 4), but from measurements of the chemical shift of calcium stannate relative to α-iron, a correction may be made and the shifts are therefore quoted relative to calcium stannate (the source material) at room temperature.

The chemical shift may be temperature dependent, but more significantly a second measurable effect is that of the temperature shift or second order Doppler shift. It is present as a result of atomic vibrations. The observed frequency may be expressed as [21]

$$\nu_0 = \nu\left[1-\frac{v}{c}\right]\left[1-\frac{v^2}{c^2}\right]^{-\frac{1}{2}} \tag{3.7}$$

where ν_0 is the frequency of the emitted γ-rays, v the atom's mean velocity and c the velocity of light. Although the first order term will average zero, the mean square velocity will not, hence there is a corresponding change in energy, $\Delta E = \frac{-\langle v^2\rangle_T E_\gamma}{2c^2}$. The resulting shift is given by [42] [43]

$$\delta(T) = \frac{-\langle v^2\rangle_T}{2c} \tag{3.8}$$

$\langle v^2\rangle$ is the mean square velocity of the nuclei and depends upon the temperature and the properties of the lattice. The Debye model may be used to describe the temperature dependence of the second order Doppler shift for a particular lattice, and this is given by [16]

$$\delta_T = \frac{-9}{4}\frac{k\theta_D}{mc}\left\{\frac{1}{4}+2\left(\frac{T}{\theta_D}\right)^4\int_0^{\frac{\theta_D}{T}}\frac{x^3dx}{e^x-1}\right\} \tag{3.9}$$

where k is Boltzmann's constant, m is the atomic mass of the isotope (in kg) and θ_D is the Debye temperature of the material. At high temperatures this quantity δ_T is proportional

to the temperature of measurement, and for ^{119}Sn the slope of this line should be -3.5×10^{-4} mms^{-1}.

3.4.2 The Electric Quadrupole Interaction and Quadrupole Splitting

A nuclear quadrupole moment arises when the nucleus deviates from spherical symmetry i.e. it has a spin quantum number $I > 1/2$. An oblate (or flattened) nucleus has a negative quadrupole moment, eQ, which is the case for the excited state of the ^{119}Sn nucleus, and a prolate (or elongated) nucleus has a positive quadrupole moment. When the electron charge density surrounding the nucleus is also not spherically symmetric, then an electric field gradient is present at the nucleus.

The interaction between the nuclear quadrupole moment and the electric field gradient (efg) at the nuclear site is the electric quadrupole interaction and results in a splitting of the nuclear levels. The efg is a tensor given by $\nabla\mathbf{E}$, but by defining suitable coordinates, this may be simplified to a diagonal form where the efg is expressed in terms of three components, V_{xx}, V_{yy} and V_{zz}. As there is no electron charge density which contributes to the efg present at the nucleus, then Laplace's equation applies, hence $V_{xx} + V_{yy} + V_{zz} = 0$. The efg may be defined by the efg along the principal axis, V_{zz}, and the asymmetry parameter, η, where $\eta = \frac{V_{xx} - V_{yy}}{V_{zz}}$. The maximum value of the efg corresponds to $V_{zz} = eq$, and η lies between 0 and 1.

The two contributions to V_{zz} may be considered to arise from valence electrons and from charges on atoms bonded to the Mössbauer atom. These terms, eq_{val} and eq_{latt}, may be of opposite sign. The effect of the efg at the nucleus, however, is modified from

the simple electrostatic case. [44 - 47]

The interaction between the nuclear quadrupole moment and the efg may be described by the Hamiltonian;

$$\mathcal{H} = \frac{eQV_{zz}}{4I(2I-1)}\left[3\hat{I}_z^2 - \hat{I}^2 + \frac{\eta}{2}(\hat{I}_+^2 + \hat{I}_-^2)\right] \qquad (3.10)$$

where I is the nuclear spin and $\hat{I}_+$ and $\hat{I}_-$ are raising and lowering operators. The quadrupole moment eQ will be fixed for a particular isotope, while V_{zz} = eq depends upon the chemical environment. Equation (3.10) can be solved [48] for I = 3/2 to give eigenvalues of

$$E_Q = \frac{e^2qQ}{4I(2I-1)}\left(3m_I^2 - I(I+1)\right)\left[1 + \frac{\eta^2}{3}\right]^{\frac{1}{2}} \qquad (3.11)$$

where m_I is the magnetic quantum number, m_I = I, (I- 1), ...-(I + 1), -I. This shows that states with m_I differing only in sign will not split.

The first excited state of ^{119}Sn will therefore split into just two sub-levels with $m_I = \pm 3/2$ and $m_I = \pm 1/2$, and there will be an energy difference of

$$\Delta E_Q = \frac{e^2qQ}{2}\left(1 + \frac{\eta^2}{3}\right)^{\frac{1}{2}} \qquad (3.12)$$

Two transitions result, and a quadrupole split doublet is observed in the Mössbauer spectrum. The energy levels and the resulting spectrum are shown in figure 3.4.

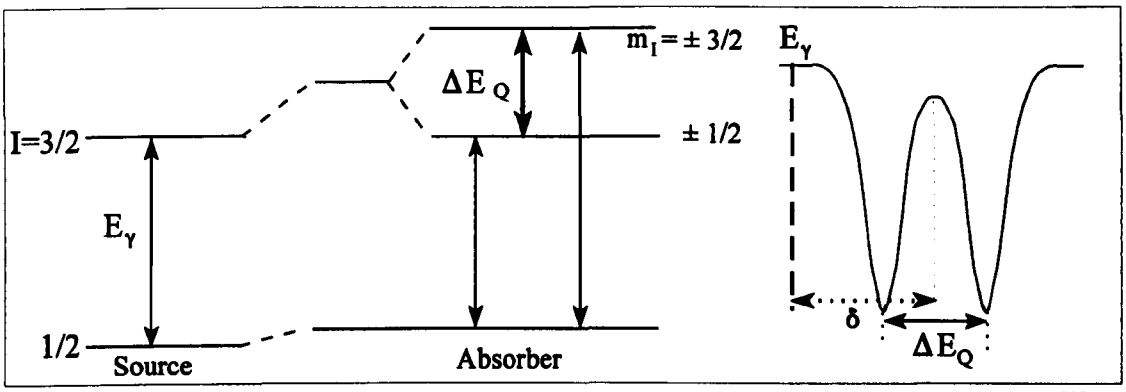

Figure 3.4 Energy level diagram and corresponding Mössbauer spectrum for ^{119}Sn in the presence of a quadrupole splitting.

The intensity of the two lines in the doublet may not be equal. It will depend on the angle θ between the γ-ray beam and the principal axis of the efg. The intensity ratio of the two transitions is given by the following when $\eta = 0$,

$$\frac{I_{\pm 3/2 \rightarrow \pm 1/2}}{I_{\pm 1/2 \rightarrow \pm 1/2}} = \frac{3(1 + \cos^2\theta)}{5 - 3\cos^2\theta} \qquad (3.13)$$

and for an absorber which is a single crystal or a polycrystalline sample which is not randomly orientated, an asymmetry in the line intensity may be observed. If however all crystallites in a polycrystalline sample are randomly arranged, then the net effect will be two lines of equal intensity.

In an amorphous sample, such effects resulting from texture, should not be seen and an asymmetry in the quadrupole split spectrum may result from anisotropy of the recoil-free fraction, known as the Goldanskii-Karyagin effect. [49] This may be confirmed by observing the changes in the relative intensities of the spectral lines over a temperature range. Asymmetry resulting from texture effects will not change with temperature.

Other possible cases of asymmetry occur when there is line broadening and as a

result of the absorber giving rise to a range of chemical shifts and quadrupole splittings. This may be the case when the Mössbauer atom is present in a number of different sites in the absorber.

3.4.3 The Magnetic Hyperfine Interaction

The magnetic hyperfine interaction or the nuclear Zeeman effect occurs when there is a magnetic field present at the nucleus which interacts with the nuclear magnetic moment. This field may be present due to the atoms own electrons or it can originate in the crystal or else it may be applied externally. No tin containing materials studied here exhibit this interaction.

An internal field does however exist in ^{57}Fe and the Zeeman splitting of the ground and excited state levels in these nuclei results in six absorption lines. This spectrum is used to calibrate the Mössbauer spectrometer set-up described in the next chapter.

Chapter 4 Experimental Apparatus and Techniques

4.1 Introduction

The simplest set-up for recording a Mössbauer spectrum was operated at room temperature. It consisted of a radioactive source of γ-radiation, the sample absorber to be measured and a γ-ray detection system which recorded the transmitted γ-rays as a function of the Doppler velocity, discussed in section 3.3.

As a result of the low recoil-free fraction of Mössbauer γ-rays for the tin isotope used, and the low abundance of tin in many glass samples, it was necessary to record most spectra at low temperatures where the Mössbauer fraction, *f*, increases. The experimental apparatus necessary for low temperature measurements is discussed in the following sections. High temperature measurements were made with samples containing larger proportions of tin by using a furnace under vacuum.

4.2 The Mössbauer Spectrometer and Detection System

The basic components of the Mössbauer system are shown in figure 4.1, which is a schematic illustration of the γ-ray detection system for ^{119}Sn γ-rays and the Mössbauer spectrometer box. The source motion was obtained using a vibrator system and the energy of the emitted γ-rays was controlled simultaneously with the same equipment which recorded the spectrum. Two γ-ray detectors were used, depending on the energy of the γ-rays. A gas filled proportional counter detected the 14.4 keV ^{57}Fe γ-rays when taking a calibration measurement, and a solid state intrinsic germanium detector was used for the 23.8 keV γ-rays of ^{119}Sn when the absorber was a tin-containing glass sample.

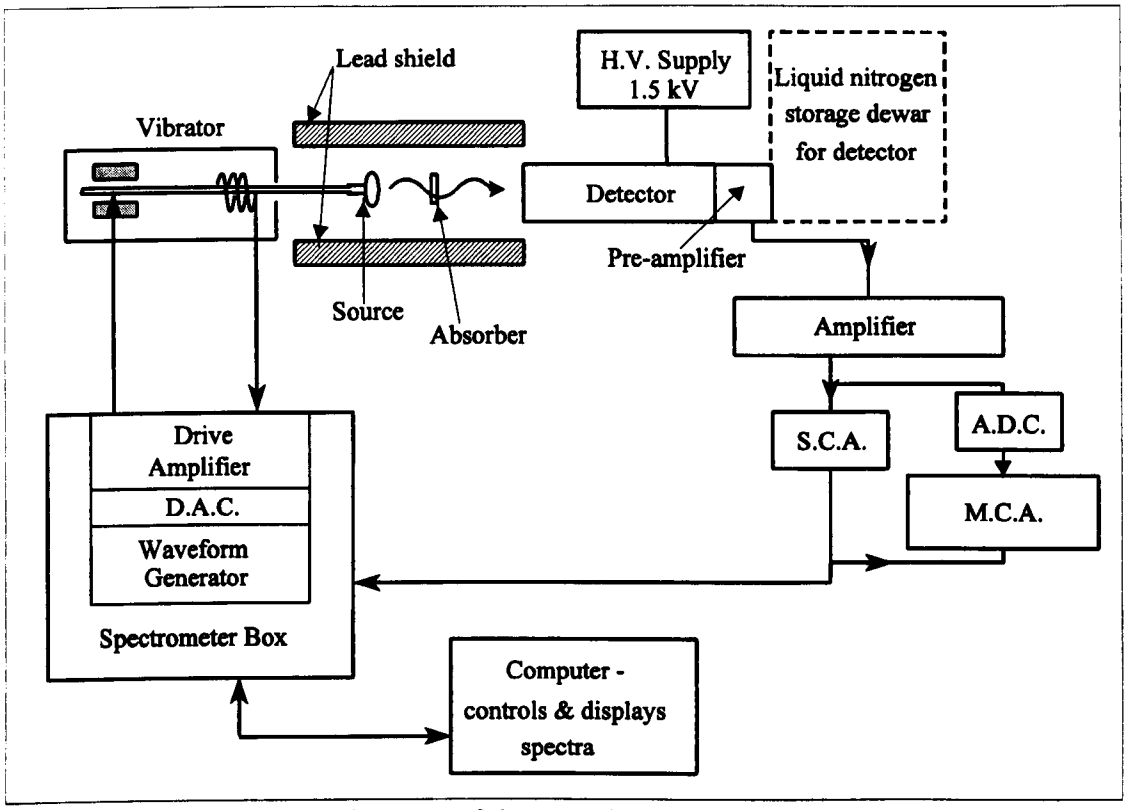

Figure 4.1 Schematic diagram of the Mössbauer spectrometer.

4.2.1 The γ-ray source and the Energy Modulation System

The radioactive source of 23.8 keV tin γ-rays was obtained from Amersham International plc. It consisted of a calcium stannate matrix, 16 mm in diameter and the most recent source had a 10.2 mCi activity when manufactured in February 1994. The source linewidth was quoted as 0.362 mms^{-1}. It was necessary to exchange the $Ca^{119}SnO_3$ source for a source of ^{57}Co in rhodium and to use a standard iron absorber when calibrating the velocity scale. This velocity calibration is described in section 4.4.1, and the different methods of γ-ray detection are discussed in the next section.

As discussed in chapter three, it is necessary to Doppler shift the energy of the γ-rays emitted from the source. This source motion was obtained by mounting it on a shaft which was driven by a vibrator. The vibrator contained magnets, coils and a spring. A

voltage was applied to the drive coil surrounding one magnet which was connected to the shaft. The induced force moves the shaft and therefore changes the source position. The signal from the drive amplifier to the vibrator may be changed by a computer; setting the attenuation altered the voltage to the drive coil. Hence the source position and the maximum velocity range scanned was variable. The waveform used to drive the shaft was triangular which corresponded to a constant acceleration of the source.

Along the shaft, a second small magnet and pick-up coil produced a feed-back signal which was proportional to the source velocity. This enabled any non-linearity of the shaft velocity to be corrected as the signal was fed back to the drive amplifier.

4.2.2 γ-ray Detection and the Pulse Height Spectrum

A relatively simple argon-methane gas-filled proportional counter is effective for detecting the 14.4 keV ^{57}Fe γ-rays necessary for calibration purposes. However, in the case of the higher energy 23.8 keV γ-rays from ^{119}Sn, several advantages were gained by using a solid-state intrinsic germanium detector. Firstly, the proportional counter becomes less efficient as the γ-ray energy increases and secondly the solid-state counter provides better resolution of the different radiations entering the detector. Preliminary results obtained using a proportional counter needed much longer counting times but the majority of the Mössbauer spectra were recorded using a germanium detector and this produced a γ-ray count rate which was increased by a factor of ten. The resolution of the 23.8 keV Mössbauer γ-rays and the 25.2 keV K_α x-rays (arising from internal conversion processes) can be seen in the pulse height spectrum of the intrinsic germanium detector which is shown in figure 4.2.

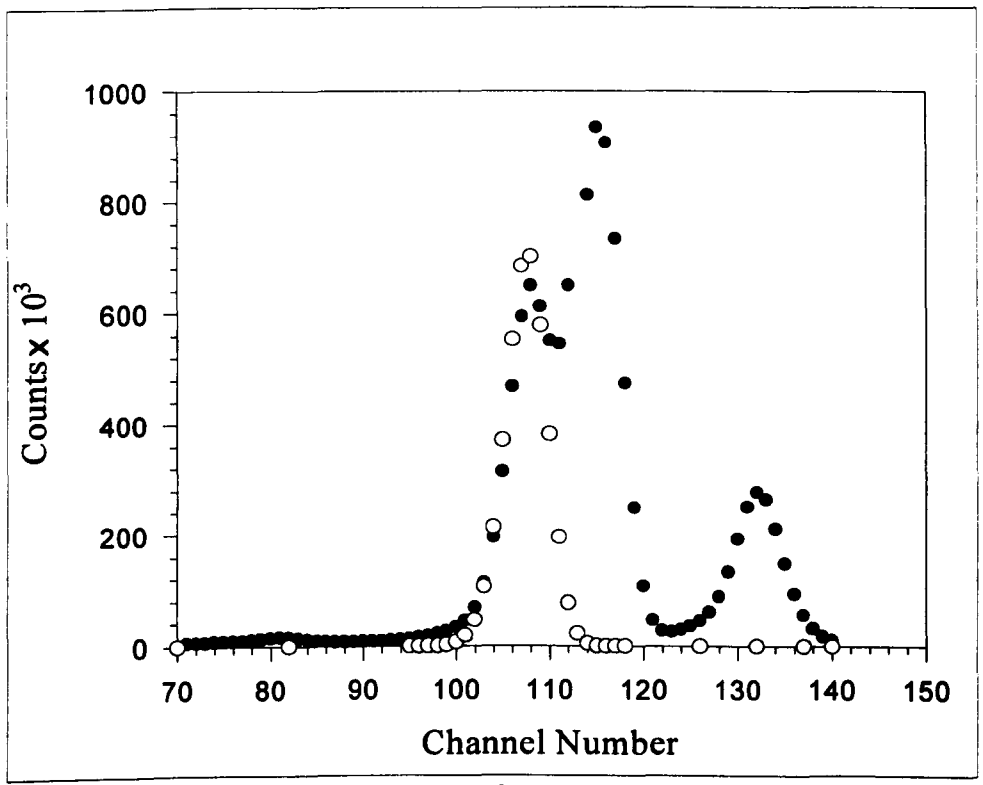

Figure 4.2 Pulse height spectrum for the $CaSnO_3$ source and solid-state germanium detector before and after a "window" was set on the 23.8 keV Mössbauer γ-rays.

The detector was chosen to have a thin germanium crystal (providing better resolution for the relatively low energy Mössbauer γ-rays), and a thin beryllium window at the front of the detector. The improved resolution compared with a gas-filled detector arises as a result of less energy being required for ionisation to occur, hence more excitations per event result.

The detector operates at low temperatures (77 K) to avoid thermal excitations leading to a "leakage current" and to reduce the associated noise.[50] The detector is kept under vacuum in a cryostat and a solid copper "finger" is connected between the crystal and the liquid nitrogen dewar. A high voltage (1500 V) is applied to the crystal causing a depletion region to be formed. Contacts on each side of the crystal collect the charge

resulting from ionisation which is produced by the incoming γ-radiation. A charge sensitive preamplifier is contained in the cryostat near to the detector (to reduce capacitance) and the output pulse from here is sent to a spectroscopy amplifier.

4.2.3 Data Collection

The output signal from the amplifier was fed into both a single channel analyser (SCA) and a multi-channel analyser (MCA). The MCA displays the pulse-height spectrum and this enabled the gate which was set on the Mössbauer peak by the SCA to be seen. (This is also shown in figure 4.2). The digital output pulses from the SCA were passed to the spectrometer box. This stored the counts in one of the 576 channels corresponding to the different position and velocity of the source and hence the different γ-ray energies.

The spectrometer box therefore contained information on the intensity of the spectrum versus the channel number and this information was passed to the computer where the data could be stored on disk . The computer also controlled the spectrometer box, for example in starting and stopping data collection.

4.3 Sample Preparation and Environments

Plastic sample holders of a fixed size (cross sectional area of about 2.84 cm^2) were used to hold the glass samples in most sets of apparatus. Samples containing a known quantity of tin were weighed out and mixed with a quantity of boron nitride so that the tin-containing material was distributed evenly across the region through which the γ

radiation was passed. Initially, to eliminate any line broadening resulting from a "thick" sample, several samples were made to different thicknesses until no reduction in linewidth was measured. This usually occurred at about one quarter of the calculated optimum thickness described in reference [38].

The float glass samples described in section 1.5.2 contained a very low concentration of tin, even in the bottom 0.1 mm. Therefore to obtain a Mössbauer spectrum with a better signal to noise ratio, the sample holders were filled entirely with the ground float glass.

Samples to be measured above room temperature were placed in a furnace and this required an aluminium sample holder to be used. The glass was placed between thin aluminium foil and this was held between two pieces of an aluminium cylinder which were screwed together.

Spectra were recorded over a range of temperatures from about 10 K to 900 K. The low and high temperature equipment is described in the following section.

4.3.1 The Nitrogen Cryostat

This was designed to maintain samples at a temperature close to that of liquid nitrogen (~78 K) whilst the Mössbauer spectrum was recorded. The sample was held at the end of a copper sample stick which was placed in an inner sample space of the cryostat. This space and the bath of liquid nitrogen were insulated by a surrounding vacuum and the sample was kept in thermal contact with the nitrogen by means of the copper cavity wall. The design is shown below in figure 4.3. Windows of mylar in the region of the sample allowed the Mössbauer γ-rays to pass through the metal cryostat.

The vacuum was maintained by connection to a diffusion pump.

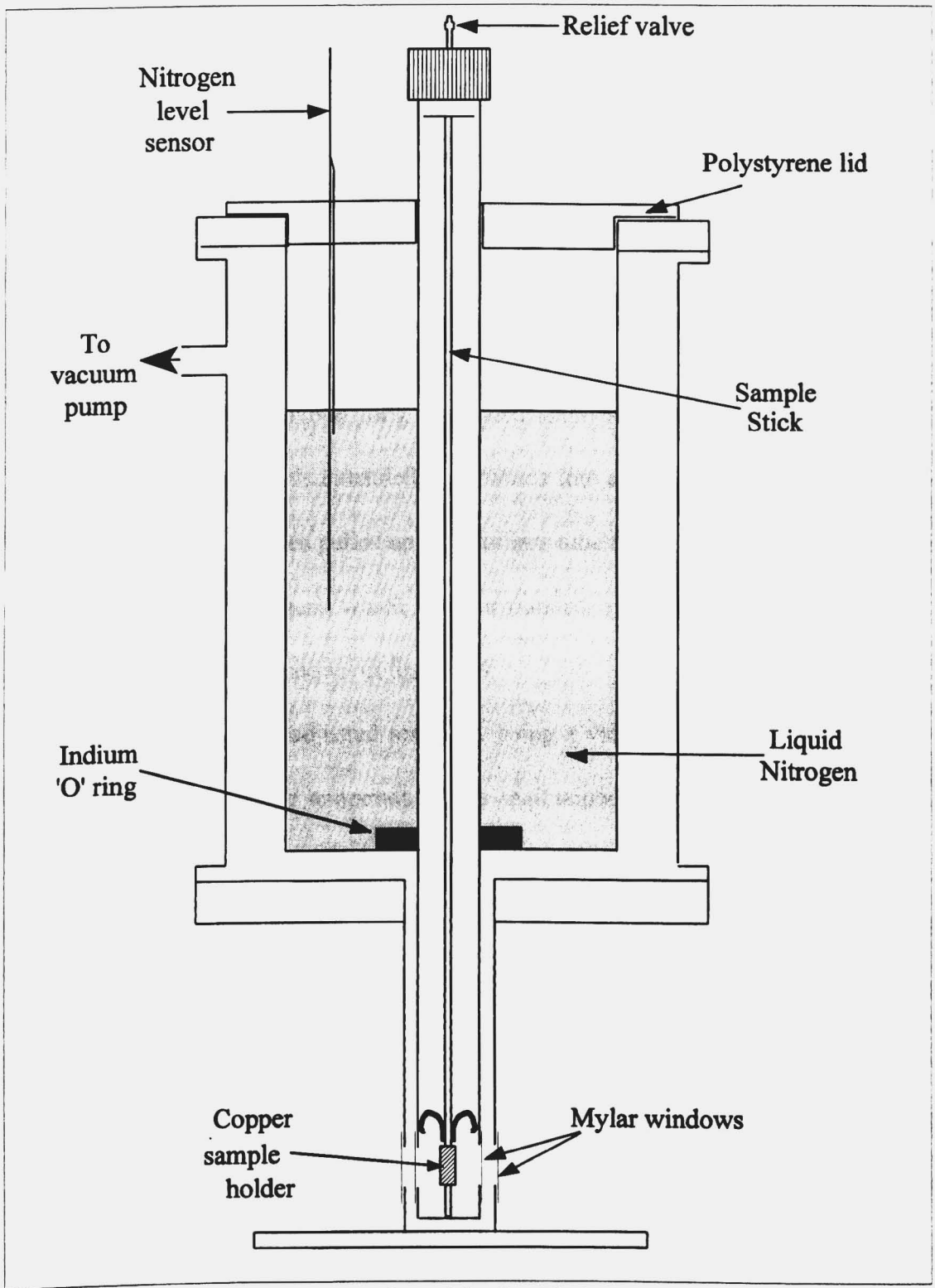

Figure 4.3 Schematic cross-section of the liquid nitrogen cryostat.

4.3.2 The Flow Cryostat

To record Mössbauer spectra of samples over a wide range of temperatures below 300 K, a continuous flow cryostat, manufactured by Oxford Instruments Ltd., was used. A stable temperature of the sample could be maintained between approximately the temperature of the liquified gas used and just above 300 K. Liquid helium was usually used as the coolant. As the temperature stability was found to improve at 10 K and above, this was the lowest temperature set.

The cryostat contains a long evacuated stainless steel tube, incorporating a capillary tube inside it. This extended downwards into a dewar storing the cryogenic liquid. The cold gas was then pulled up the capillary tube by a pump, to cool the sample space (via a heat exchanger), which was surrounded by an outer vacuum cavity. A diagram of the cryostat is shown in figure 4.4.

The gas flow was adjusted manually using a valve to roughly set the chosen temperature. The accurate temperature was maintained by means of an automatic temperature controller (ITC4 - Oxford Instruments Ltd.) which was connected to a copper block near the sample. A resistance thermometer sensed the temperature, and the voltage to a heater was adjusted to obtain the set temperature. The heater voltage was regulated by other settings and for different temperatures these were chosen according to a method described by S.R. Brown (Ph.D thesis 1992). At temperatures below about 50 K helium exchange gas was used in the sample space. This brought the temperature into equilibrium with the outer temperature.

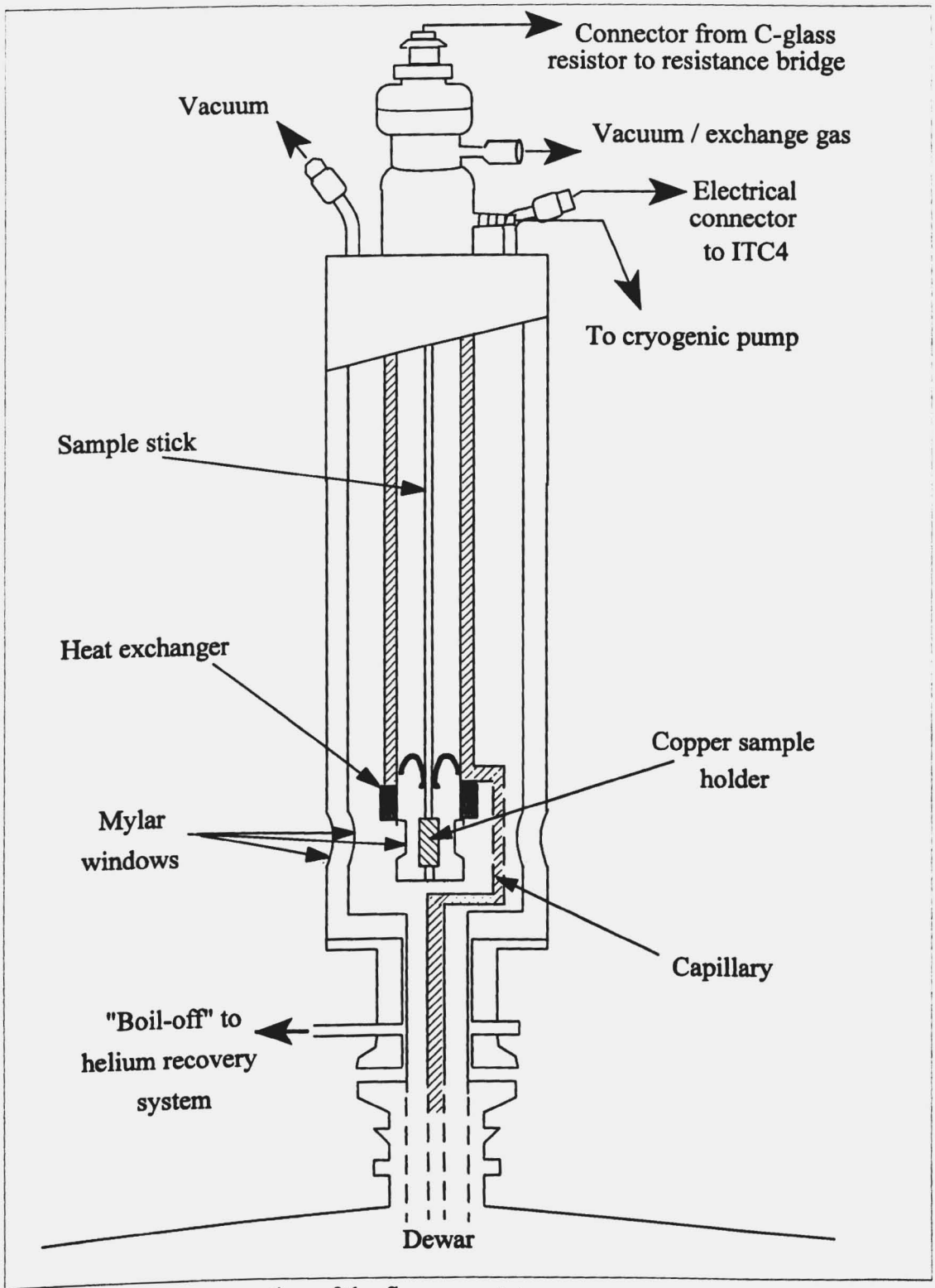

Figure 4.4 Cross section of the flow cryostat.

The sample was held in a copper holder at the end of a stainless steel stick containing a carbon-glass resistor to measure the actual temperature. Connection to a resistance bridge enabled the value to be read and the temperature was then obtained from the calibration of the resistor.

In measuring the f-factor of several samples, a series of spectra was recorded over a range of temperatures from 10 to 300 K. In order to obtain a consistent set of results, it was necessary to maintain the same geometrical set-up of the flow cryostat, i.e. the cryostat had not to be moved to re-fill the storage dewar. This was possible to achieve if the dewar was filled with over 80 litres of liquid helium.

4.3.3 The Furnace

A furnace was used to continue recording variable temperature results above room temperature. With the aluminium sample holder described earlier, results were obtained up to 900 K. The sample was placed in the centre of the cylindrical furnace and held by a solid ceramic block of boron nitride. It was evacuated using a diffusion pump so that oxidation did not occur at high temperatures. A heater surrounded the sample and this was connected to an external regulating power supply. Several concentric radiation shields surrounded the central region. A connection from the centre was also made to a thermocouple which was used to measure the sample temperature. The regions described are shown in the diagram of the furnace in figure 4.5.

The voltage was increased gradually until the required temperature was reached as indicated from the thermocouple calibration tables of voltage and temperature. As the reference thermocouple wires were held in air and not at 0°C, a correction equivalent to

the laboratory temperature was made when setting the voltage. Although the scale of the temperature controller indicated that the temperature remained stable, it was necessary to allow for about a 2° fluctuation in the temperature of the room.

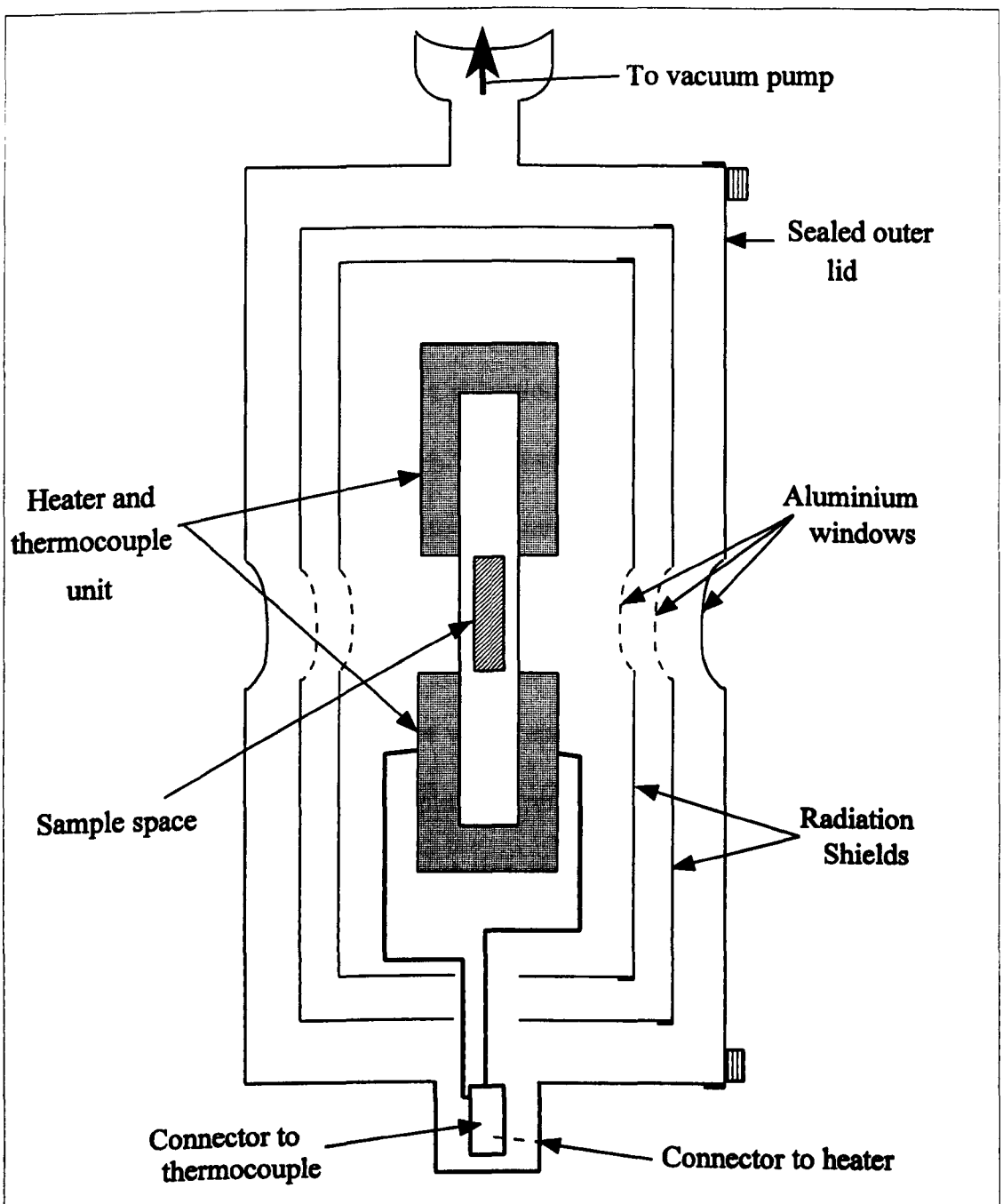

Figure 4.5 Schematic cross-section of the furnace.

4.4 Computer Analysis

In order to obtain information about Mössbauer parameters from the recorded spectra a computer fit to the experimental spectrum was produced.

4.4.1 Velocity Calibration

It was necessary to calibrate the channel number in terms of the relative velocity between the source and absorber for each spectrometer. This was achieved by measuring the spectrum of an iron foil at room temperature as the hyperfine parameters of this material were accurately known.[51] Calibration parameters were obtained when this spectrum was fitted as described in 4.4.2 and these included the centre and the scale. The centre was the channel corresponding to the centre of the iron spectrum and the scale was the velocity increment per channel.

The ^{57}Co:**Rh** source and iron absorber were used as there was no suitable standard tin absorber. A tin-containing garnet was prepared by V.K. Sankaranarayanan in an attempt to produce a magnetically split spectrum which could be used to calibrate the motion with a tin source. However, as this contained only small quantities of tin, a spectrum with a low signal to noise ratio resulted. A large velocity range was required to scan the energies of the observed lines and this was not attainable with the vibrators used. It was therefore necessary to change both the source and the detector to carry out a calibration measurement. In order to quote the centre shift relative to an appropriate tin compound several spectra of the source material, $CaSnO_3$, were recorded and then the centre shift of this absorption line relative to iron (0.113 mms^{-1}) was subtracted from the

measured shift of each subsequent tin spectrum. Hence the centre shifts are quoted relative to calcium stannate at room temperature.

4.4.2 Computer Fitting of Spectra - Data Analysis

The data file of counts collected from the spectrometer box and stored on a disk was transferred to the UNIX system where it could be analysed. To obtain the Mössbauer parameters (centre shift, quadrupole splitting, linewidth and relative absorption area) of a particular spectrum it was necessary for a calculated spectrum to be produced which "matched" the experimental data.

If an initial set of values for the parameters was set, then the main program evaluated the counts per channel and generated a theoretical Mössbauer spectrum. This process was repeated for however many components existed in any one spectrum (i.e. when different sites existed for the tin atoms). When this spectrum had been calculated it was passed to a second core program which referred to a NAG minimisation routine. The parameters were then varied incrementally to achieve the best fit to the experimental spectrum. This should have occurred when the χ^2 parameter was minimised over all channels. This measure of "goodness of fit" is given by

$$\chi^2 = \frac{\sum_i \frac{(E_i - Th_i)^2}{\sqrt{E_i}}}{(n_i - n_f)} \qquad (4.1)$$

where n_i is the total number of channels, n_f is the number of variable parameters and $E_i - Th_i$ is the difference between the experimental and the theoretical spectrum.

A value of χ^2 close to unity resulted when there was a low signal to noise ratio and therefore this was only used to compare fitted spectra with similar signal to noise ratios.

The program used to fit the single line or quadrupole split doublet tin spectra, called Ffita, produced a theoretical spectrum of Lorentzian lines. Each Mössbauer parameter could be fixed or allowed to vary. With more than one tin site present in the material, the area of one component was fixed to equal one, whilst the areas of the other components were allowed to vary. Hence the relative area of each absorption line could be calculated.

Chapter 5 A Mössbauer Study of the Binary Tin Oxide-Silica Glass System

5.1 Introduction

Before considering the complex float glass system, the simplest glass containing tin, i.e. SnO-SiO_2, was studied. Previous work on similar glasses was mentioned in chapter 2. The binary glass samples were prepared at the University of Warwick by Dr. M.M. Karim as described in chapter 1.

The powdered glass was weighed to produce the appropriate thickness and this was mixed with boron nitride. The powder was held in a plastic sample holder and Mössbauer spectra were recorded in transmission geometry over a range of temperatures from 10 K to about 300 K. Preliminary results were recorded at room temperature, but as the recoil-free fraction was low at this temperature the measurements were repeated at liquid nitrogen temperature to compare glasses of different composition.

5.2 Characteristics of the Mössbauer Spectra

In all the SnO-SiO_2 glass samples the tin was found to exist predominantly in the 2+ state. The chemical shift and quadrupole splitting of each spectrum were greater than those measured for crystalline tin oxide. The spectrum of the 40.9 mol.% SnO sample is compared to that obtained for black stannous oxide in figure 5.1, and their Mössbauer parameters at 77 K are listed in table 5.1. The linewidth measured for all the glasses was also greater than that of SnO, which is commonly the case for amorphous materials. An improved fit to the spectra and a corresponding lower chi-squared could be obtained if two components were used to represent two Sn^{2+} sites with different chemical shifts and

quadrupole splittings. The spectrum fitted this way is shown in figure 5.1(c). Although the linewidths could be reduced to values close to that found for the crystalline oxide (~ 0.9 mms^{-1}), it was not possible to consistently fit each spectrum in this way. Therefore, with a few exceptions, just one component was fitted to the Sn^{2+} doublet.

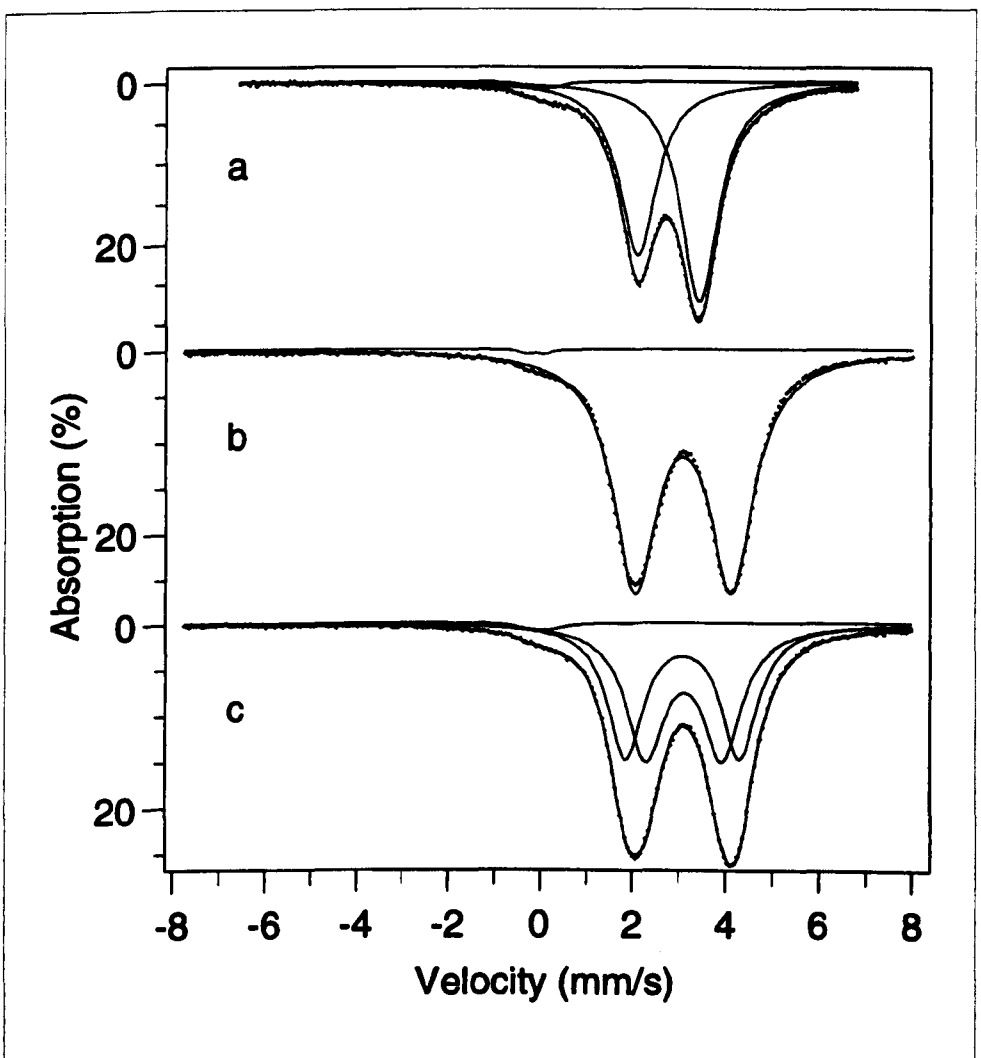

Figure 5.1 Mössbauer spectra of (a) crystalline SnO and (b) and (c) 40.9 mol.% SnO binary glass.

Table 5.1

Absorber	Chemical Shift (δ) mms^{-1}	Quadrupole Splitting (Δ) mms^{-1}	Linewidth (Γ) mms^{-1}
Crystalline SnO	2.767 ± 0.0006	1.327 ± 0.0006	0.975 ± 0.002
40.9 mol.% SnO-SiO_2 glass	3.092 ± 0.001	2.070 ± 0.001	1.153 ± 0.001
	3.080 ± 0.001	2.452 ± 0.001	0.930 ± 0.008
	3.110 ± 0.001	1.648 ± 0.001	1.008 ± 0.007

5.2.1 Effect of Tin Concentration

The glass samples were analysed at Warwick University and the tin concentrations (ranging from 16.8 mol.% to 71.5 mol.% SnO) and other physical properties are shown in table 5.2. The variations of density and molar volume with tin concentration are plotted in figure 5.2. The decrease of volume V with concentration c is given by $\partial(\ln V)/\partial c = -(0.16 \pm 0.11)\ mol^{-1}$.

Table 5.2

Nominal SnO content (mol.%)	Analysed Composition (mol.%) ±3%		Density $\times 10^3$ ($kg\ m^{-3}$)	Molar Volume $\times 10^{-6}$ ($m^3\ mol^{-1}$)	Expansivity $\alpha \times 10^7$ (K^{-1}) (303 - 673K)
	SnO	SiO_2			
0	0	100	2.20	27.31	5.7
20.0	16.8	83.2	2.678	27.12	25.8
32.0	28.2	71.8	3.081	26.33	-
33	29.6	70.4	3.116	26.37	44.1
40.0	32.6	67.4	3.318	25.44	42.5
47.2	39.7	60.3	3.579	25.06	-
50.0	40.9	59.1	3.738	24.24	43.9
60.0	49.4	50.6	3.864	25.09	50.1
65.0	53.5	46.5	3.955	25.28	53.2
70.0	55.4	44.6	4.065	24.95	54.1
75.0	64.0	36.0	4.391	24.56	61.6
80.0	71.5	28.5	4.538	24.99	-

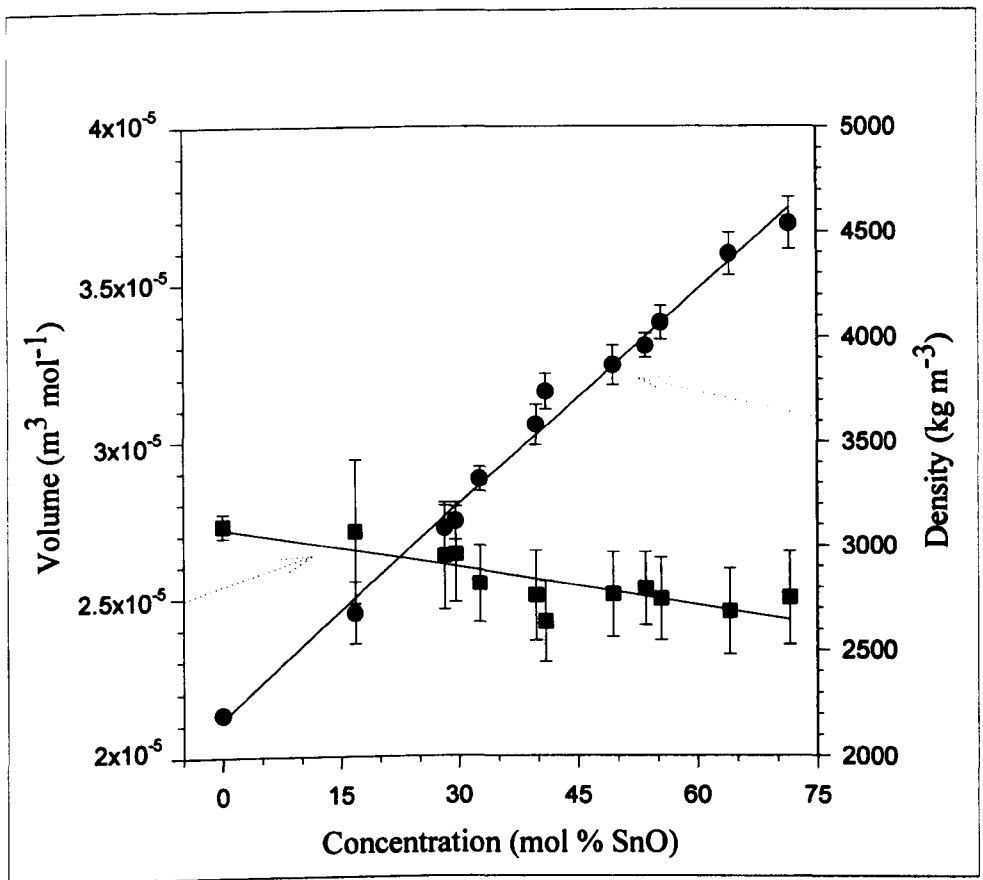

Figure 5.2 Variation of density and molar volume with tin concentration.

5.2.2 Dependence of the Mössbauer Parameters on Concentration

Mössbauer spectra of all the glasses were recorded at 77 K and these are shown in figure 5.3. A small amount of Sn^{4+} could be seen in each of the spectra and therefore two components were fitted; one to the doublet corresponding to Sn^{2+} and one to the unresolved quadrupole split peak of the Sn^{4+}.

The measured chemical shifts and quadrupole splittings are plotted against tin concentration in figure 5.4. Both quantities decreased with increasing concentration. The broad linewidths arose from a distribution of chemical shifts and quadrupole splittings corresponding to a random distribution of tin sites in the glass. The observed asymmetry,

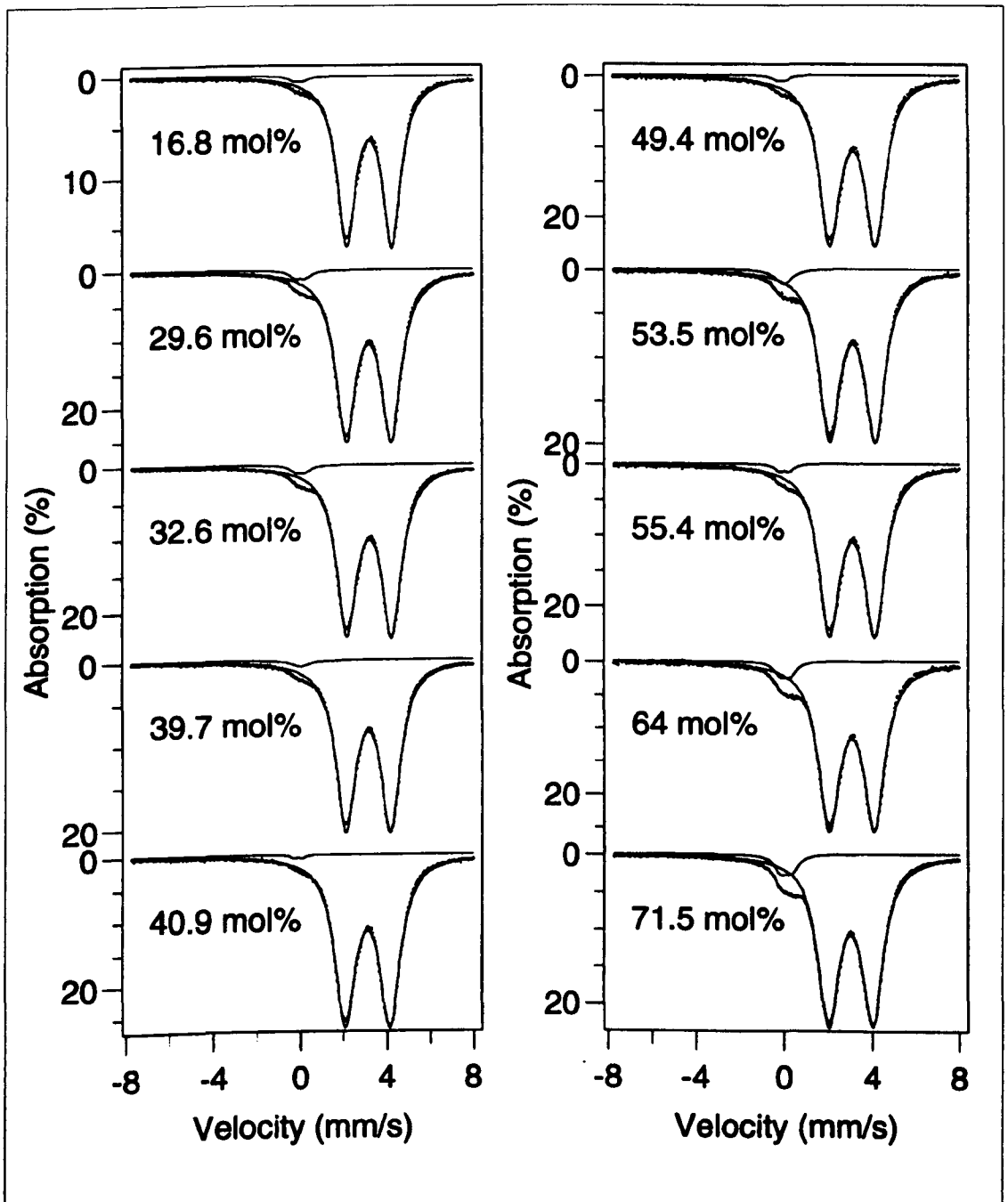

Figure 5.3 Mössbauer spectra of each concentration of the binary SnO-SiO$_2$ glasses at ~77 K.

however, may not have arisen solely because of this reason. The variation of the chemical shift and quadrupole splitting was therefore considered as follows. Both these parameters decreased with increasing tin concentration, so if a range of values was present in one sample, then the higher energy line would be broader and have a correspondingly smaller

absorption depth. The spectra show that there is an unequal intensity of the quadrupole split lines, but that the larger intensity occurred for the higher energy line. This therefore suggests that the different intensities were caused by an anisotropy of the f-factor i.e. the Gol'danskii-Karyagin effect. [49]

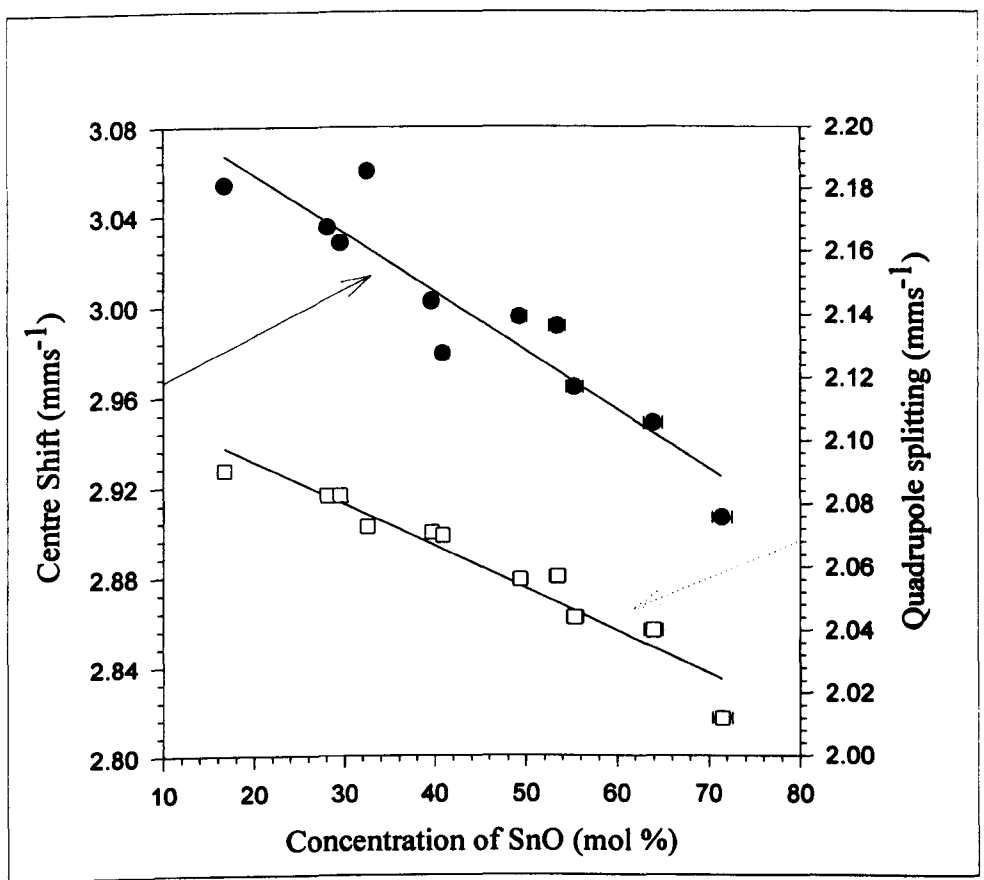

Figure 5.4 Variation of the average centre (chemical) shift (●) and quadrupole splitting (□) with SnO concentration.

As discussed in chapters 2 and 3, the decrease in the chemical shift (as the tin content increased) corresponds to a decrease in the electron density at the nuclei. The decrease in quadrupole splitting suggests that there is decreasing distortion around the tin atoms as the concentration increases and a reduction in the p electrons associated with the tin atoms. A decrease in chemical shift would be consistent with increased covalency in the glasses as the amount of SnO increases. The changes in the shifts and splittings

with concentration, c, according to a least-squares fit to the data were found to be $\frac{\partial \delta}{\partial c} = -(0.277 \pm 0.009)\ mms^{-1}mol^{-1}$ and $\frac{\partial \Delta}{\partial c} = -(0.135 \pm 0.009)\ mms^{-1}mol^{-1}$. The change in chemical shift with concentration is discussed further in section 5.4.

5.3 Temperature Dependence of Mössbauer Spectra

Mössbauer spectra of two of the binary glass samples were recorded over a temperature range between 10 K and 300 K. The spectra of the 32.6 mol.% SnO sample and the 53.5 mol.% SnO glass at different temperatures are shown in figures 5.5 and 5.6 respectively.

The spectra were fitted in two ways; by two doublets as described above and also by representing the asymmetry of the Sn^{2+} doublet with two single Lorentzian lines of different intensities but equal linewidths. The second method showed that the areas of the two single lines became more equal as the temperature decreased, (figure 5.7), which was consistent with the Gol'danskii-Karyagin effect, (see 3.4.2).

5.3.1 Variation of the Recoil-Free Fraction

From the two component computer fits to the spectra, it was possible to calculate the absorption area of the Sn^{2+} and Sn^{4+} lines. As the f-factor is proprtional to the area then this was also estimated. The small quantity of Sn^{4+} present in each of the glass samples introduced a large error into the area calculated and therefore these results were not pursued. The area of the Sn^{2+} absorption lines was found to increase at lower temperatures.

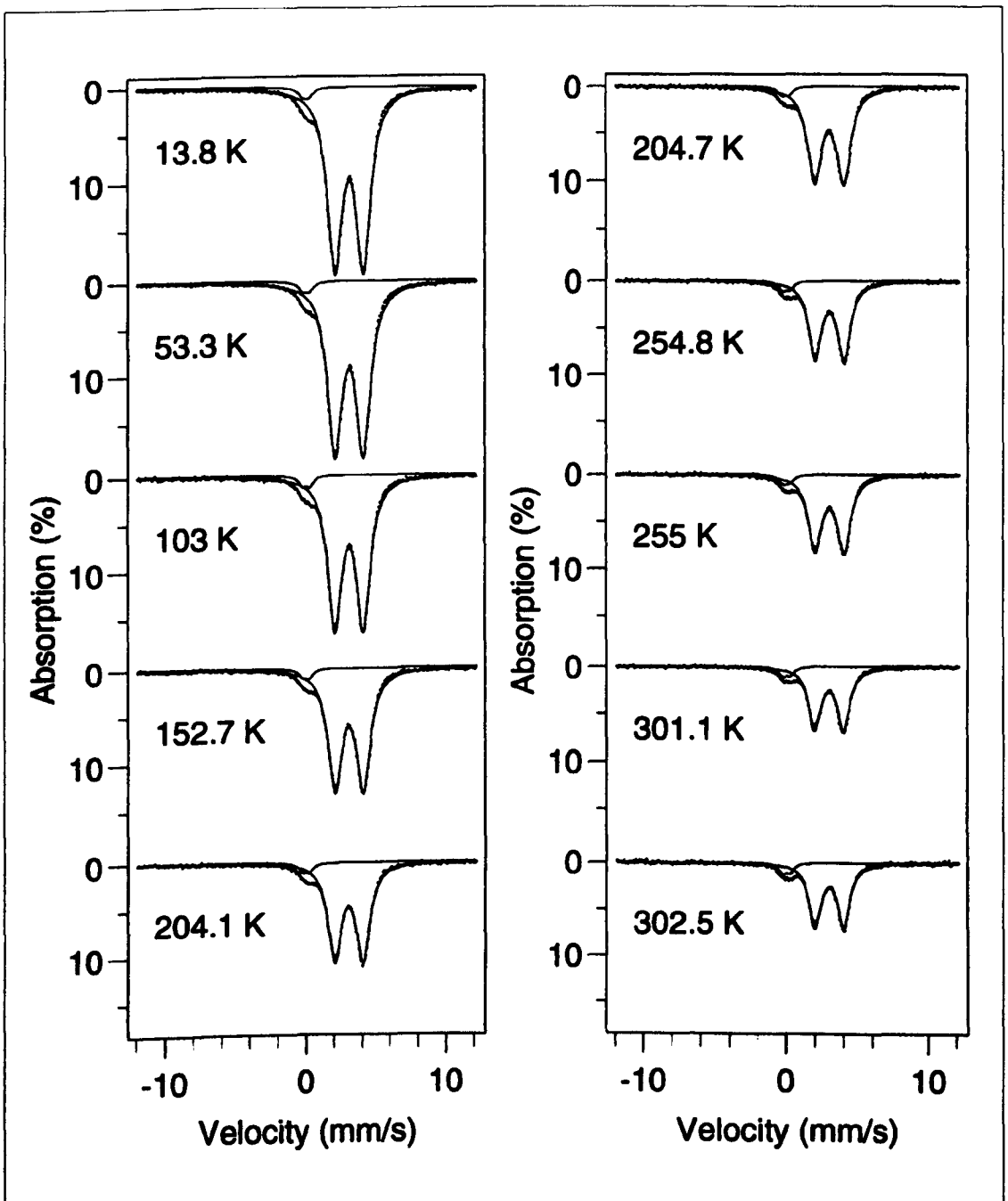

Figure 5.5 Mössbauer spectra of the 53.3 mol.% SnO glass between 13.8 K and 302.5 K.

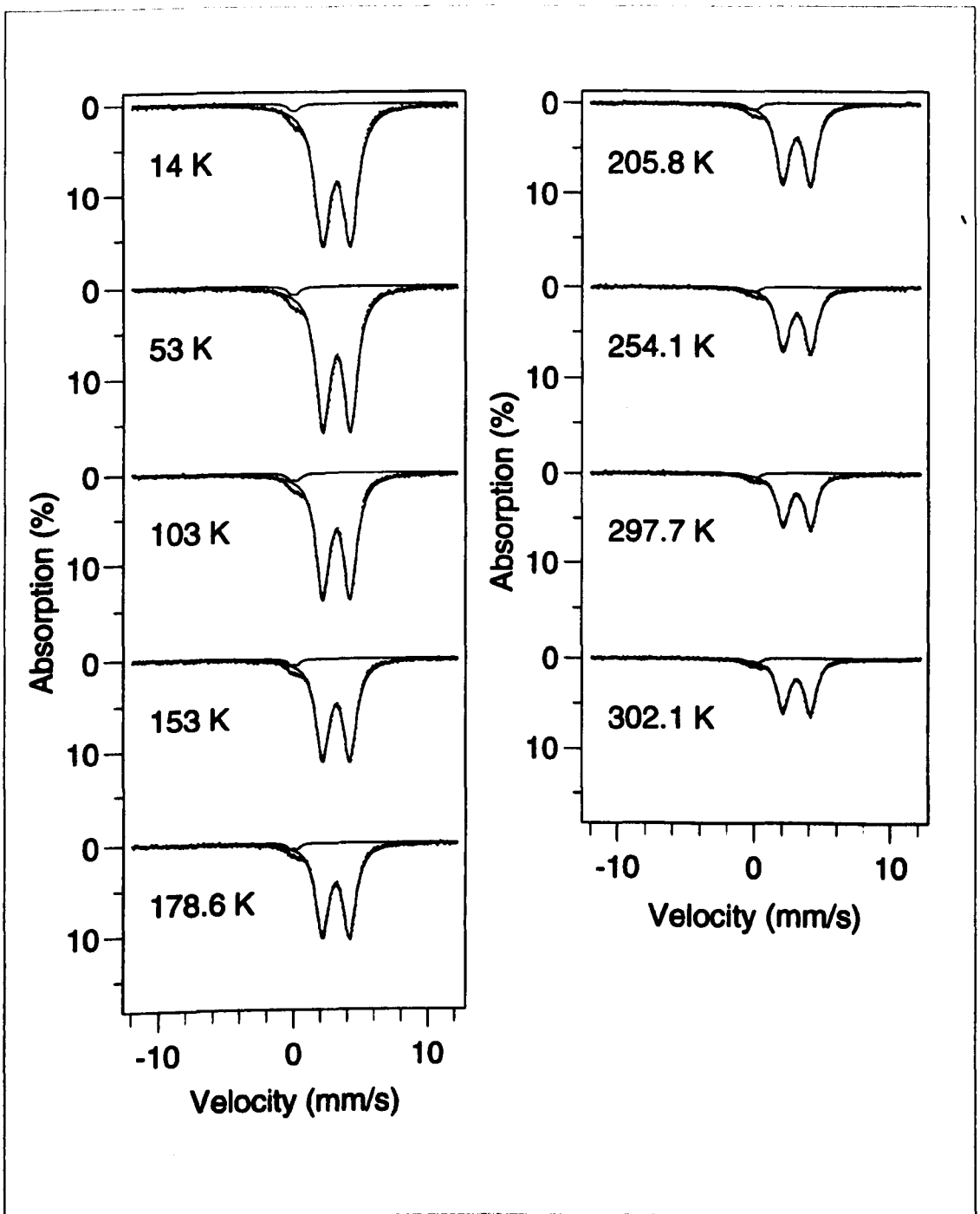

Figure 5.6 Mössbauer spectra of the 32.6 mol.% SnO glass between 14 K and 302 K.

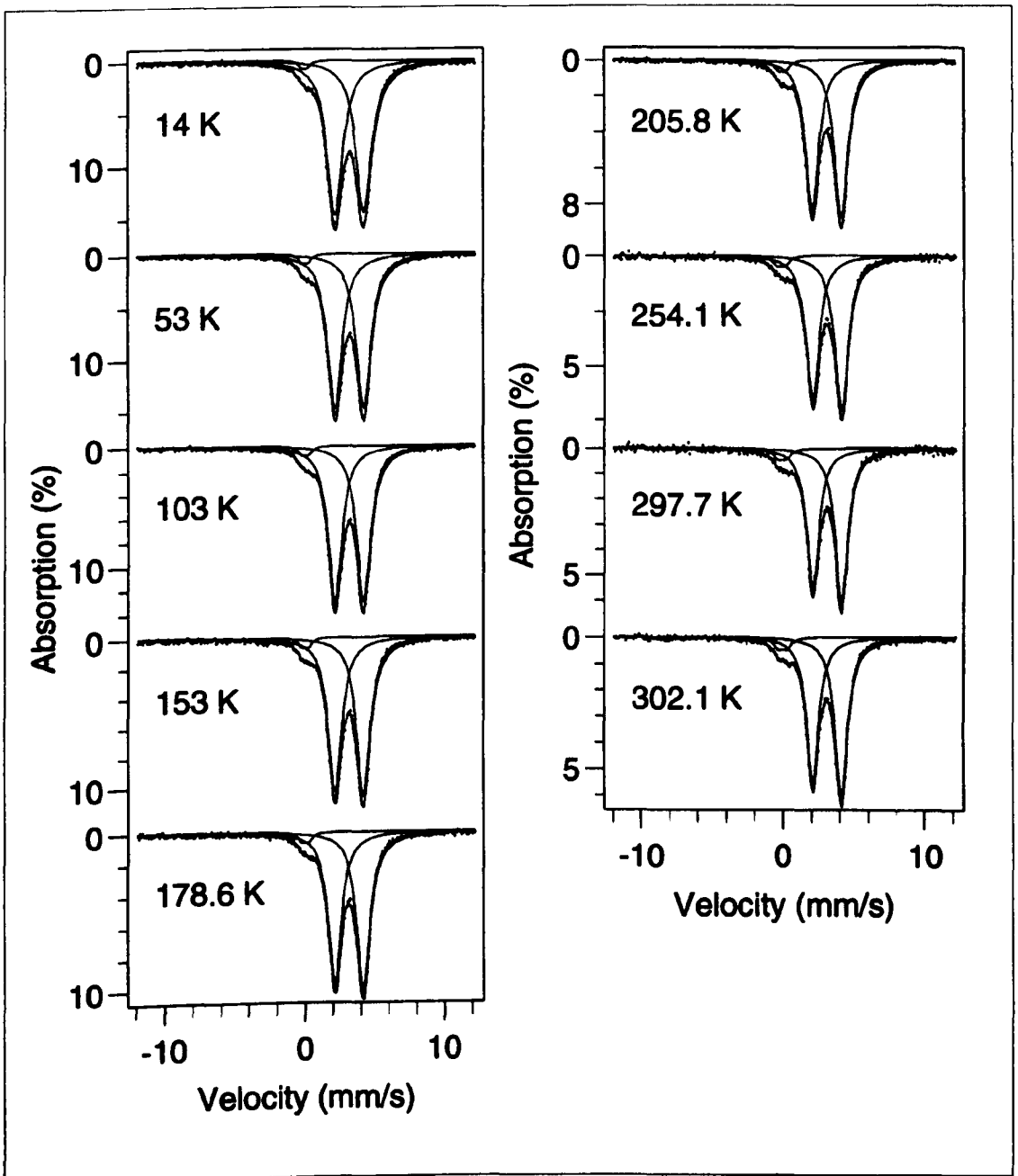

Figure 5.7 Mössbauer spectra of the 32.6 mol.% SnO glass between 14 K and 302 K with the Sn^{2+} asymmetrical doublet fitted with 2 components of equal linewidth but different absorption areas.

The dependence of the absorption area on temperature was initially plotted and this curve was used to produce a plot of ln(f) against temperature. The absorption area incorporated factors such as a dependence upon the concentration of tin present. These could be eliminated if the data points were shifted so that the line through the high temperature

points was extrapolated back to pass through zero on the ln(area) axis (as described in appendix I). The high temperature slope remains the same and could be used to determine the Debye temperature of the tin in the glass. The data is plotted in figure 5.8 as well as the curves obtained from the Debye model.

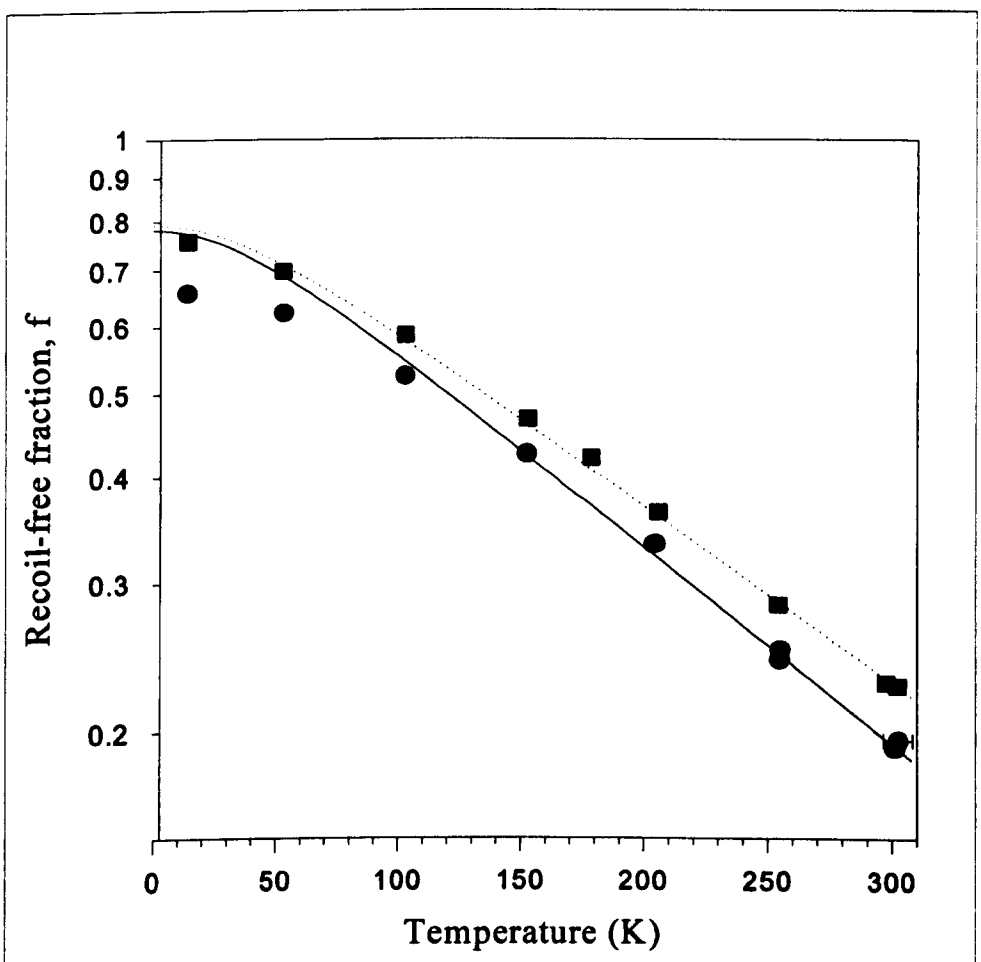

Figure 5.8 Temperature variation of the f-factor for the 32.6 mol.% (■) and the 53.5 mol.% (●) SnO glasses with the curves corresponding to θ_D=191 K and 181 K respectively.

5.3.2 The Debye Model and Debye Temperature

The variation of the f-factor according to the Debye model was given in equation 3.3. At high temperatures, i.e. $T \geq \theta_D/2$, the expression reduces to $\ln f = \frac{-6E_R T}{k\theta_D^2}$ where

E_R is the ^{119}Sn γ-ray recoil energy equal to 2.572×10^{-3} eV, k is Boltzmann's constant and θ_D is the Debye temperature. The slope $\partial(\ln f)/\partial T$ may be used to estimate θ_D and the results give values of 191 K and 181 K for the 32.6 mol.% and the 53.5 mol.% samples respectively. The differences can be seen in figure 5.8. The results are lower than that found for crystalline SnO, i.e. 204 K, and this is discussed further in chapter 8.

5.3.3 Temperature Dependence of the Centre Shift

The variation of the centre shift with temperature includes a small temperature dependence of the chemical shift but is mostly caused by the second order Doppler shift which is described in section 3.4.1. The expression for the contribution to the centre shift by the S.O.D.S. according to the Debye model was given in equation 3.9.

The centre shift is plotted against temperature for the two glass samples in figure 5.9. The line through the data points could not be completely described by the second order Doppler shift. In the Debye model the high temperature region is given by $\delta = \frac{-3kT}{2Mc}$, i.e. it is independent of θ_D. The corresponding slope of the δ versus T line is -3.5×10^{-4} mms^{-1}. However, the calculated slope for each of the samples was found to be $\partial\delta/\partial T = (-2.80 \pm 0.10) \times 10^{-4}$ mms^{-1} K^{-1}. This implies that the temperature dependence of the chemical shift is given by $\partial\delta^{IS}/\partial T = (+0.70 \pm 0.1) \times 10^{-4}$ mms^{-1} K^{-1}. At low temperatures the intercept of the curve should provide an alternative value for the Debye temperature. This may be obtained from $\theta_D = \frac{16mc\delta_T}{9k}$ when T = 0, and gave 168 K and 153 K for the 32.6 mol.% and the 53.5 mol.% SnO glasses respectively. At high temperatures δ_T is proportional to the temperature of measurement and independent of θ_D, (from equation 3.9), but at low temperatures the shift is proportional to θ_D. In

determining the Debye temperature from measurements of the chemical shift at low temperatures, only phonons excited at these temperatures contribute. However, measurements of the recoil-free fraction were made over a wide range of temperatures, and a greater number of data points were obtained to determine θ_D by this method. The results obtained from the temperature dependence of ln(f) should therefore be more accurate. The quadrupole splitting also showed a dependence on temperature. This was calculated to be $\partial\Delta/\partial T = (-2.50 \pm 0.10) \times 10^{-4}$ mms^{-1} K^{-1}.

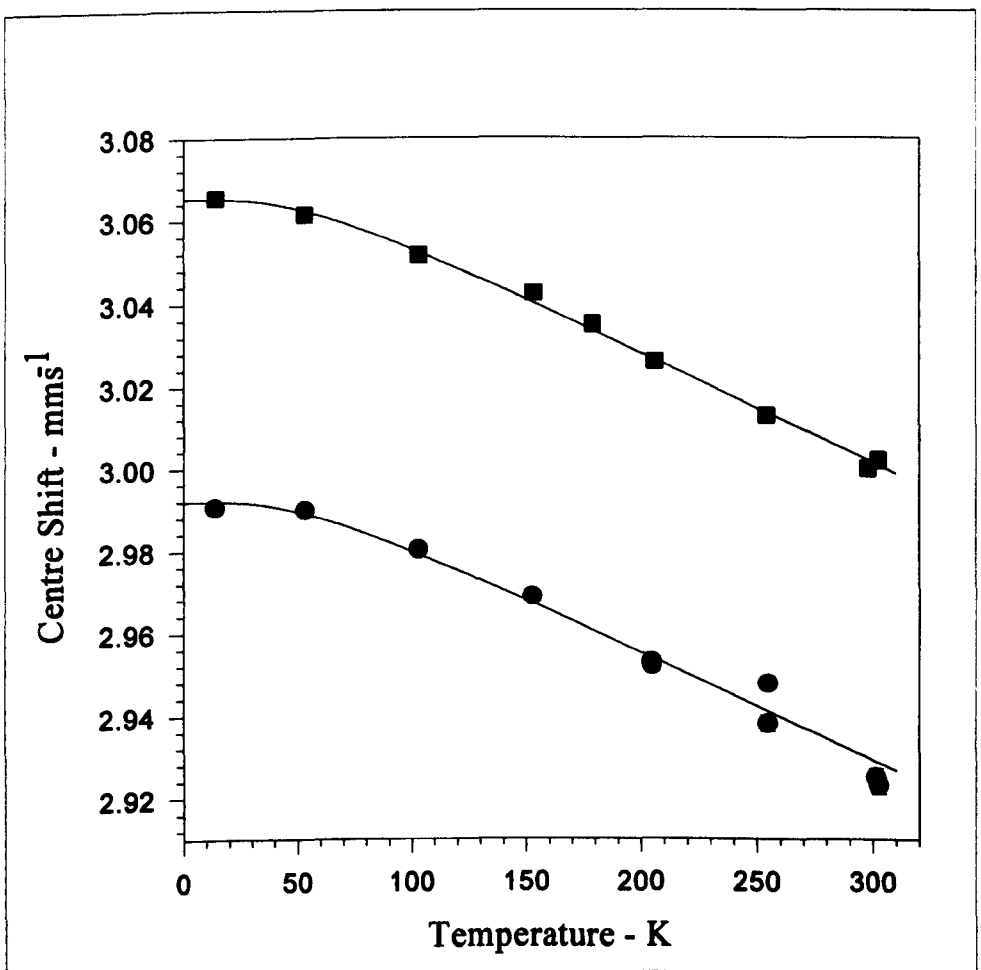

Figure 5.9 Temperature variation of the centre shift for the 32.6 mol.% (■) and the 53.5 mol.% (●) SnO glasses with the curve corresponding to the measured Debye temperatures.

5.4 Dependence of the Mössbauer Spectra on Volume

The chemical shift changed as both the concentration of tin in the glasses was varied and at the different temperatures of measurement. The molar volume decreased as the concentration increased as shown in figure 5.2. Similarly a change in molar volume could be related to the increase in electron density at the nuclei as the temperature increased. Assuming the dependence on volume to be related to thermal expansion, then the two observed changes in chemical shift may be connected by

$$\frac{\partial \delta^{IS}}{\partial T} = \beta \frac{\partial \delta^{IS}}{\partial c} / \frac{\partial \ln V}{\partial c} \qquad (5.1)$$

The volume expansivity β may be calculated from 3α, and α is given in table 5.2. Thus from the calculated results of $\partial \ln V/\partial c$ and $\partial \delta^{IS}/\partial T$ a value for $\partial \delta^{IS}/\partial c$ of (-0.74 ± 0.51) mms^{-1} mol^{-1} was obtained. This differed from the measured result of -0.277 mms^{-1} mol^{-1} quoted above and suggested that a correction to the chemical shift dependence on concentration was necessary. Allowing for this correction, the change of chemical shift with concentration instead became $\left(\frac{\partial \delta^{IS}}{\partial c}\right)_{corr^d} = (+0.46 \pm 0.51)\, mms^{-1} mol^{-1}$, i.e. it increased with concentration.

5.5 Effect of Heat Treatment

Three of the binary glass samples underwent a series of heat treatments to study the changes which occurred. These treatments and D.T.A. measurements were carried out by Dr. Karim at Warwick University. The production of a crystal phase upon heating was reported by Carbó-Nóver and Williamson [10] and this was mentioned in chapter 2.

5.5.1 Heat Treatment Conditions

The heat treatment temperatures were chosen using information provided by D.T.A. traces obtained in air. The 40.9 mol.%, 49.4 mol.% and 55.4 mol.% SnO glasses were heated. The D.T.A trace for the 40.9 mol.% sample (figure 5.10) shows crystallisation, decomposition and oxidation at ~660°C, ~740°C and ~780°C respectively.

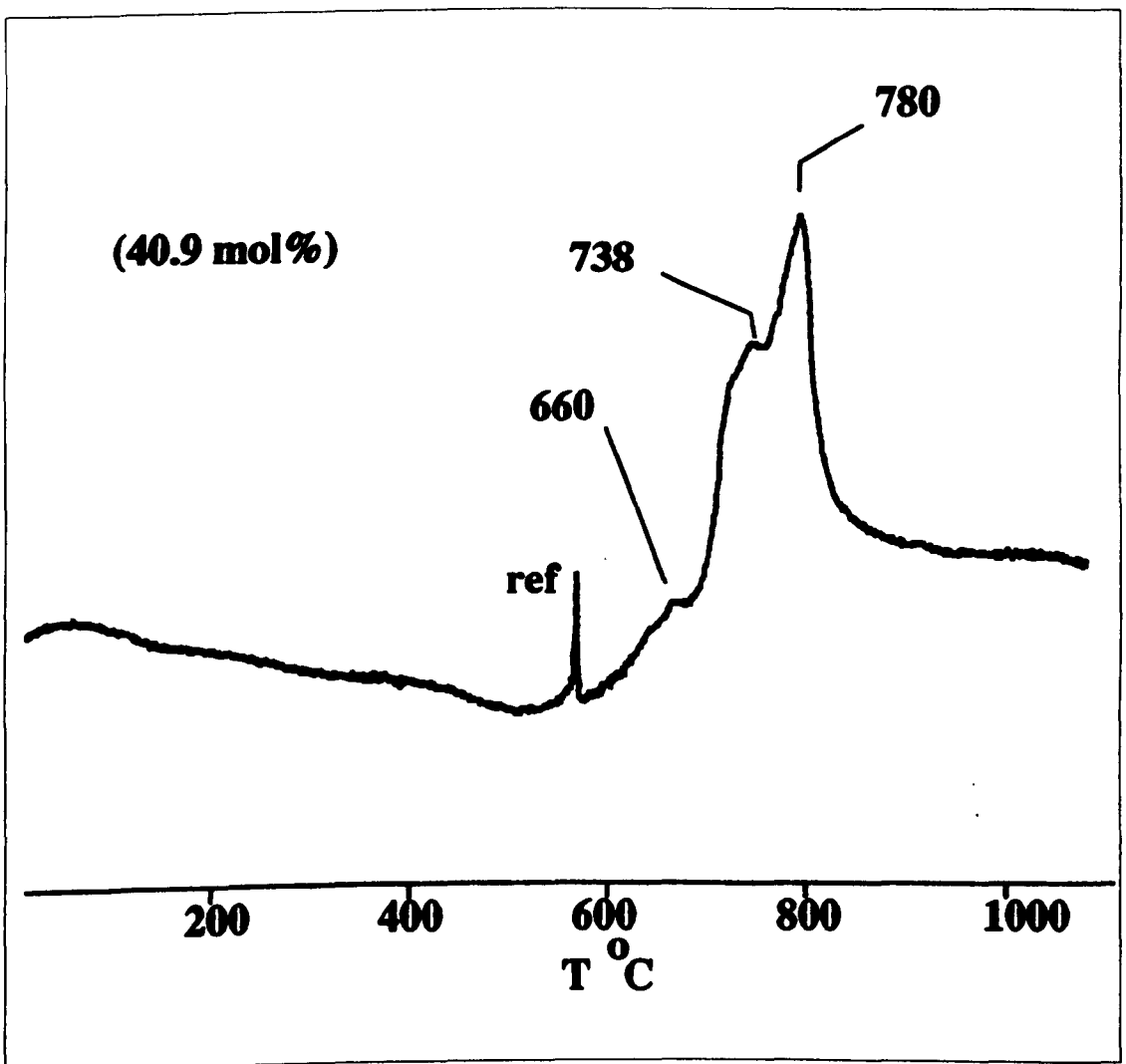

Figure 5.10 D.T.A. trace of the 40.9 mol.% SnO glass heated in air.

The chosen conditions were therefore (1b) 3 hours at 670°C, (1c) 4 hours at 730°C and (1d) 5 hours at 770°C. Similarly for the 49.4 mol.% glass, it was heated for (2b) 2 hours at 570°C, (2c) for 3 hours at 620°C, (2d) for 4 hours at 720°C and (2e) for 5 hours at

780°C. The 55.4 mol.% glass underwent heating for (3b) 2 hours at 570°C, (3c) for 3 hours at 620°C, (3d) for 4 hours at 720°C and (3e) for 5 hours at 780°C. These temperatures were chosen to reduce the chance of the next reaction occurring as the lengths of times of the treatments were considerable, (see figure 5.10).

One sample of each of the three different concentrations was also heated in a non-oxidative atmosphere of argon. These treatments were carried out at (1a) 600°C for 4 hours, (2a) 600°C for 4 hours and (3a) 590°C for 5 hours for the 40.9 mol.%, the 49.4 mol.% and the 55.4 mol.% SnO glasses. All resulting samples were analysed by x-ray diffraction and these spectra showed that crystallisation had occurred. SiO_2, SnO_2, SnO and $SnSiO_3$ were found to be present.

5.5.2 Mössbauer Spectra of Heat Treated Binary Glasses

Mössbauer spectra of the heat treated glasses were recorded at 77 K and are shown in figures 5.11 and 5.12. The results are given in table 5.3. The spectra of the samples heated in argon showed that there had been some change in the chemical shift and quadrupole splitting. No oxidation of Sn^{2+} to Sn^{4+} was seen.

The spectra of the glasses which were heated in air, however, showed that more changes had occurred, for example Sn^{4+} had been produced by oxidation. The amount of Sn^{4+} present increased as the temperature and time of heating was increased. It was possible to fit the Sn^{2+} absorption with two doublets of slightly different chemical shifts and different quadrupole splittings. The quadrupole splitting of about 1.3 mms^{-1} may correspond to the presence of crystalline SnO, whilst the larger quadrupole split doublet may incorporate both the Sn^{2+} of $SnSiO_3$ and any Sn^{2+} still present in the glass.

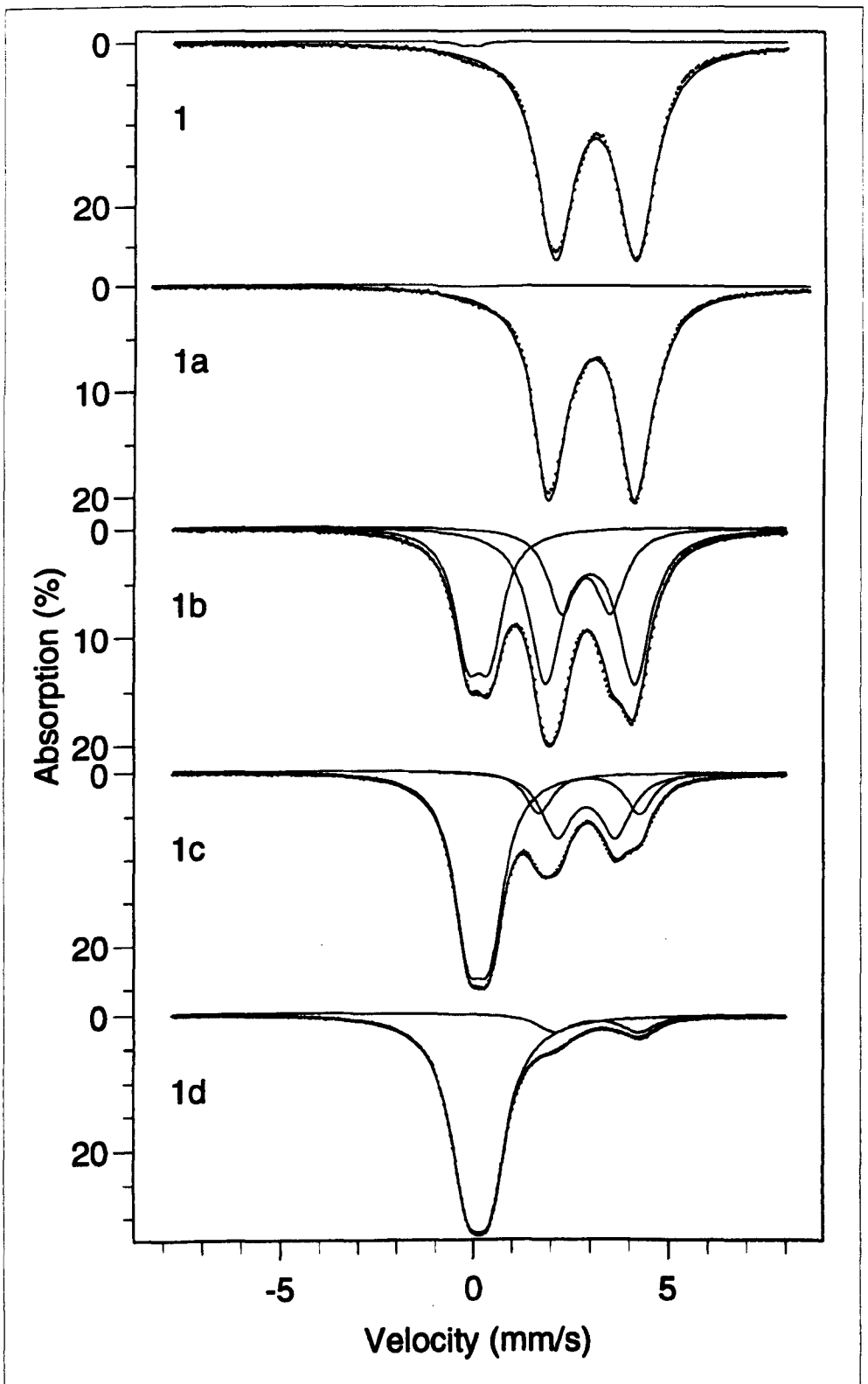

Figure 5.11 Mössbauer spectra at ~77 K of the 40.9 mol.% SnO glass (1) unheated, (1a) heat treated in argon for 4 hours at 600°C, when heat treated in air for (1b) 3 hours at 670°C, (1c) 4 hours at 730°C, (1d) 5 hours at 770°C.

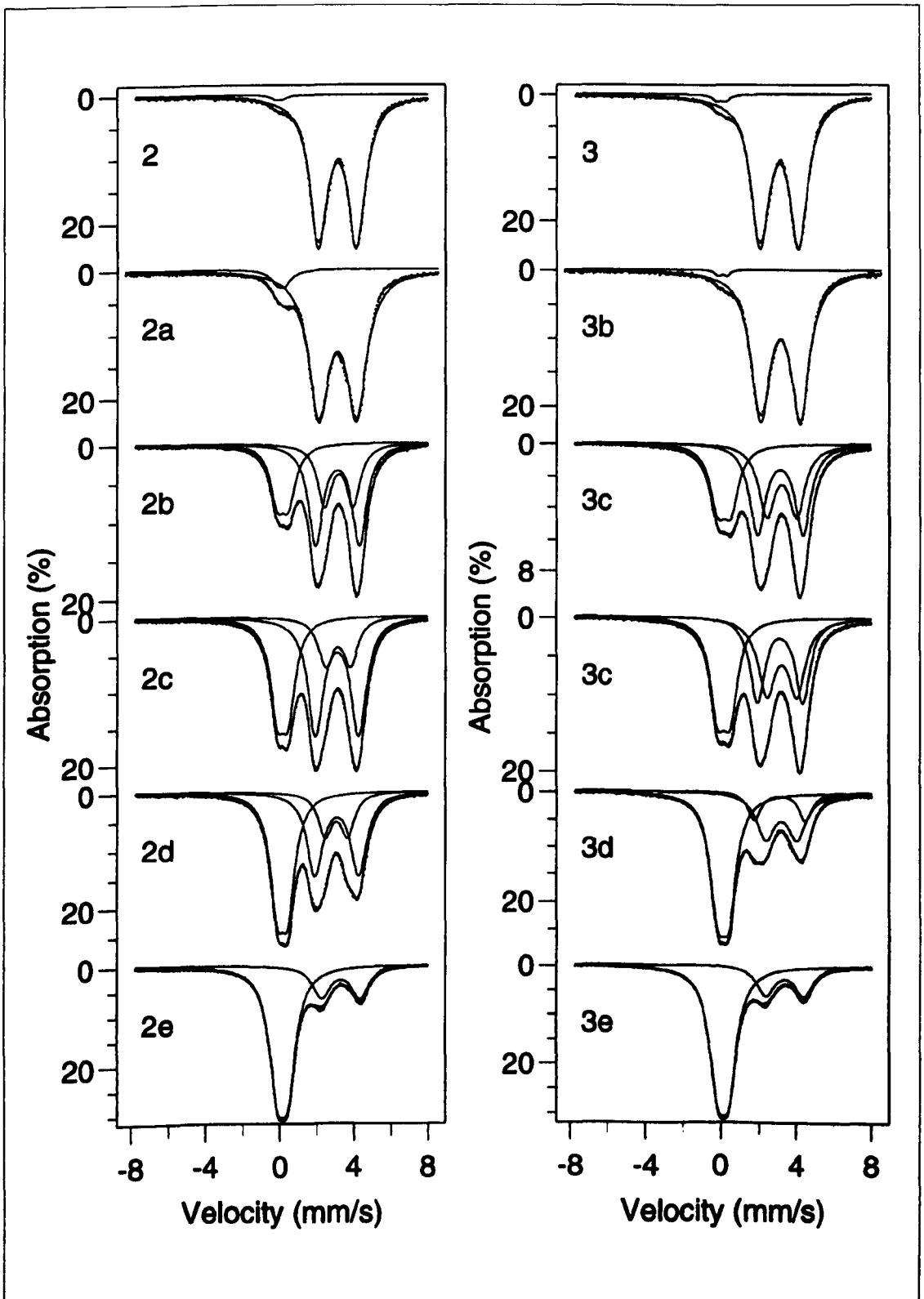

Figure 5.12 Mössbauer spectra at ~77 K of (2) the 49.4 mol.% SnO glass, before and after undergoing the heat treatments (2a) to (2e) described above, and of (3) the 55.4 mol.% SnO glass, before and after undergoing the heat treatments (3a) to (3e) described above.

Table 5.3

Glass Sample	δ_1 (mms^{-1})	Δ_1 (mms^{-1})	δ_2 (mms^{-1})	Δ_2 (mms^{-1})	δ_3 (mms^{-1})	Δ_3 (mms^{-1})
1	2.979	2.070	-	-	-	-
1a	2.926	2.203	-	-	-	-
1b	2.885	2.277	2.792	1.253	0.018	0.569
1c	2.871	2.584	2.799	1.500	0.030	0.563
1d	3.067	2.151	-	-	0.027	0.601
2	2.995	2.056	-	-	-	-
2a	3.000	2.027	-	-	-	-
2b	3.080	1.531	3.003	2.364	0.049	0.615
2c	3.039	1.340	2.982	2.325	0.032	0.599
2d	2.970	2.359	2.942	1.202	0.032	0.586
2e	3.182	2.062	-	-	0.030	0.597
3	2.965	2.044	-	-	-	-
3a	3.007	2.096	-	-	-	-
3b	3.094	1.582	3.009	2.401	0.064	0.685
3c	3.102	1.587	3.016	2.399	0.057	0.662
3d	3.073	1.658	2.996	2.701	0.035	0.596
3e	3.264	2.023	-	-	0.028	0.601

5.6 Conclusions

The correction applied to the chemical shift from the change in volume led to an increase in shift with tin concentration in the glasses. As this implies there was an increased electron density at the tin nuclei then it is possible to deduce that the tin

bonding became less covalent in the glass as its concentration increased. The decrease in the quadrupole splitting with increasing tin concentration (i.e. less p electrons at the tin sites), was consistent with a change in covalent character.

A greater Debye temperature of the tin was found for the lower concentration glass. This showed that the strength of binding was higher in the more covalently bonded SnO-SiO_2 glasses.

Chapter 6 A Mössbauer Study of Tin-Doped Float Composition Glass

6.1 Introduction

The preparation of these glass samples, as described in 1.4.2, provided two sets of samples. These will be referred to as the "alumina" samples and the "silica" samples as this indicates the different crucibles used in the preparation process. The alumina set contained considerably larger quantities of aluminium oxide and this led to noticeable differences in their Mössbauer spectra.

Mössbauer spectra of the twelve glasses of different compositions were recorded at 77 K in the nitrogen cryostat. The glasses with the highest percentage by weight of tin oxide in both the alumina and silica sets were used to compare the spectra at different temperatures. The flow cryostat was used for temperatures up to about 300 K and then further results were obtained up to 900 K with the glass samples held in the furnace.

6.2 Compositional Analysis and the Mössbauer Spectra

6.2.1 Chemical Analysis

The samples were chemically analysed (at Pilkington Technology Centre) and the full compositions are displayed in tables 6.1 and 6.2. Some of the results obtained from the Mössbauer spectra are also shown and this comparison is discussed in 6.4.

The percentage of stannous tin was found chemically by titration. The glass was dissolved in acid and the stannous ions are "replaced" by ferrous ions which then take part in the titration. [52] The total tin content was obtained by atomic absorption spectrophotometry. [53]

Table 6.1 Chemical Analysis of the "Alumina" Samples.

Sample / Oxide (Wt %)	2.5 %	5 %	7.5 %	10 %	12.5 %	15 %
SiO_2	66.4	59.2	54.5	58.0	56.7	54.9
Al_2O_3	8.5	15.6	20.8	13.2	12.6	13.0
Fe_2O_3	0.126	0.107	0.097	0.098	0.097	0.089
TiO_2	0.03	0.03	0.03	0.04	0.04	0.04
CaO	7.5	6.8	6.1	6.4	6.1	6.0
MgO	3.6	3.1	2.9	3.0	2.9	2.8
Na_2O	10.6	10.1	9.1	9.6	9.4	9.1
K_2O	0.5	0.5	0.4	0.5	0.5	0.4
SO_3	0.05	0.05	0.05	0.05	0.05	0.05
Tin oxide	2.7	4.6	6.1	9.2	11.7	13.7
% Sn^{2+} - Chemical	39	45	29	35	41	34
% Sn^{2+} - Mössbauer	31.9	42.8	28.6	34.0	40.3	34.1
SnO mol %	0.356	0.850	0.780	1.378	2.108	2.121
SnO_2 mol %	0.759	1.136	1.946	2.675	3.123	4.099

Table 6.2 Chemical Analysis of the "Silica" Samples.

Sample / Oxide (Wt %)	2.5 %	5 %	7.5 %	10 %	12.5 %	15 %
SiO_2	71.1	71.2	68.0	65.3	64.7	63.6
Al_2O_3	1.1	1.1	1.0	1.0	0.9	0.8
Fe_2O_3	0.125	0.120	0.109	0.098	0.108	0.097
TiO_2	0.04	0.03	0.03	0.04	0.04	0.04
CaO	8.0	7.8	7.4	7.2	7.0	6.9
MgO	3.9	3.8	3.6	3.5	3.5	3.3
Na_2O	12.0	11.8	11.1	10.8	10.4	10.3
K_2O	0.5	0.5	0.5	0.5	0.5	0.5
SO_3	0.19	0.16	0.05	0.06	0.03	0.04
Tin oxide	2.9	3.4	8.2	11.5	12.8	14.4
% Sn^{2+} - Chemical	5	5	33	28	37	48
% Sn^{2+} - Mössbauer	0	1.9	32.0	30.1	35.0	51.8
SnO mol %	0	0.026	1.086	1.460	1.955	3.229
SnO_2 mol %	1.160	1.340	2.310	3.398	3.506	3.004

The remaining compounds are all characteristic of float composition glass, i.e. predominantly a soda-lime-silica glass with small quantities of magnesium oxide, potassium oxide and ferric oxide. Aluminium oxide would normally be present at low levels of about 1%. The presence of up to 20% Al_2O_3 in the alumina samples arose because of contamination from the crucibles.

6.2.2 Mössbauer Spectra of the Alumina Contaminated Samples

Mössbauer spectra of each of these glasses, ranging in composition from 2.7 to 13.7 weight percent tin oxide, were initially recorded at room temperature and also at 77 K. The large temperature dependence of the f-factor was apparent from a comparison of the absorption in the spectra. The results obtained at liquid nitrogen temperature are shown in figure 6.1(a) and both Sn^{4+} and Sn^{2+} were seen to be present in each glass sample.

6.2.3 Mössbauer Spectra of the Alumina Free ("Silica") Samples

The spectra of the "silica" samples (from 2.9 to 14.4 weight percent tin oxide) showed some differences when compared to the alumina spectra (figure 6.1(b)). No Sn^{2+} doublet was found in the 2.9 wt% sample and a very small amount of Sn^{2+} (1.9% of the total tin) was detectable in the 3.4 wt% glass. Both the chemical shift and quadrupole splitting were consistently different and the linewidth was narrower than that measured for the alumina samples (0.91 - 0.99 mms^{-1} for the Sn^{2+} linewidth compared with 0.91 - 1.05 mms^{-1}, and 0.80 - 0.91 mms^{-1} compared with 0.80 - 0.98 mms^{-1} for Sn^{4+}).

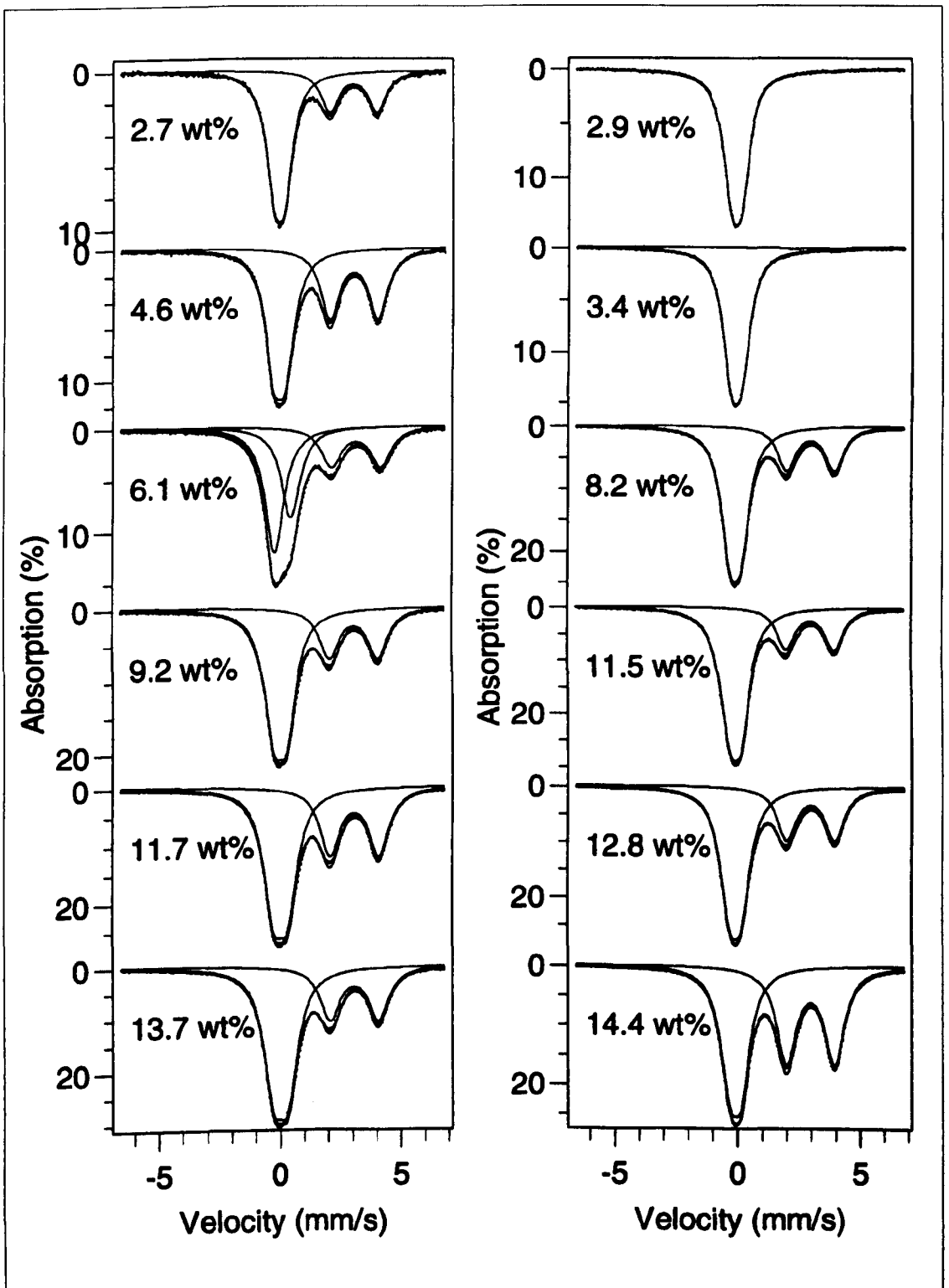

Figure 6.1 Mössbauer spectra recorded at ~77 K of (a) the "alumina" and (b) the "silica" tin-doped float composition glasses ranging nominally in concentration from 2.5 weight % to 15 weight % tin oxide.

6.3 Variation of the Hyperfine Parameters with Tin Concentration

The general trend in the chemical shift was to increase as the tin concentration increased. There was also an increase in the quadrupole splitting. However, an anomaly was apparent for the results of the alumina samples. The results are plotted in figure 6.2 for both the tin 4+ oxidation states, and the tin 2+ parameters are plotted in figure 6.3.

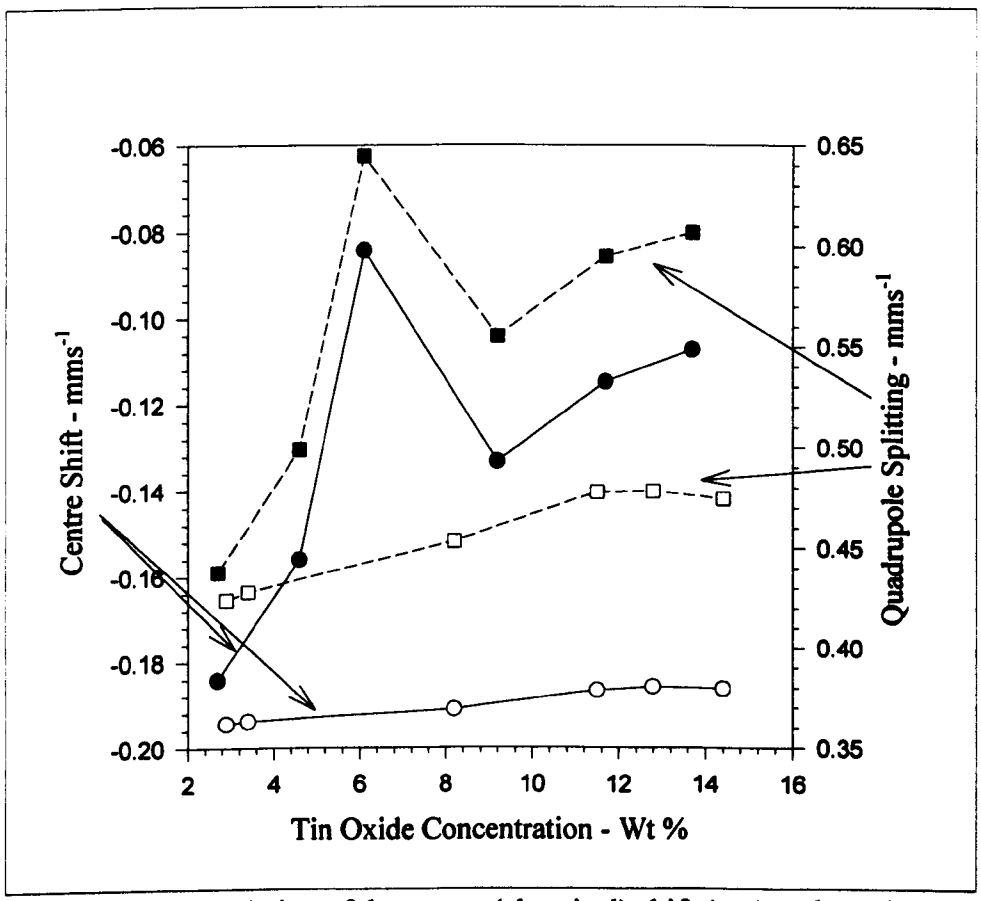

Figure 6.2 Variation of the centre (chemical) shift (●○) and quadrupole splitting (■□) of Sn^{4+} for the "alumina" (●■) and the "silica" (○□) samples.

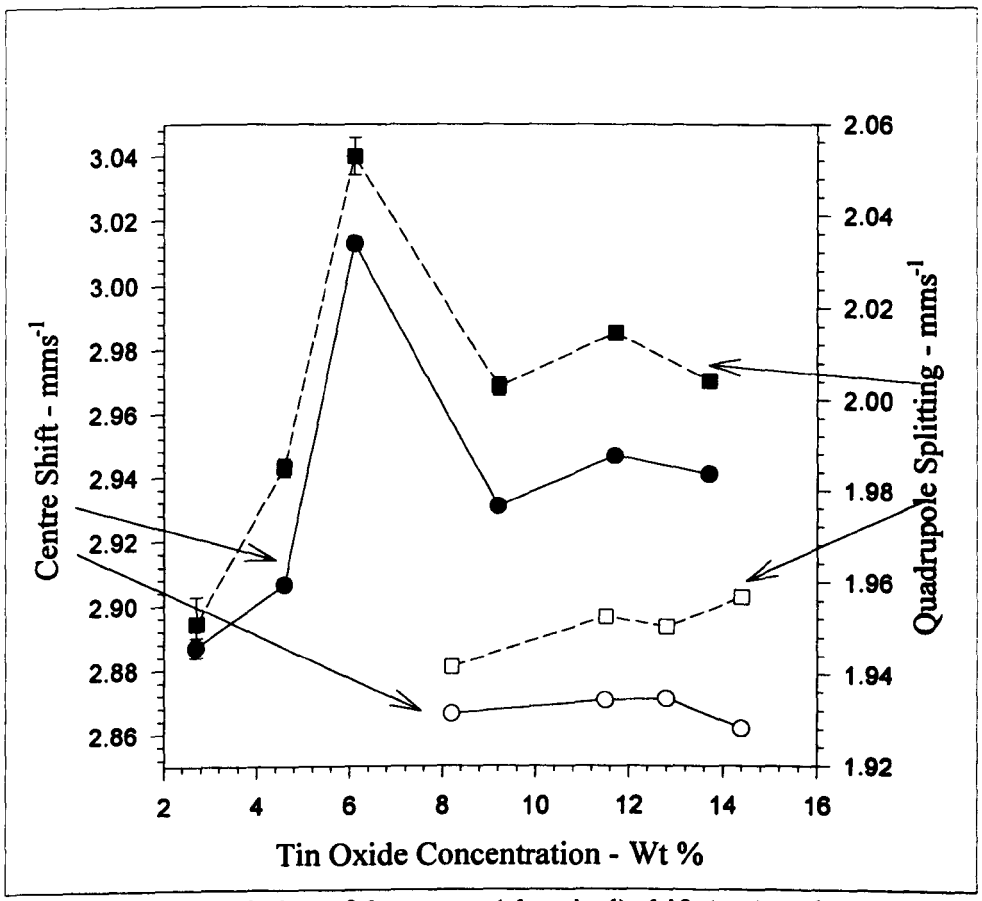

Figure 6.3 Variation of the centre (chemical) shift (●○) and quadrupole splitting (■□) of the Sn^{2+} for the "alumina" (●■) and the "silica" (○□) samples.

6.3.1 "Alumina" Glass Samples

The chemical shift and quadrupole splitting of the Sn^{4+} were seen to increase with tin concentration and the same general trends were observed for the Sn^{2+}. However, for the glass containing 6.1 wt% tin oxide, a large increase in both the chemical shifts and the quadrupole splittings were seen. These were even greater in each case than the corresponding value for the 13.7 wt% sample.

A possible explanation of the anomaly at 6.1 wt% tin oxide may be obtained from

the chemical compositions of the glasses. At this tin concentration the highest level of aluminium oxide occurs, i.e. 20.8 wt% Al_2O_3, whereas the other samples have an average of only about 12% alumina. Al_2O_3 is an intermediate and may either take part in the silica glass network or occupy the holes between SiO_4 tetrahedra. [54] In this case it appears to affect the resultant sites occupied by the tin ions such that they are in a more distorted environment (increased quadrupole splitting). The greater shift in the "alumina" samples suggests that the Sn^{4+} ions are situated in a more covalently bonded site whilst the Sn^{2+} ions would be more ionically bonded.

6.3.2 "Silica" Glass Samples

The chemical shift and quadrupole splitting of both the Sn^{4+} and Sn^{2+} showed little variation with tin concentration. A small increase in the quadrupole splitting as the amount of tin increases could be seen. The measured values were all lower than those recorded for the alumina samples.

A comparison of the chemical analysis of both sets of glasses shows that all quantities e.g. Na_2O, CaO, MgO, are similar except for the high concentration of Al_2O_3 and the corresponding difference in the weight percentage of silica in the glasses. The "silica" glasses should be closer to the composition of industrially produced float glass, except of course that the quantity of tin is greatly different. The small variation of hyperfine parameters for the silica samples reinforces the idea that the presence of the aluminium oxide is the reason for the observed differences in the "alumina" samples.

6.4 Comparison of Oxidation State Ratios

One of the aims of the analysis was to establish the relative abundance of the two tin oxidation states in the glasses with different tin concentrations. This could be estimated from the absorption areas of the Sn^{4+} and Sn^{2+} lines in the low temperature spectra. A more accurate result was obtained for the 15 wt % tin oxide samples from the variable temperature results (which are discussed in 6.5).

6.4.1 "Alumina" Samples

The percentage of tin existing as Sn^{2+} varied between 28.4% and 42.8%. There seems to be no relation between the ratio of the oxidation states and the total tin concentration. The percentage of Sn^{2+} is plotted in figure 6.4 and it is possible that the lower percentage of stannous ions in the 6.1% glass is again somehow due to the high alumina content.

6.4.2 "Silica" Samples

A general increase in the percentage of tin existing as Sn^{2+} in the glass was observed as the amount of tin increased (figure 6.4). In the absence of excess Al_2O_3 this increase may have been steeper as a limit to the solubility of Sn^{4+} ions in the glass was reached.

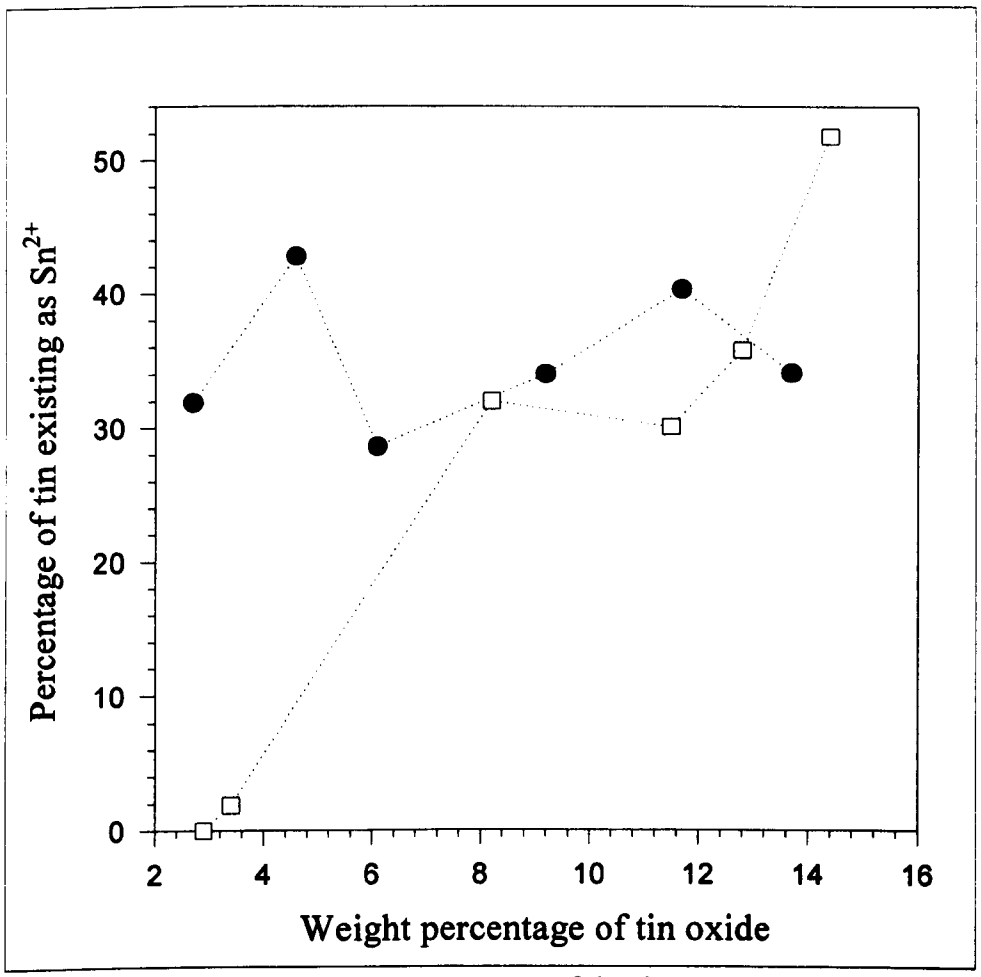

Figure 6.4 Variation of the percentage of the tin 2+ oxidation state with total tin oxide concentration for the "alumina" (●) glass samples and the "silica" (□) glass samples.

6.5 Variable Temperature Measurements

The spectra recorded over the temperature range from about 15 K to 900 K were used to measure the variation of the centre shift and the quadrupole splitting with temperature. A calculation of the temperature dependence of the f-factor was also made, as described in chapters 3 and 5, to obtain information on the strength of binding of the two tin oxidation states in the doped glasses.

6.5.1 The Mössbauer Hyperfine Parameters

The centre shift and quadrupole splitting of the Mössbauer spectra of both the alumina and silica samples showed a similar decrease in value with increasing temperature. The shifts of the Sn^{4+} components are plotted in figure 6.5, and also those of the Sn^{2+} components. A straight line fit to the high temperature region produced the slopes of $\partial\delta/\partial T$ which are given in table 6.3. The data for the variation of the quadrupole splitting with temperature for each set of samples is also shown in the table.

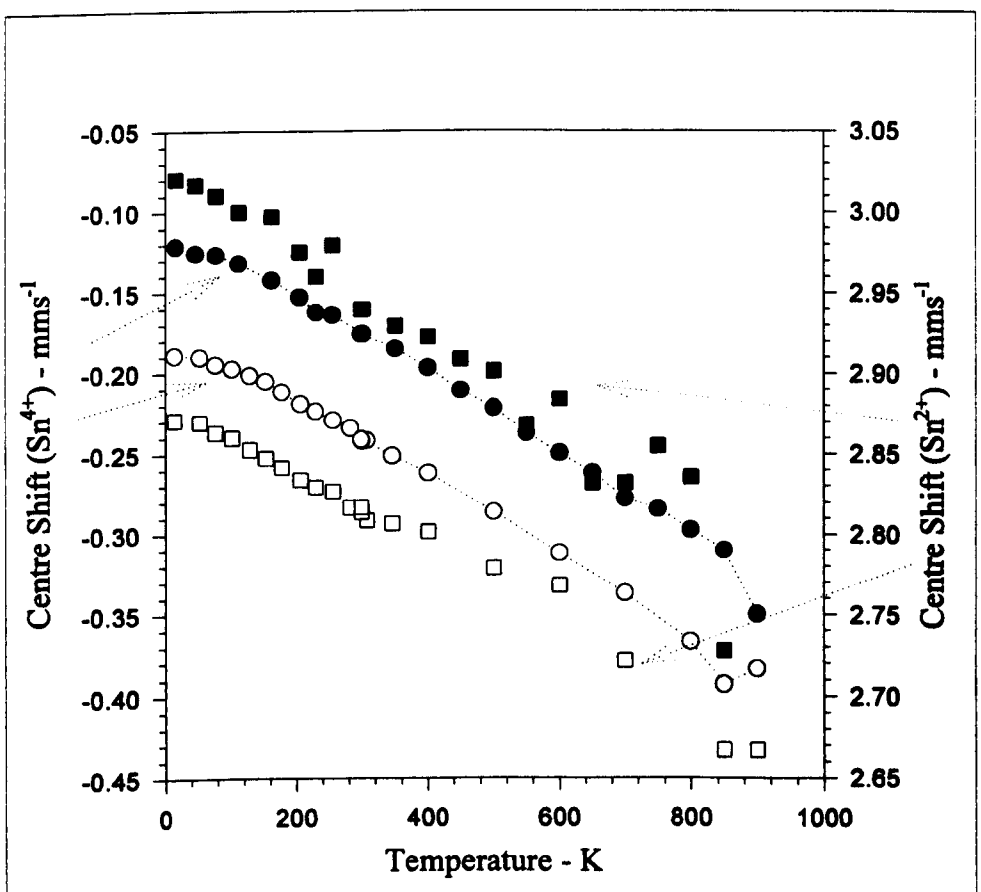

Figure 6.5 Temperature variation of the centre (chemical) shift for Sn^{4+} (●○) and Sn^{2+} (■□) for the "alumina" (●■) and the "silica" (○□) samples.

Table 6.3

Tin State / Slope		"Alumina"	"Silica"
Sn^{4+}	$\partial\delta/\partial T$	$(-2.447 \pm 0.05) \times 10^{-4}$	$(-2.446 \pm 0.01) \times 10^{-4}$
	$\delta_{T=0}$	(-0.090 ± 0.003)	(-0.1666 ± 0.0006)
	$\partial\Delta/\partial T$	$(-1.639 \pm 0.09) \times 10^{-4}$	$(-1.379 \pm 0.2) \times 10^{-4}$
	$\Delta_{T=0}$	(0.6771 ± 0.005)	(0.547 ± 0.007)
Sn^{2+}	$\partial\delta/\partial T$	$(-2.997 \pm 0.16) \times 10^{-4}$	$(-2.059 \pm 0.02) \times 10^{-4}$
	$\delta_{T=0}$	(3.017 ± 0.02)	(2.878 ± 0.0007)
	$\partial\Delta/\partial T$	$(-1.35 \pm 0.5) \times 10^{-4}$	$(-1.769 \pm 0.07) \times 10^{-4}$
	$\Delta_{T=0}$	(2.018 ± 0.02)	(1.959 ± 0.003)

6.5.2 Temperature Dependence of the f-factor

As described earlier (and detailed in appendix I), the dependence of the f-factor on temperature was calculated from the absorption areas of the fitted spectra. The large decrease in f for the Sn^{2+} component was particularly apparent at the high temperatures (~ 900 K), where the doublet was only just visible. The spectra recorded over the full temperature range are shown in figures 6.6 and 6.7 for the "alumina" and the "silica" samples respectively.

The resultant data for lnf versus temperature are plotted in figures 6.8 and 6.9. The curves obtained from a Debye model fit to the data are also shown. The Debye temperature of each oxidation state was calculated from the slopes of the high temperature straight line regions. From the graphs of ln(absorption area) against temperature, the intercepts of these lines gave the concentration of one oxidation state relative to the other, (as described in appendix I). The results, including the Debye

temperature, θ_D, which is given by $\theta_D = \sqrt{\frac{6E_R}{k[d(\ln A)/dT]}}$, are listed in table 6.4.

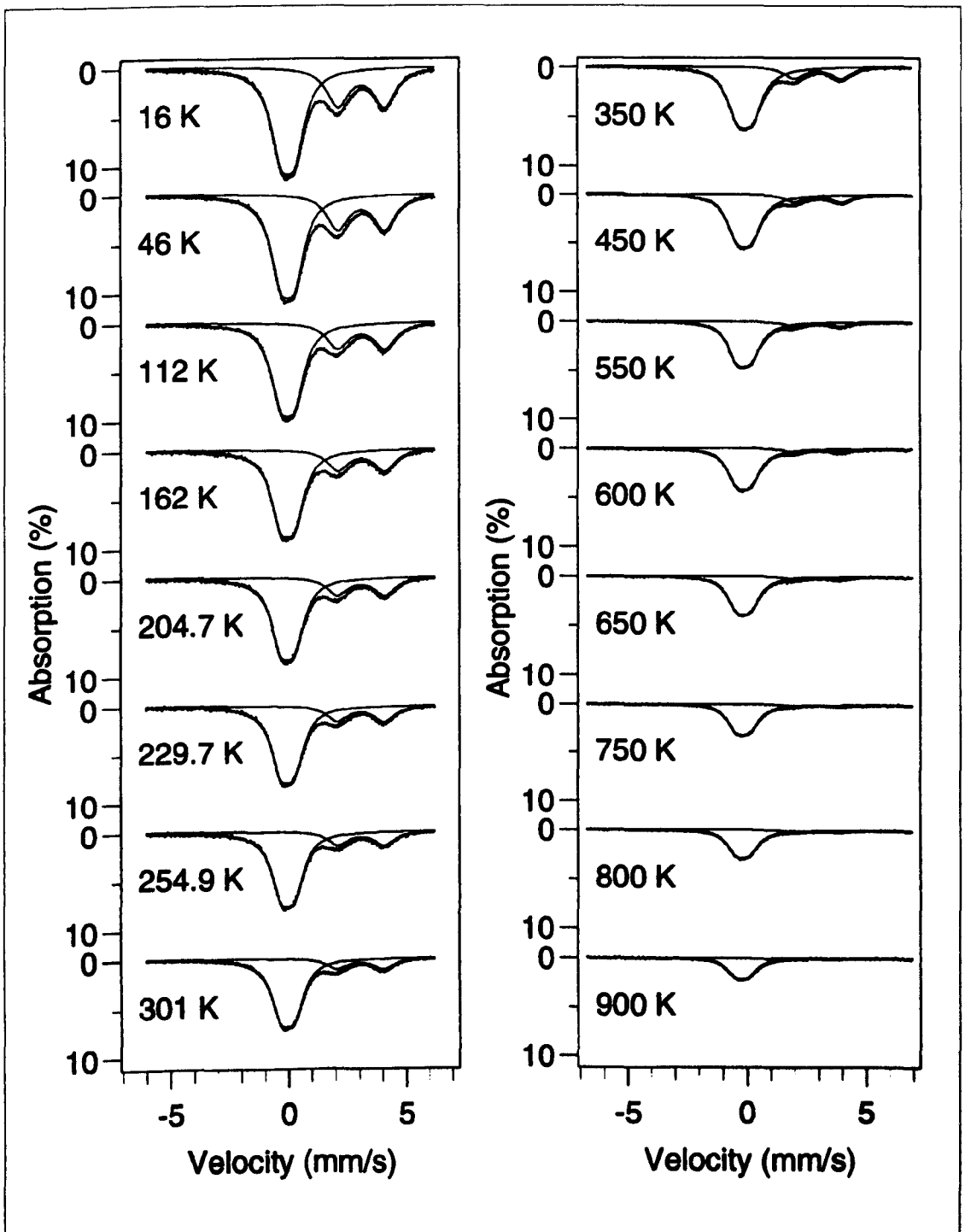

Figure 6.6 Mössbauer spectra of the 13.7 wt% tin oxide "alumina" doped-float glass sample recorded between 16 K and 900 K.

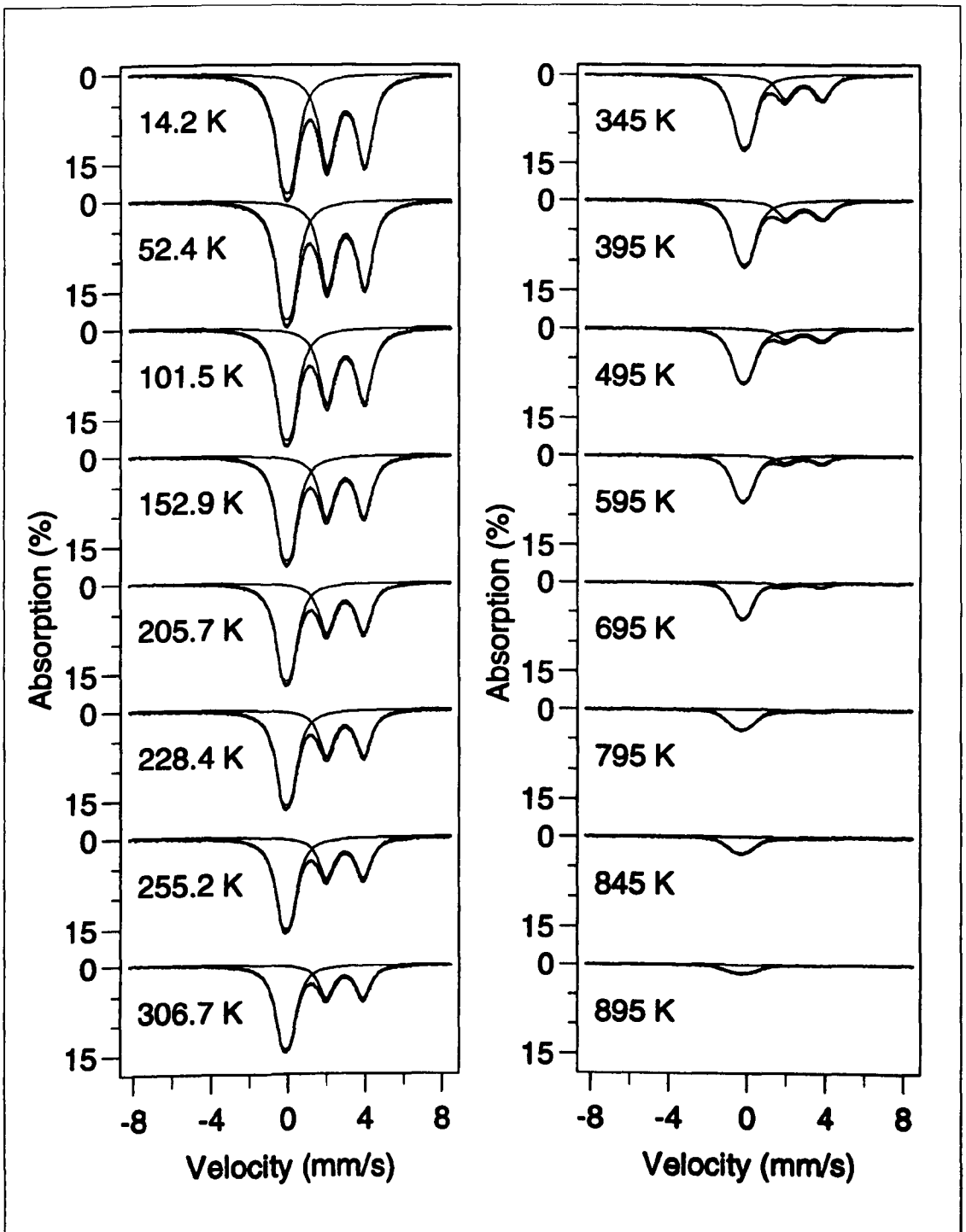

Figure 6.7 Mössbauer spectra of the 14.4 wt% tin oxide "silica" doped-float glass recorded between 14.2 K and 845 K.

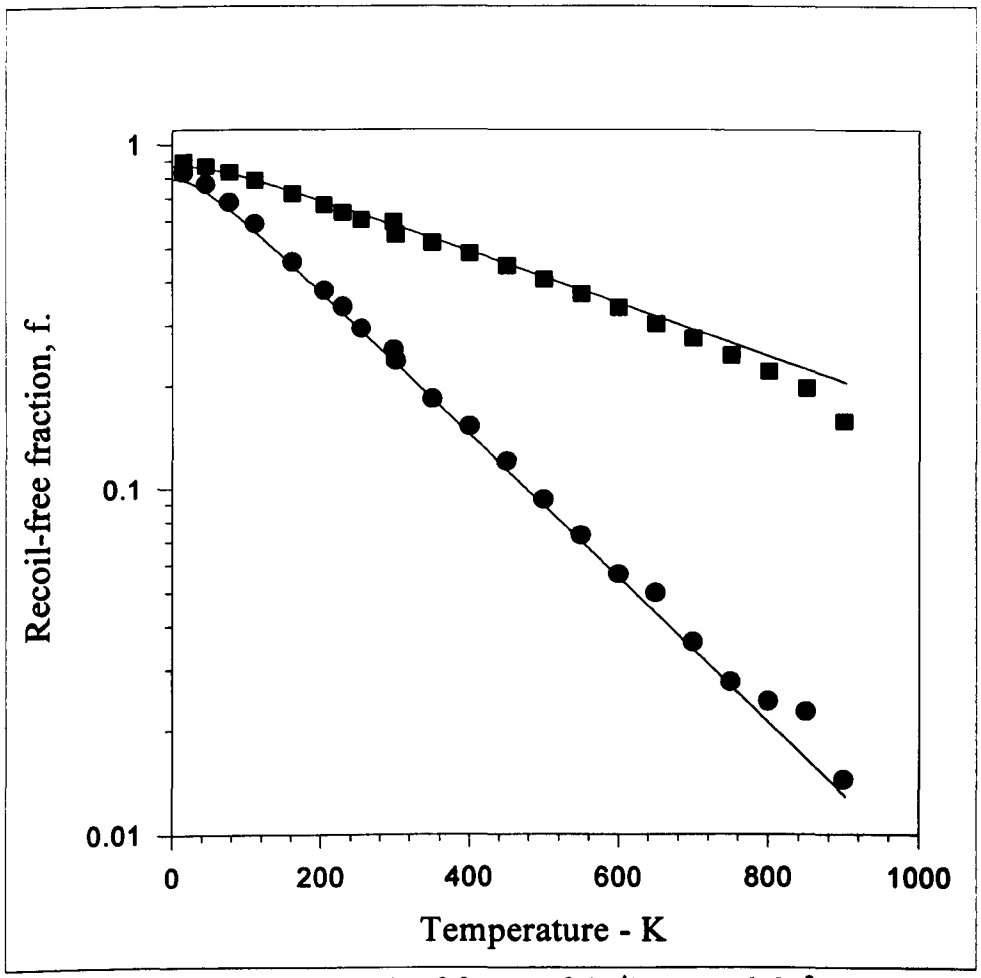

Figure 6.8 Variation of the f-factor of Sn^{4+} (■) and Sn^{2+} (●) in the 13.7 wt% tin oxide "alumina" doped-float composition glass with the curves fitted to the Debye temperatures calculated from the high temperature slopes.

Table 6.4

Tin State	"Alumina"			
Sn^{4+}	d(lnA)/dT	$(-1.776\pm0.008)\times10^{-3}$	θ_D	(318 ±0.7) K
	$lnA_{(T=0)}$	(0.461±0.003)	Rel.Conc.	61.4 %
Sn^{2+}	d(lnA)/dT	$(-4.757\pm0.01)\times10^{-3}$	θ_D	(194 ±0.2) K
	$lnA_{(T=0)}$	$(-2.939\pm6)\times10^{-3}$	Rel.Conc.	38.6 %

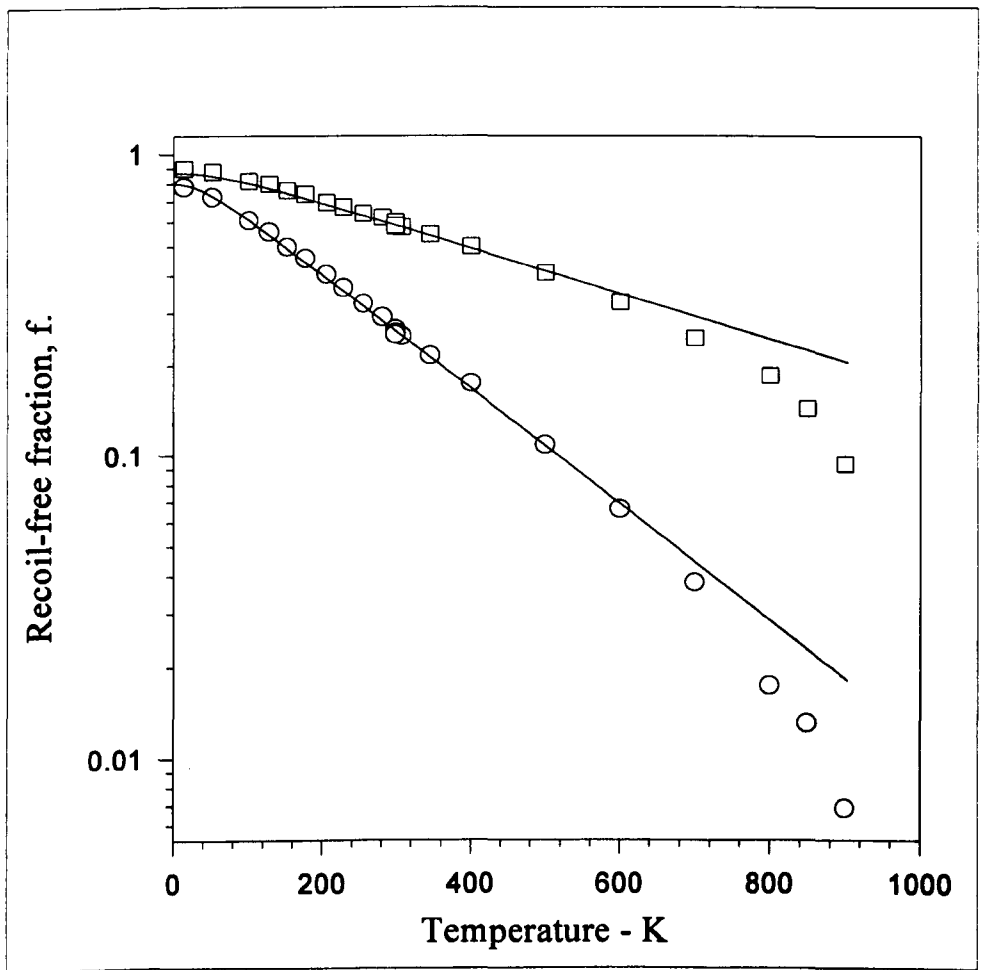

Figure 6.9 Variation of the f-factor of Sn^{4+} (□) and Sn^{2+} (○) in the 14.4 wt% tin oxide "silica" doped-float composition glass and the curves fitted to the Debye temperatures calculated from the high temperature slopes.

Table 6.4 (continued).

Tin State	"Silica"			
Sn^{4+}	d(lnA)/dT	$(-1.761\pm0.007)\times10^{-3}$	θ_D	(319 ±0.6) K
	$lnA_{(T=0)}$	(0.942±0.003)	Rel.Conc.	41.4 %
Sn^{2+}	d(lnA)/dT	$(-4.455\pm0.008)\times10^{-3}$	θ_D	(200 ±0.2) K
	$lnA_{(T=0)}$	(1.289±0.002)	Rel.Conc.	58.6 %

For both the "alumina" and the "silica" glass samples the data points fell below the Debye lines at the higher temperatures, however there was a much larger difference between the curve and the data for the silica sample. The glass transition temperatures of both samples have been measured (all results are shown in table 6.5). T_g for the 13.7 weight percent and the 14.4 weight percent tin oxide glasses was found to be 650°C for the "alumina" sample and 570°C for the "silica" sample. Therefore at the highest temperatures used to record the Mössbauer spectra the glasses were approaching their transformation temperatures, especially in the case of the "silica" sample which was found to have a lower T_g.

The values obtained for the Debye temperatures of Sn^{4+} and Sn^{2+} in both samples show that the average strength of binding of the tin in each glass is similar. The Sn^{2+} ions are much less strongly bound in both cases.

6.6 Properties of the Glass Samples

The density, coefficient of linear thermal expansion and the glass transition temperature, T_g, were measured at the University of Warwick. The results are shown in table 6.5 and show that for both cases the density and the transformation temperature increase as the weight percentage of tin oxide in the samples increases.

Table 6.5

"Alumina"				"Silica"			
Wt%	ρ (gcm^{-3})	T_g (±5°C)	α × 10^7 K	Wt%	ρ (gcm^{-3})	T_g (±5°C)	α × 10^7 K
0	2.494	535	89.7 ± 1.8	0	2.494	535	89.7 ± 1.8
2.7	2.534	570	85.2 ± 2.2	2.9	2.540	555	89.1 ± 1.4
4.6	2.550	585	80.3 ± 1.6	3.4	2.554	575	86.2 ± 1.5
6.1	2.606	595	77.0 ± 1.5	8.2	2.623	580	83.2 ± 1.4
9.2	2.644	615	73.1 ± 1.8	11.5	2.707	595	79.3 ± 1.4
11.7	2.704	640	69.3 ± 1.5	12.8	2.705	590	78.6 ± 1.6
13.7	2.749	650	65.9 ± 2.5	14.4	2.704	570	77.2 ± 1.4

6.7 Conclusions and Comparisons between Samples

The presence of excess aluminium oxide in a glass of float compostion was seen to affect the tin Mössbauer hyperfine parameters. It does not, however, alter the strength of binding of the tin ions in the glass. A tetrahedral unit of AlO_4 in a glass network would have a (-1) charge associated with it and this may influence a nearby Sn-O bond.

The measured Debye temperatures show that Sn^{4+} is more strongly bound in the glass network than Sn^{2+}. These results are discussed further in chapter 8, where a comparison with commercial float glass samples is made.

Chapter 7 Mössbauer Spectra of Float Glass

7.1 Introduction

The float process was discussed in chapter 1 where it was mentioned that a small amount of tin diffuses into the lower surface of the glass ribbon. Tests at the float plants suggest that this occurs because of the unavoidable presence of a small quantity of oxygen (a few parts per million) in the molten tin. The "surface" described here refers to approximately the first 30 μm of the bottom of the float glass ribbon. This is the region which differs in composition and consequently in physical properties from the bulk glass and is the depth in which the diffused tin may be found.

In studying the float surfaces containing tin, it was useful to compare samples from several different manufacturing float plant lines. Comparisons between glass from different positions across the bath were also made. The other factors which were considered included the glass-tin contact time, the bath atmosphere and the effect of heat treatments. In each case the ratios of the tin oxidation states were noted and for some glass samples the Debye temperatures of the tin were measured.

Specially treated glasses which had been coated with a layer of tin oxide were also studied. Different thicknesses of coatings were compared to see if any Sn^{2+} was present.

For analysis by Mössbauer spectroscopy, each sample of the thinned glass (0.1 mm of the bottom surface) was crushed and placed in the sample holder. Unground samples were also analysed to check that no significant changes occurred on grinding for just a short time (less than 10 seconds). The coated glasses were prepared as discs which could fit inside the sample holder.

7.2 Experimental Techniques for Analysing Float Glass Surfaces

The samples were characterised at Pilkington Technology Centre by techniques such as XPS, EMPA and XRF. These are described briefly in the following sections. The most suitable method for obtaining the oxidation state of tin in a float glass surface is that of Mössbauer spectroscopy.

An atomic force microscope, (AFM), was used to obtain images of certain float glass surfaces. The AFM operates by monitoring the surface forces using a probe tip attached to a cantilever. The reflection of light from the cantilever is deflected and the image is built up as the surface is scanned.

7.2.1 X-ray Photoelectron Spectroscopy (XPS)

XPS was used in the near surface analysis of several of the constituent oxides of float glass, e.g. SiO_2, MgO, CaO, Na_2O and also tin oxide. X-rays are directed at the sample which results in the electrons being ejected from the core levels of the atoms. The kinetic energy of these electrons is recorded to establish which atoms are present from the peaks corresponding to certain energy levels. A quantitative analysis is possible from the measured intensities of the peaks. This technique is suitable to a depth of about 30 Å but the surface may be etched with argon ions, so a profile to a depth of approximately a few thousand Ångstroms may be obtained.

Previous work has been carried out on similar float samples. [55] [56] Verita [55] et al found that a steep tin concentration gradient existed in the outer 50 nm of the surface.

7.2.2 Electron Microprobe Analysis (EMPA)

As tin penetration is found to be greater than that easily measurable by XPS, it is convenient to measure a tin profile by electron microprobe analysis. In this process an electron beam is applied to a polished glass cross section. The emission of photoelectrons produces core vacancies, which, on being filled emit characteristic x-rays whose wavelengths are then analysed by Bragg spectrometers. Profile results may therefore be obtained up to 30 μm into the surface. Pantano [56] et al found that tin may be present up to 40 μm into the glass. They also showed that the penetration depth increased with contact time, as did the tin concentration.

7.2.3 X-Ray Fluorescence (XRF)

The sample is bombarded with x-rays and the fluorescent L_α x-rays are measured. The amount of tin in the glass surface is obtained on a relative scale from the number of counts recorded over a few seconds.

7.3 The Effect of Variable Float Process Parameters

Several factors may affect the amount and the chemical state of tin picked up by the glass in the float bath and some of these are discussed below.

Samples were obtained from four different float lines which will be referred to as L1, L2, L3 and L4. The line sizes and atmospheric conditions differed slightly between each line, for example L2 was considerably smaller than the other three float plant lines.

Tin profiles of these samples showed that the penetration depth of up to 15 μm for line L2 was consistently less than that for L1 and L3 (up to ~30 μm).

Representative Mössbauer spectra of samples from each of the lines are shown in figure 7.1. The ratio of tin oxidation states was calculated for each sample, and the results repeatedly show that there are differences between the lines. The average percentage of tin existing as Sn^{4+} was found to be 30-36 % for L1, 20-26 % for L2 and 30-35 % for L3. The results for L3 are perhaps less representative of an average for that line as different samples were all obtained in one day. Only a few samples were studied from L4. The Mössbauer parameters for each of these spectra are shown in table 7.1. Although the spectra are similar to those obtained by Principi et al [33] (using C.E.M.S) the values of the chemical shift are slightly lower, ~2.9 mms^{-1} compared with ~3 mms^{-1}, although his reference material was not quoted.

Table 7.1

Float Line	Tin State	δ (mms^{-1})	Δ (mms^{-1})	Γ (mms^{-1})
L1	Sn^{4+}	-0.070 ± 0.008	0.393 ± 0.026	0.778 ± 0.036
	Sn^{2+}	2.958 ± 0.005	1.958 ± 0.009	0.885 ± 0.013
L2	Sn^{4+}	-0.187 ± 0.008	0.457 ± 0.008	0.858 ± 0.008
	Sn^{2+}	2.899 ± 0.008	1.979 ± 0.008	0.934 ± 0.008
L3	Sn^{4+}	-0.170 ± 0.008	0.387 ± 0.008	0.829 ± 0.008
	Sn^{2+}	2.843 ± 0.008	1.954 ± 0.008	0.934 ± 0.008
L4	Sn^{4+}	-0.187 ± 0.008	0.395 ± 0.008	0.847 ± 0.008
	Sn^{2+}	2.904 ± 0.008	1.982 ± 0.008	0.941 ± 0.008

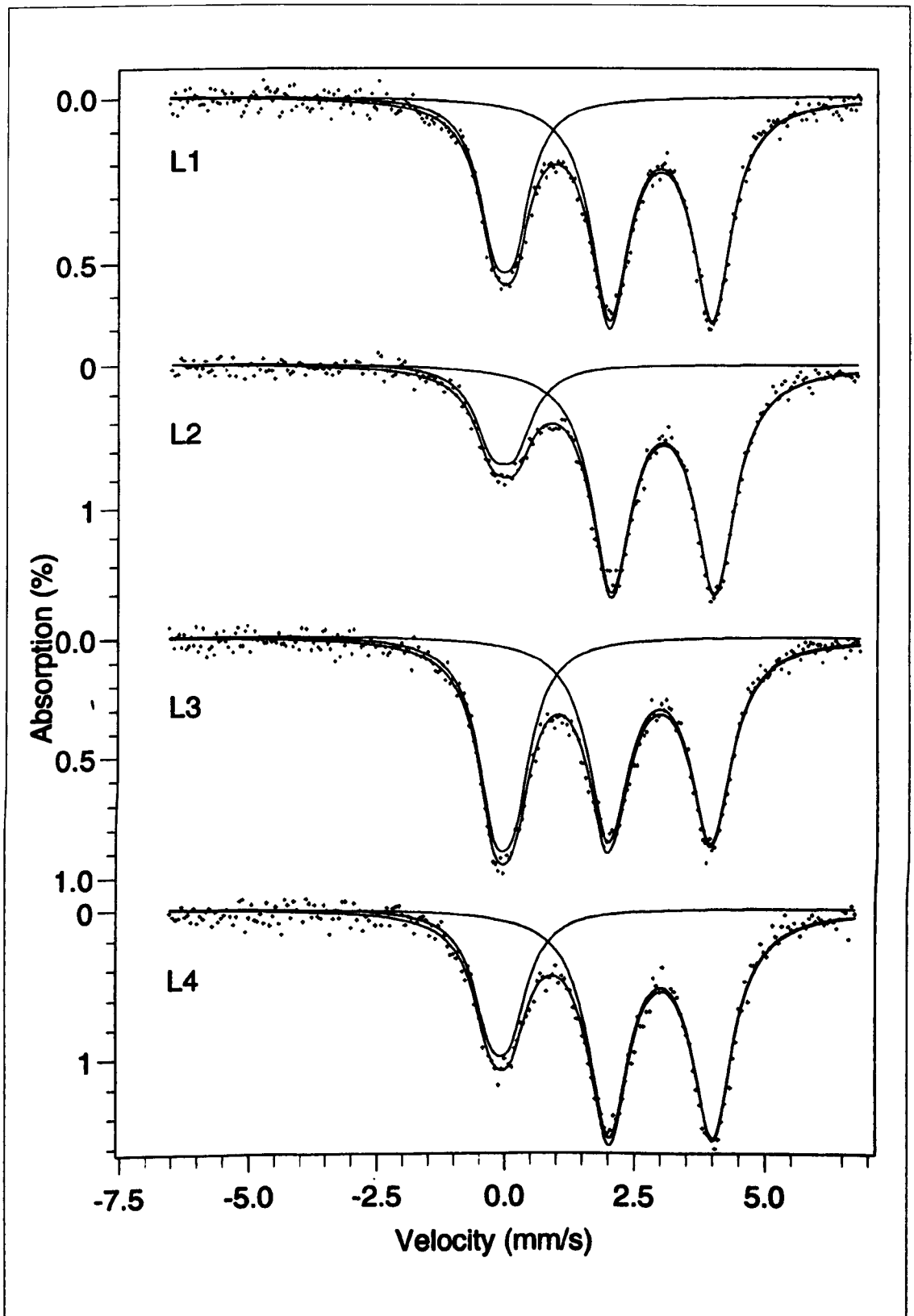

Figure 7.1 Representative Mössbauer spectra recorded at ~77 K of each different float line.

7.3.1 Position across the Float Bath Width

To discover what effect, if any, the position that the glass was obtained from across the bath width caused, samples were taken from the centre and edge of the ribbon. Two separate sets from different plants (L1 and L4), were analysed and the spectra are shown in figure 7.2. The XRF tin counts were found to be greater at the edges than in the centre for both float plant lines.The fitted spectra show that the percentage of Sn^{4+} is less at the edges than in the centre, also in both cases. The results are given in table 7.2 and are also similar to those obtained by Principi et al. The percentage of Sn^{4+} is therefore less when the tin content is greater. A similar effect was seen in results obtained for glass with a higher than average tin count from L1 and L2. These also showed a lower than average ratio of stannic to stannous ions.

Table 7.2

Float Line	Position	Tin Count	Percentage Sn^{4+} ($\pm \leq 1\%$)
L1	Edge	1800	30.3
	Centre	1400	36.6
L4	Edge	1200	25.5
	Centre	1000	27.2

The higher concentration of diffused tin occuring at the edges may be understood by considering the oxygen contamination of the tin bath. The glass ribbon lies across most of the molten tin. However, towards the sides a small width of tin is exposed to the bath atmosphere allowing for an increased amount of dissolved oxygen to be found in the edge regions compared with the centre. It is assumed that the presence of oxygen causes the formation of tin ions and therefore the possibility of diffusion into the glass is increased.

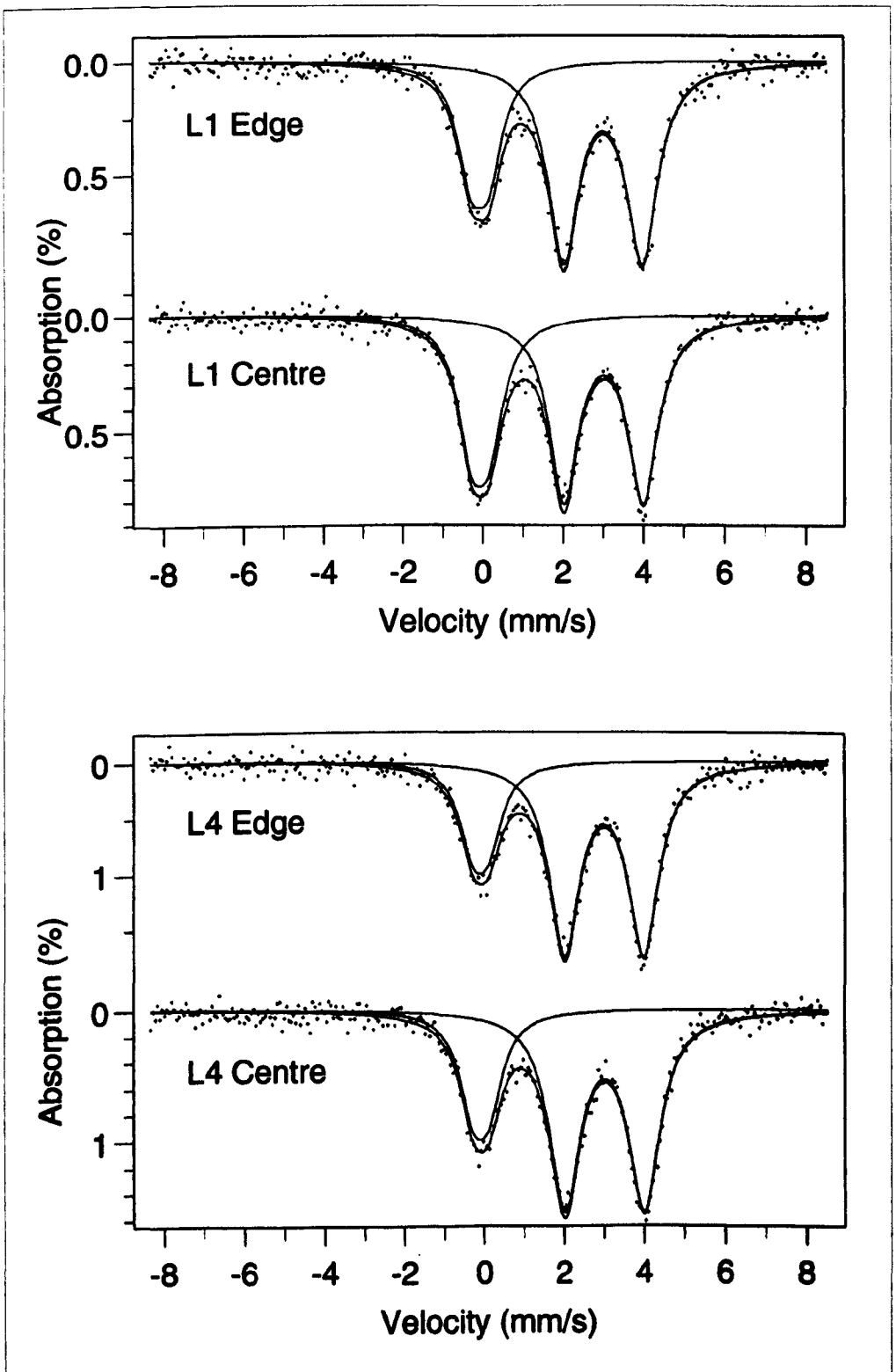

Figure 7.2 Mössbauer spectra at ~77 K of glass from the centre and edge of two different float plant lines.

The result that the ratio of oxidation states also varies when the total concentration is different suggests that under the conditions in the float bath there may be a limit to the amount of stannic tin which can exist in the glass, ie. greater tin concentration does not lead to an equal increase of both tin oxidation states.

7.3.2 Glass Thickness and Contact Time

Float glass is manufactured to thicknesses of between 0.5-25 mm. A tractive force is applied for thin glass manufacture and by restricting the outward glass spread and reducing the volume flow, thick glass may be produced. [57] The time of glass-tin contact therefore varies with glass thickness and will be longer the thicker the glass that is produced. No information on the actual times was available. Samples of 10, 12, 15 and 25 mm glass from L1 were compared. The spectra are shown in figure 7.3, and the tin counts and oxidation states are listed in table 7.3. There is little increase in tin count for increased thickness (and hence contact time), and also no observable trend in the oxidation state ratios. The samples were obtained over several weeks and it is therefore possible that other conditions may have been changed. This information was however not available.

Table 7.3

Glass Thickness - mm	Tin Count	Percentage of Sn^{4+} ($\pm\leq$ 1%)
10	1601	33.5
12	813	35
15	893	31
19	827	32.1
25	921	34

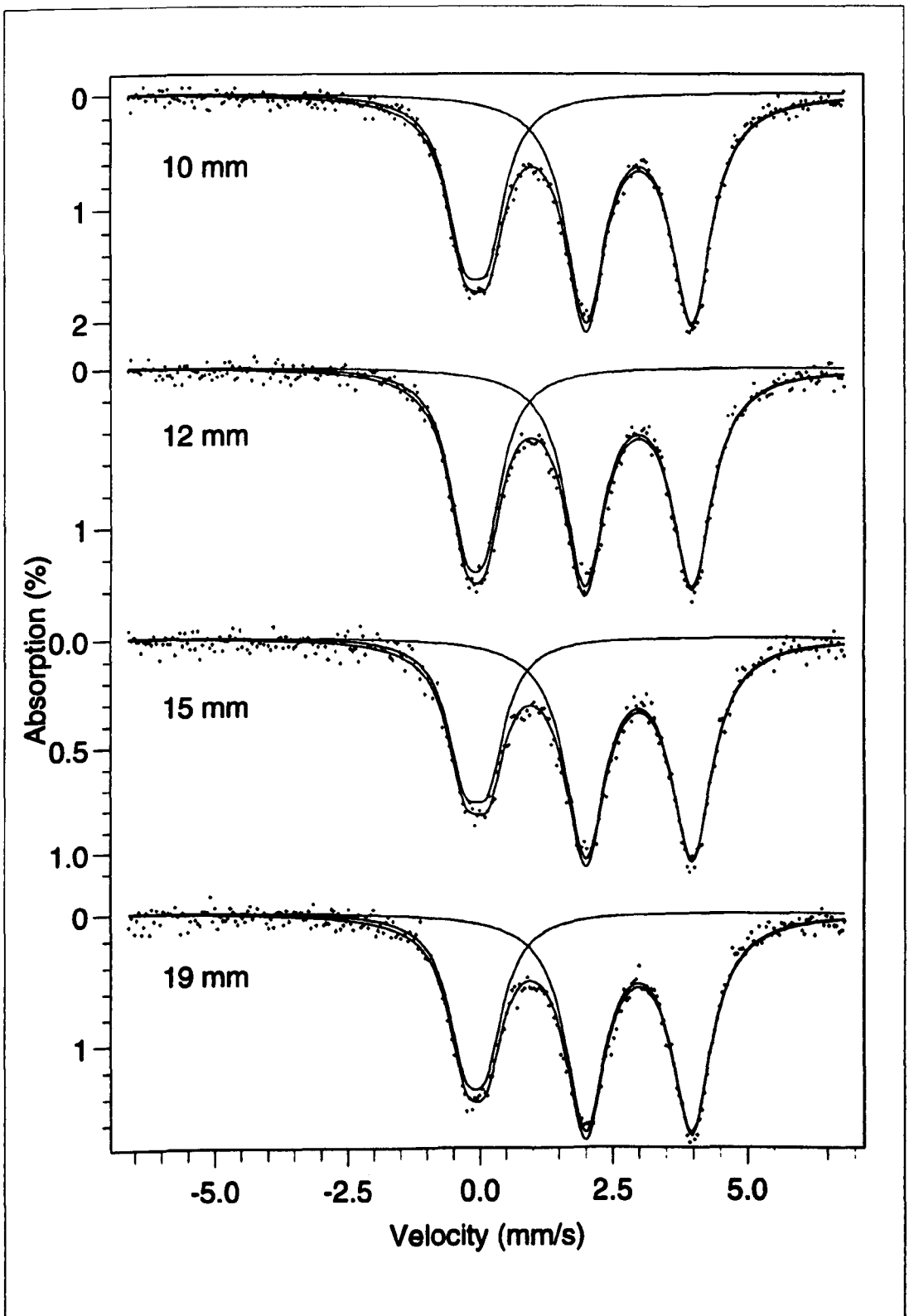

Figure 7.3 Mössbauer spectra at ~77 K of float glass samples obtained from glass manufactured to different thicknesses.

7.3.3 Float Bath Atmosphere

A reducing atmosphere is usually maintained over the bath and this keeps the oxygen contamination of the molten tin to a minimum. It consists of a mixture of nitrogen and hydrogen. Any change to a particular float bath atmosphere may be considered to affect the uptake of tin. On two occasions when such a change occurred, samples of glass were obtained and subsequently analysed. The first results were recorded for six samples taken from line L3 and the second set were obtained at a different time from line L2.

Glass from L3 was obtained in a day, with variable time gaps between each sample. The spectra which were recorded are shown in figure 7.4 for float samples 1 to 6. The reducing nature of the bath atmosphere was lowered until sample 4, but it then reverted back to its original level when the last two samples were obtained.

Following the idea that an increased presence of oxygen promotes the diffusion of tin into the glass it would be expected that the tin counts may be higher for a less reducing atmosphere. As discussed in 7.3.1 an increased tin concentration was associated with a reduced Sn^{4+} to Sn^{2+} ratio in the glass.

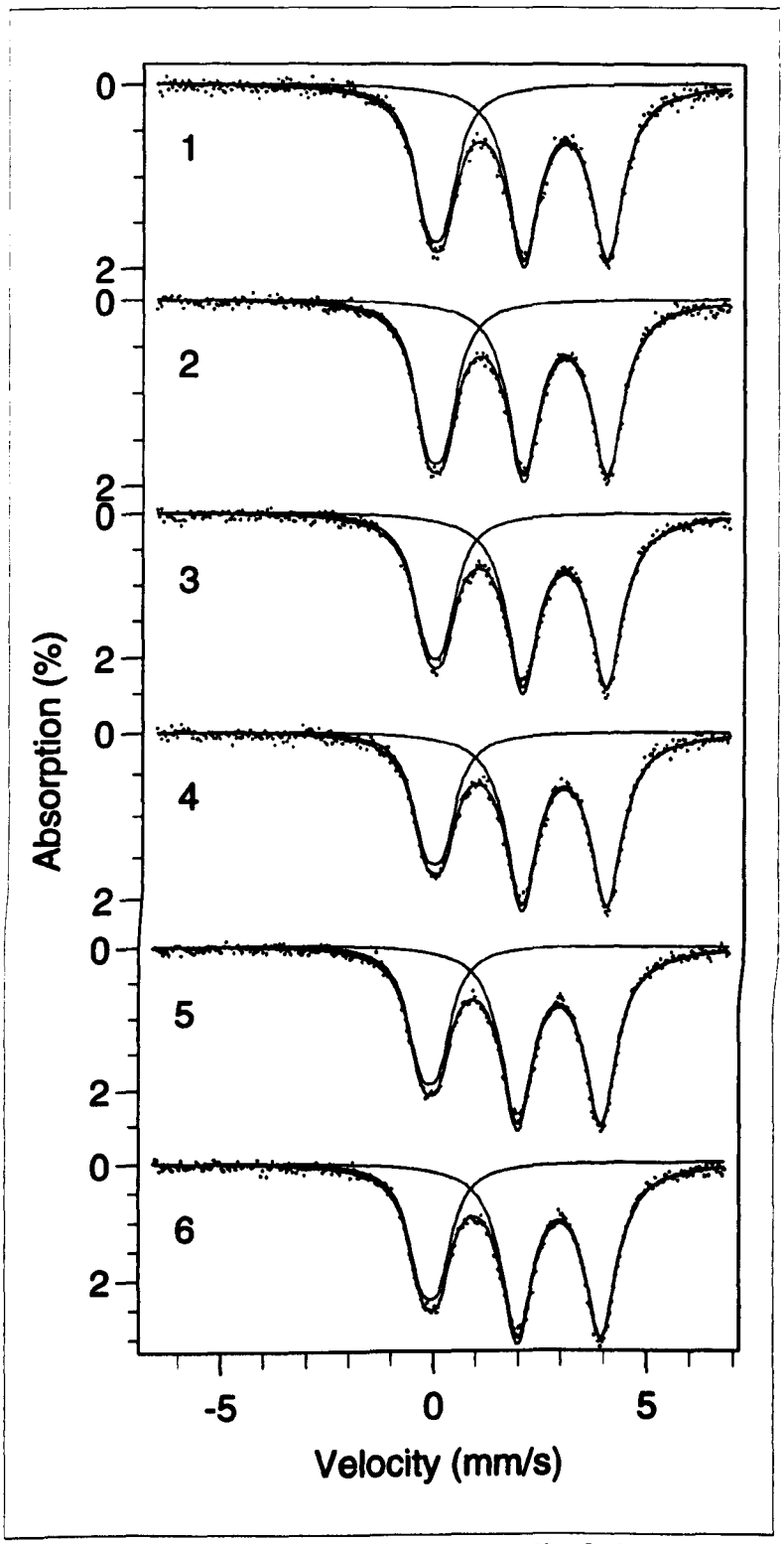

Figure 7.4 Mössbauer spectra at ~77 K of glass samples obtained from line L3 as the reducing atmosphere was decreased.

Table 7.4 shows the relevant figures and the Sn^{4+} percentage is plotted in figure 7.5.

Table 7.4

L3 Sample	Bath Atmosphere	Tin Count	Percentage Sn^{4+} ($\pm\leq$ 1%)
1	Start - Reducing X%	2460	34.5
2	Less reducing Y%	2346	35.3
3	Less reducing Y%	3403	32.7
4	Less reducing Y%	3195	31.2
5	Reducing X%	3132	30.96
6	End - Reducing X%	3015	31.4

The percentage of stannic tin measured after float sample 1 was heated is also shown in this graph, and this is discussed below in 7.4.1. From the graph and the details listed in the table the following points may be noted. Firstly, the tin count, i.e. tin concentration in the glass, can be seen to change with time, and tends to be increased during a lower reducing atmosphere. Secondly the Sn^{4+} to Sn^{2+} ratio decreased, and then increased again. The lowest percentage of Sn^{4+} was found to occur after a normal reducing atmosphere had been restored, whereas the highest tin count was measured for sample 3, obtained during a low reducing atmosphere. A possible explanation of the minimum in the oxidation state ratio after the atmosphere was returned to normal is that a time lag occurs. This would mean that the lower reducing atmosphere does not produce an immediate increase in the dissolved oxygen, and similarly the normal reducing atmosphere does not take effect instantly. The highest tin count does not coincide with the lowest Sn^{4+} to Sn^{2+} ratio which suggests that there may be some other effect occurring.

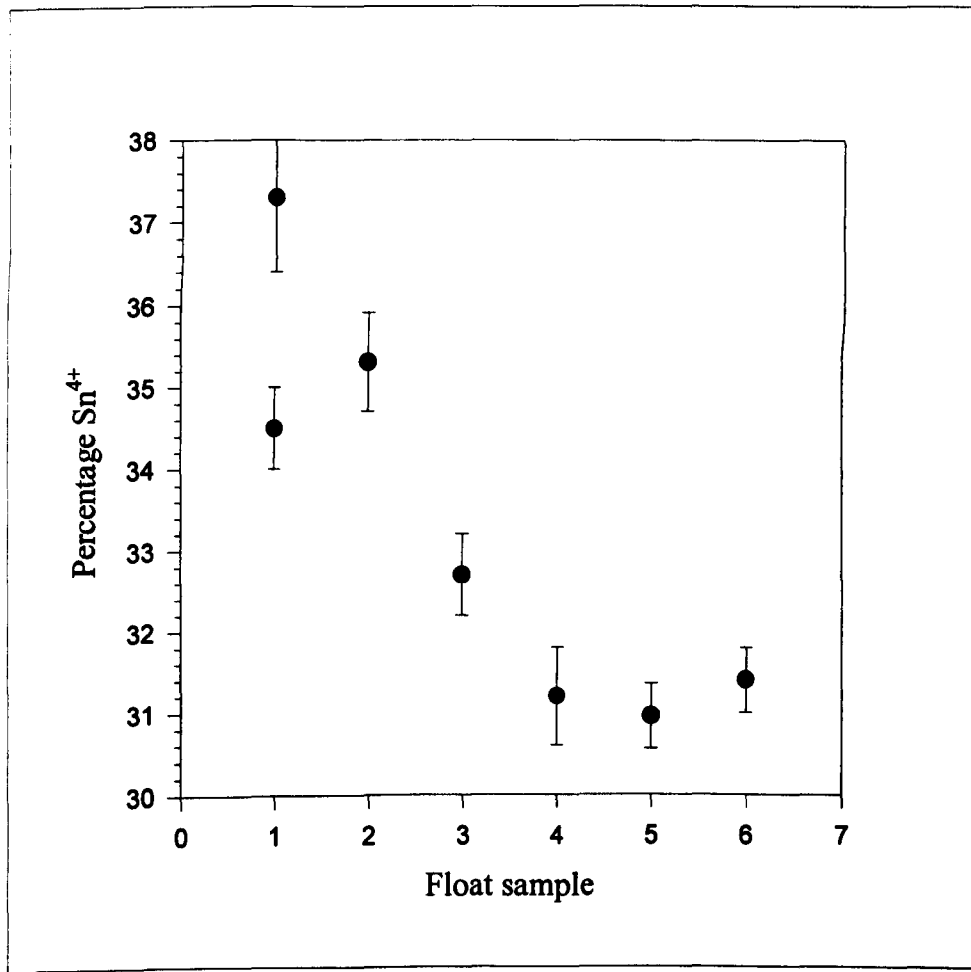

Figure 7.5 Percentage of tin existing as Sn^{4+} in float glass obtained as the bath atmosphere was changing.

Nine glass samples were obtained from L2 during a six day period when the reducing nature of the atmosphere was lowered, maintained low, increased and finally decreased again. The spectra are shown in figure 7.6 and the results are given in table 7.5.

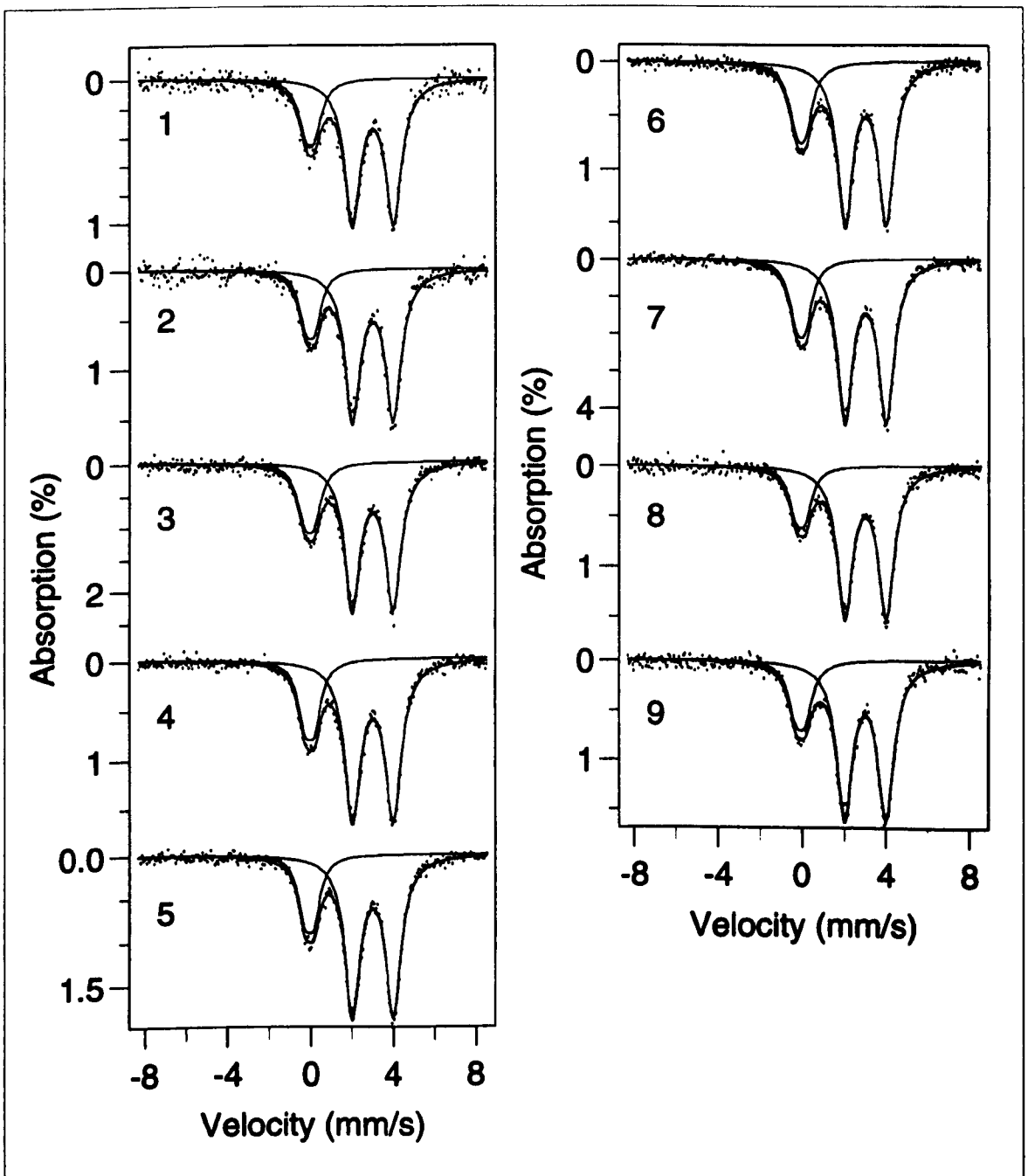

Figure 7.6 Mössbauer spectra at ~77 K of glass samples obtained from float line L2 at different times when the float bath atmosphere was changed.

Table 7.5

L2 Sample	Bath Atmosphere	Tin Count	Percentage Sn^{4+} (±≤ 1%)
1	Start - Reducing S%	1333	22.2
2	Less Reducing 0%	1470	21.3
3	Less Reducing 0%	1808	23.4
4	Less Reducing 0%	2162	22.6
5	Less Reducing 0%	2735	22.4
6	Less Reducing 0%	2893	23.9
7	Less Reducing 0%	3252	22.7
8	More Reducing R%	1181	19.8
9	End - Reducing S%	-	21.5

These figures show that the tin uptake was increased when the reducing nature of the atmosphere was less. It can also be seen that the effect became greater as the length of time without a reducing atmosphere increased. The ratio of oxidation states do not show a similar trend. However, it may be significant that these results were obtained from the float line which consistently produces a lower percentage of Sn^{4+}. The tin counts are also lower than those measured for L3, therefore it is possible that the limiting amount of Sn^{4+} may not have been reached, hence no change in the ratio would be observed.

7.3.4 Alternative Processes during Manufacture

Special products may undergo a slightly different process during manufacture, for example when producing coloured or surface modified glass. Several such samples were analysed to see if any differences could be observed in their Mössbauer spectra. Fourteen out of fifteen results were very similar to those of ordinary float glass, however one spectrum showed a noticeable difference to the Sn^{2+} doublet. It was possible to fit this spectrum with a third component which had parameters which were consistent with those

of tin metal, i.e. $\delta \approx 2.6$ mms^{-1}. Figure 7.7 shows this spectrum together with one of a sample consisting of float glass and powdered tin metal as a means of comparison. It is therefore possible to observe the presence of metallic tin,Sn^0, as well as Sn^{2+} and Sn^{4+} in float glass.

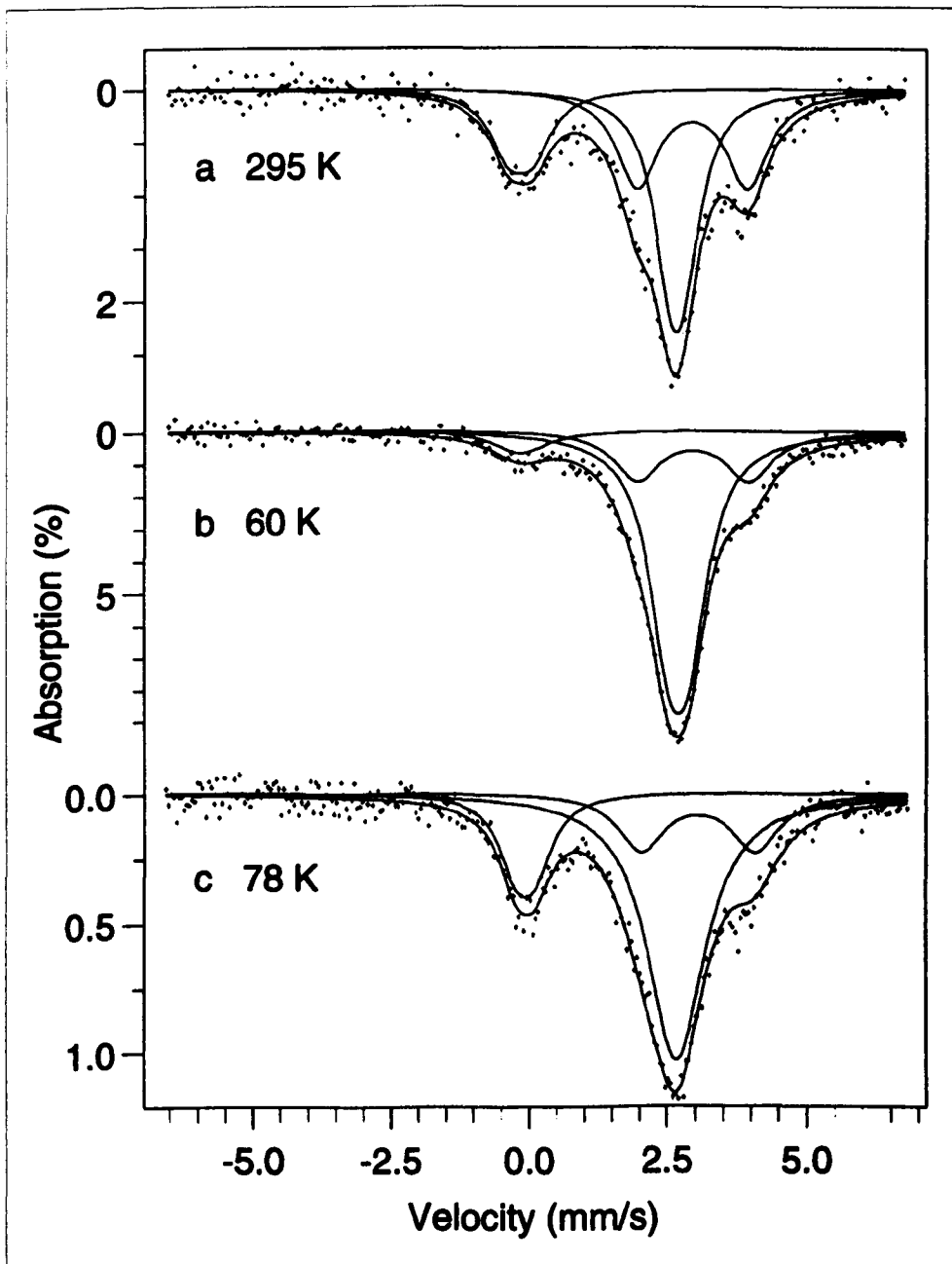

Figure 7.7 Mössbauer spectra of untreated float glass mixed with powdered tin metal at (a) 295 K and (b) 60 K, to provide a comparison to (c) float glass containing tin metal after undergoing treatment during manufacture.

7.4 Heat Treatment of Float Glass

Float glass is heated after production as a means of strengthening or shaping the glass. The uses were mentioned in chapter 1, and the changes occurring to the tin are discussed below. The surface wrinkling effect of bloom can be seen under a microscope and also in an AFM image (Figure 7.8). Figure 7.9 shows an optical micrograph of a bloomed float glass surface compared with the surface of untreated glass. The depth of the surface ridges visible in figure 7.8 can be seen to be about 200 nm. The presence of these ridges will cause diffuse light scattering from the surface, which results in reduced transmission and the creation of the hazy appearance known as bloom.

7.4.1 Mössbauer Spectra of Bloom Tested Samples

Glass from lines L2 and L3 underwent bloom testing. The tin Mössbauer spectra of the glass before and after heating are shown in figure 7.10. The changes in the Sn^{4+} to Sn^{2+} ratios are 14.5 % to 21.9 % Sn^{4+} for L1 and 34.5 % to 37.3 % Sn^{4+} for L3. These results show that a small amount of the Sn^{2+} has been oxidised to Sn^{4+}. A depth profile measured by XPS shows that some movement of the tin has also occurred. Figure 7.11 illustrates this result, which was obtained by Miss J. Greengrass and Dr. B.P. Tilley at Pilkington Technology Centre, and is consistent with results reported previously. [55] [56]

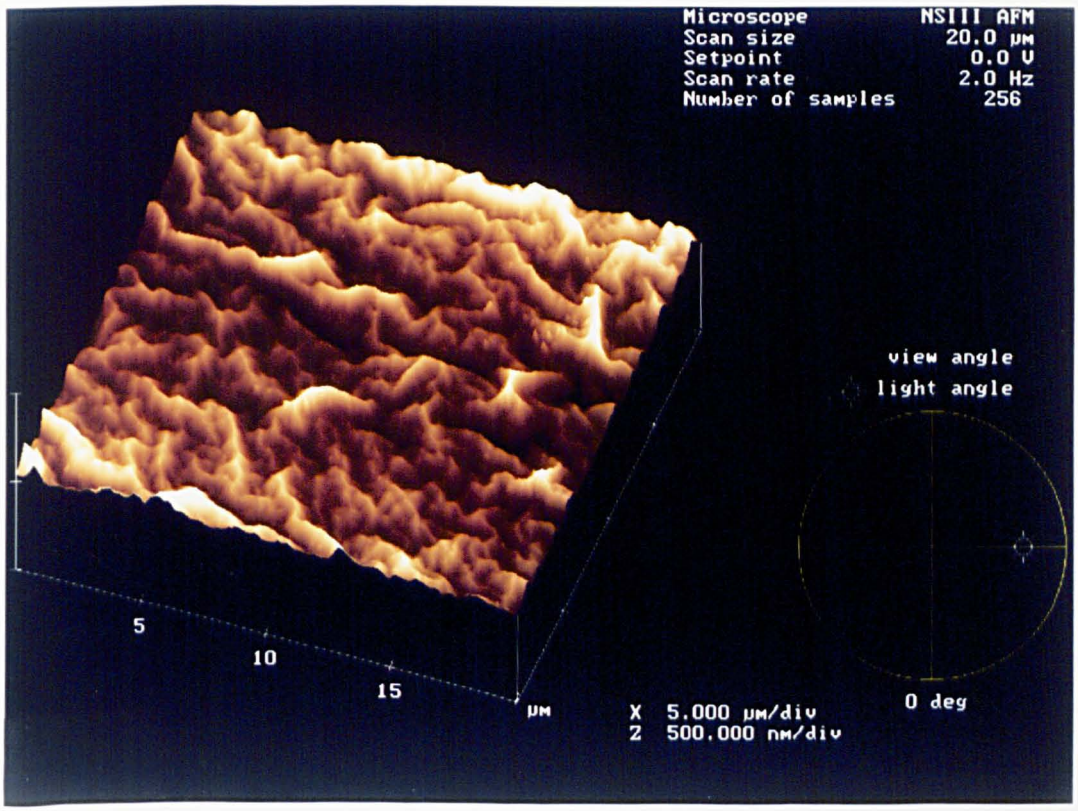

Figure 7.8 AFM image of the surface of float glass after it has undergone a bloom test at ~730°C.

(a)

(b)

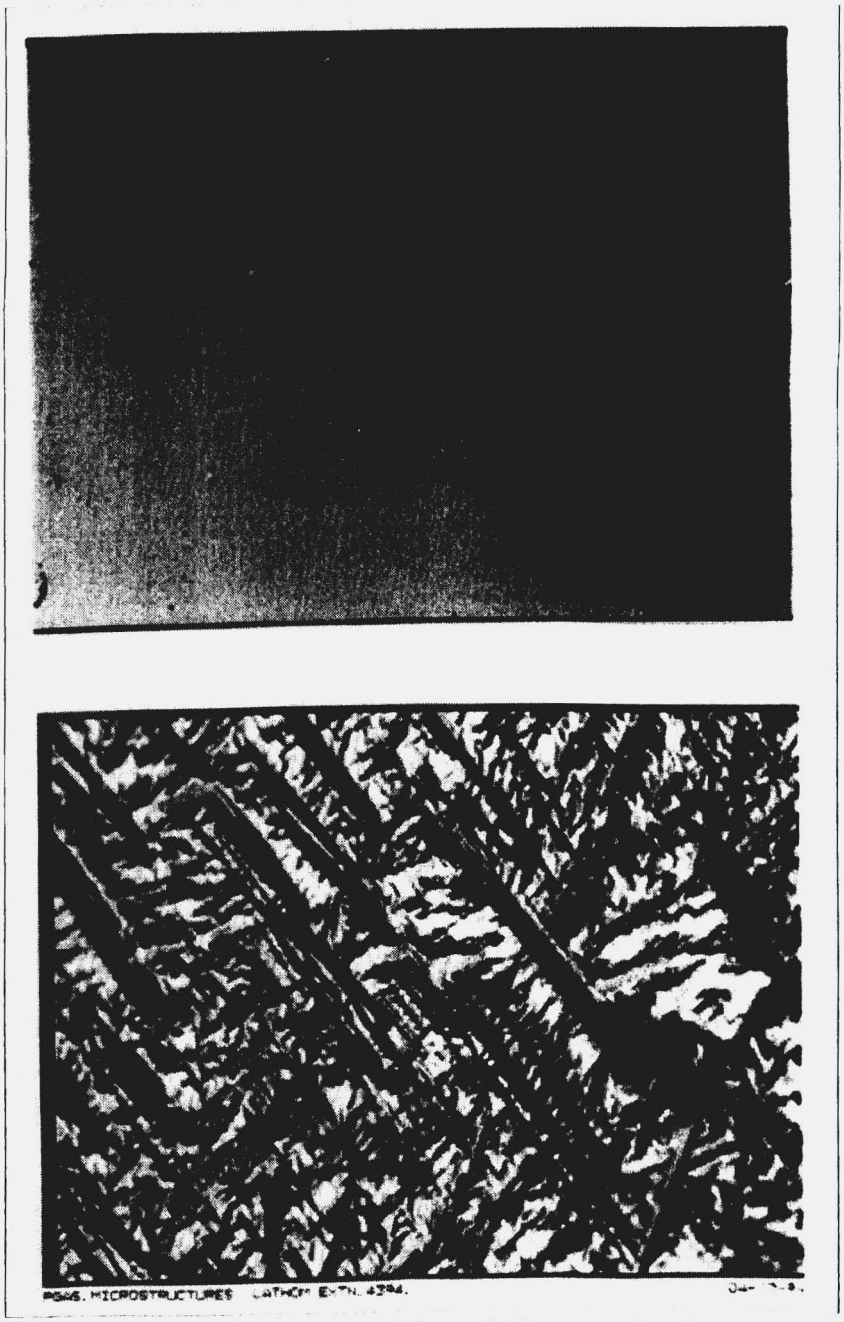

Figure 7.9 Photograph (with × 325 magnification) of the surface of float glass (a) unheated (b) after heating for 30 minutes at ~730°C.

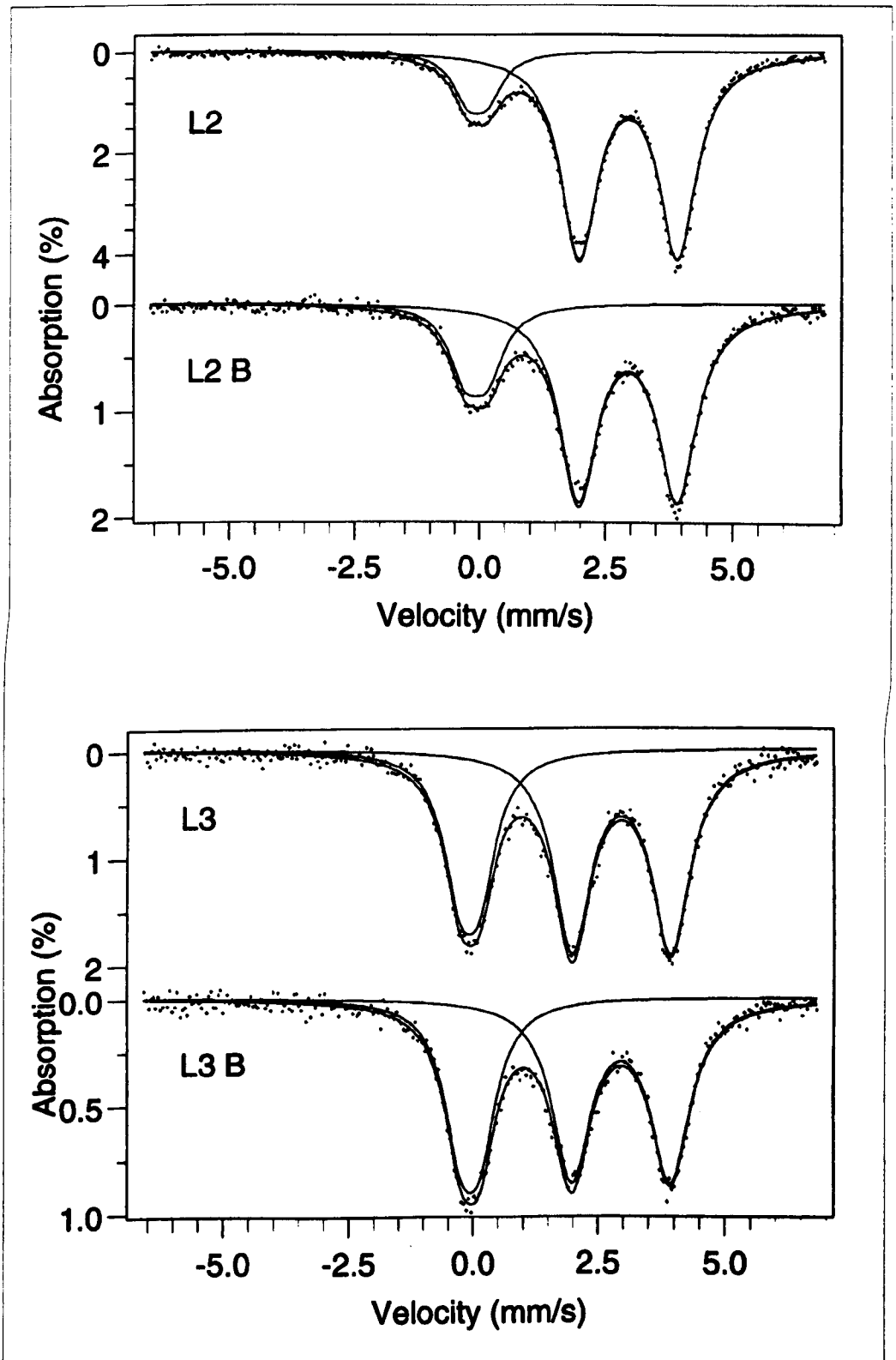

Figure 7.10 Mössbauer spectra at ~77 K of float glass from lines L2 and L3 before and after undergoing a bloom test at ~730°C.

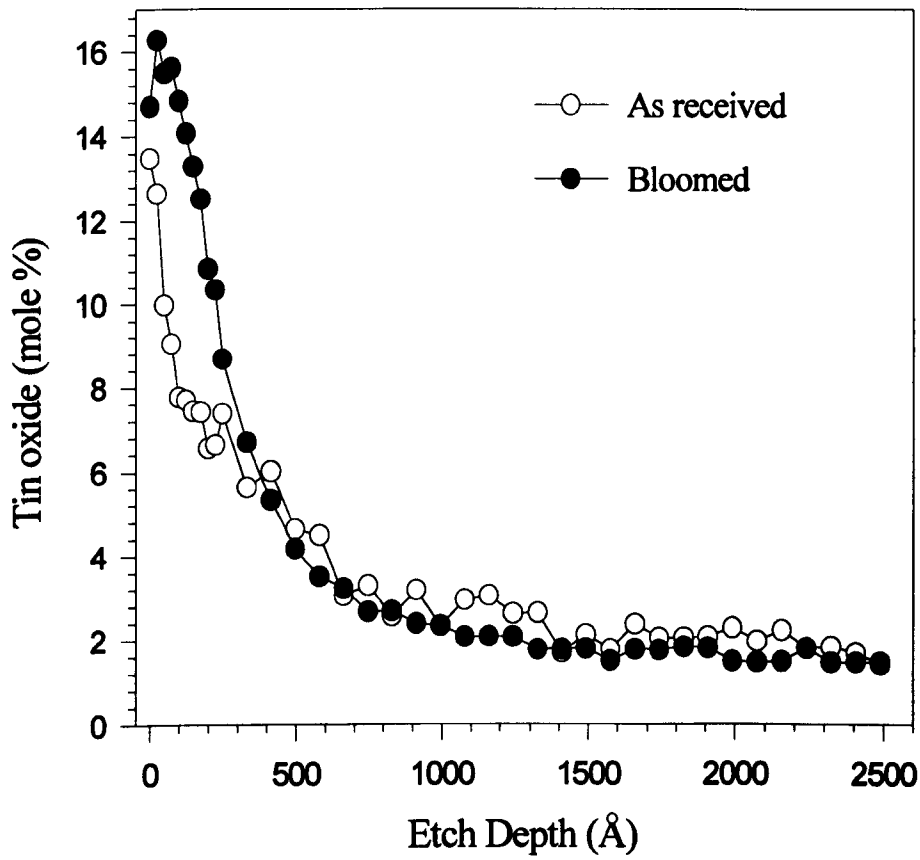

Figure 7.11 XPS tin depth profile before and after a bloom test (heating at ~730°C for a few minutes).

7.4.2 Heat Treatment Experiments to Measure Oxidation

Following the measurements of the bloom tested glass several heat treatments were planned to gain further information on the changes occurring after heating. One float glass was chosen (from line L1) and several samples were heated for between 0.5 hour and 345 hours at temperatures of 500°C, 600°C and above 700°C. The glass was placed in a muffle which was not under vacuum. A further heat treatment was carried out above the liquidus temperature, at 1050°C for 10-15 minutes; it was then quenched in water.

The XRD pattern of the glass heated at ~730°C for 338 hours showed that it had

devitrified and cassiterite, SnO_2, was seen to be present. The spectrum is shown in figure 7.12.

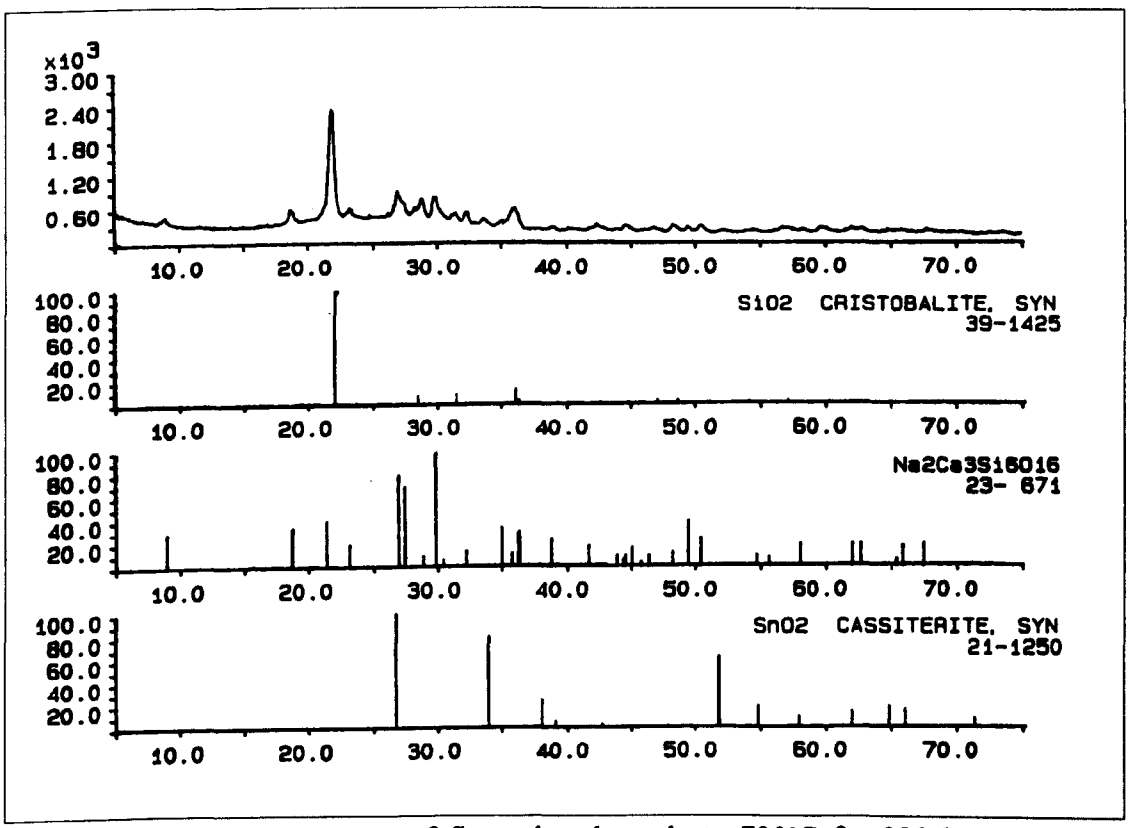

Figure 7.12 XRD spectrum of float glass heated at ~730°C for 338 hours and the positions of different crystalline species.

The Mössbauer spectrum of each new sample was recorded at 77 K and the results obtained for each of the different conditions are shown in figures 7.13, 7.14, 7.15 and 7.16. The spectra show that the greatest oxidation occurs at the highest temperatures, however even after 345 hours at about 720°C some Sn^{2+} still remains. Above 1000°C all the Sn^{2+} was converted to Sn^{4+}.

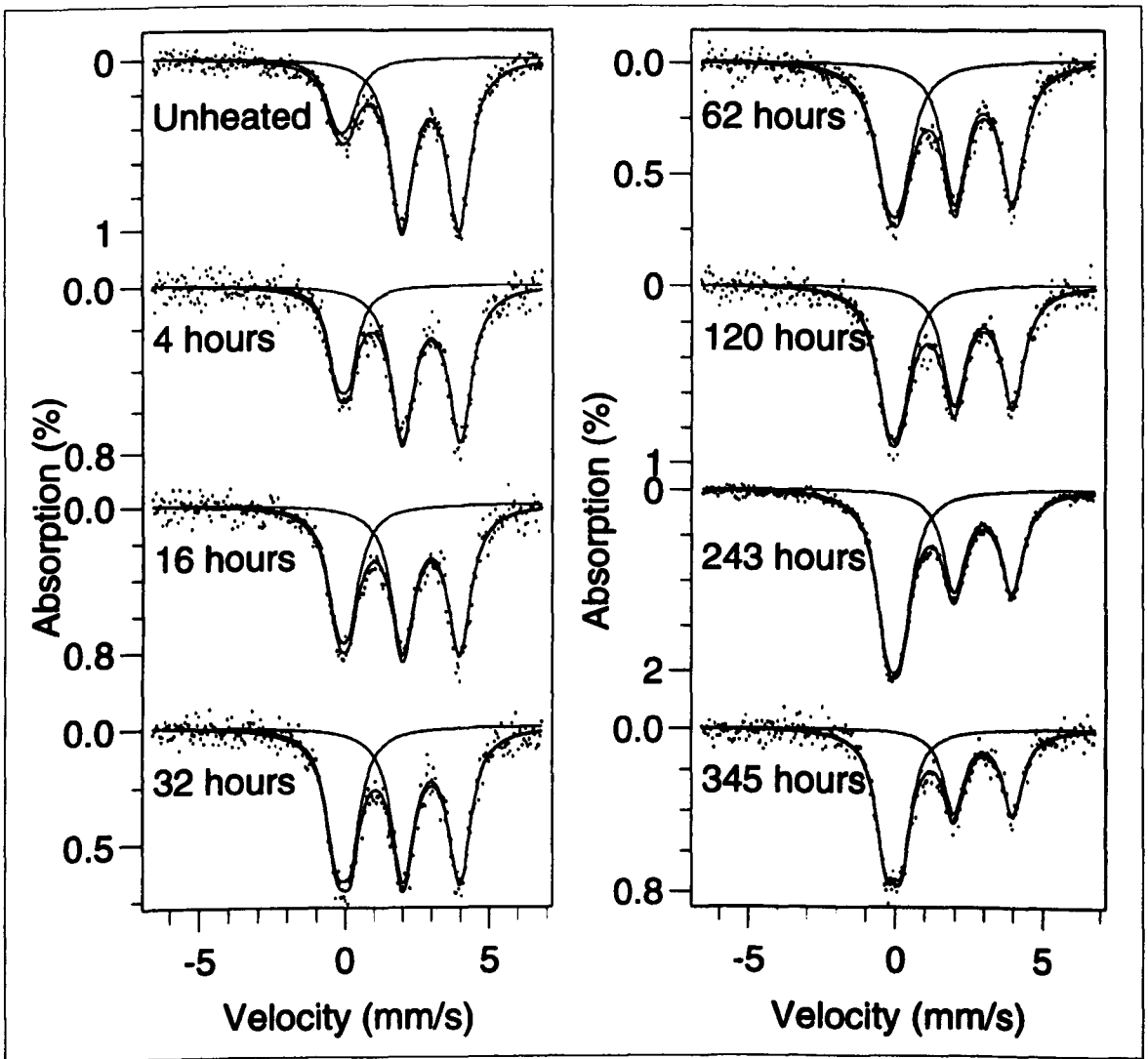

Figure 7.13 Mössbauer spectra at ~77 K of float glass heated at 500°C for up to 345 hours.

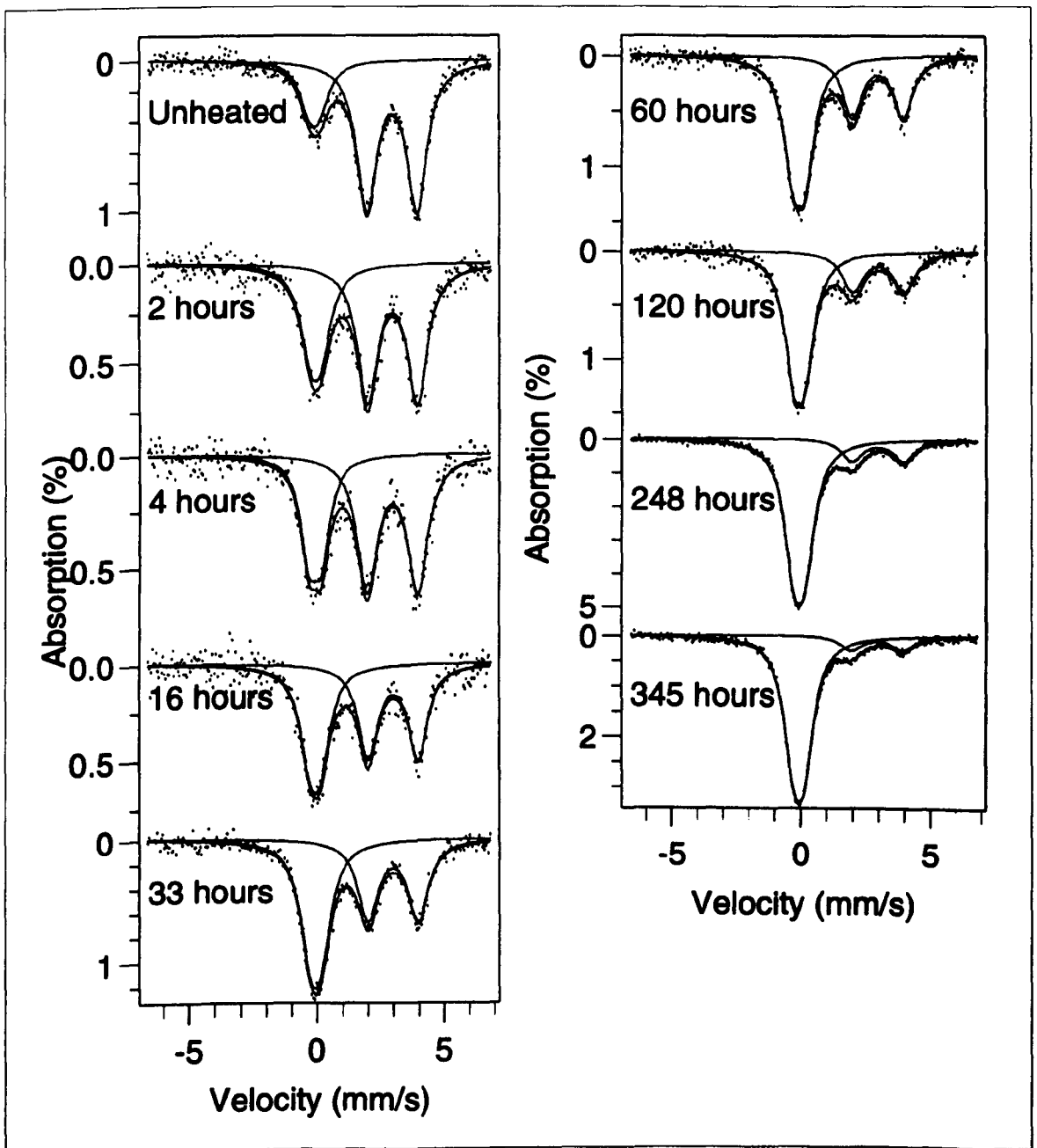

Figure 7.14 Mössbauer spectra at ~77 K of float glass heated at 600°C for up to 345 hours.

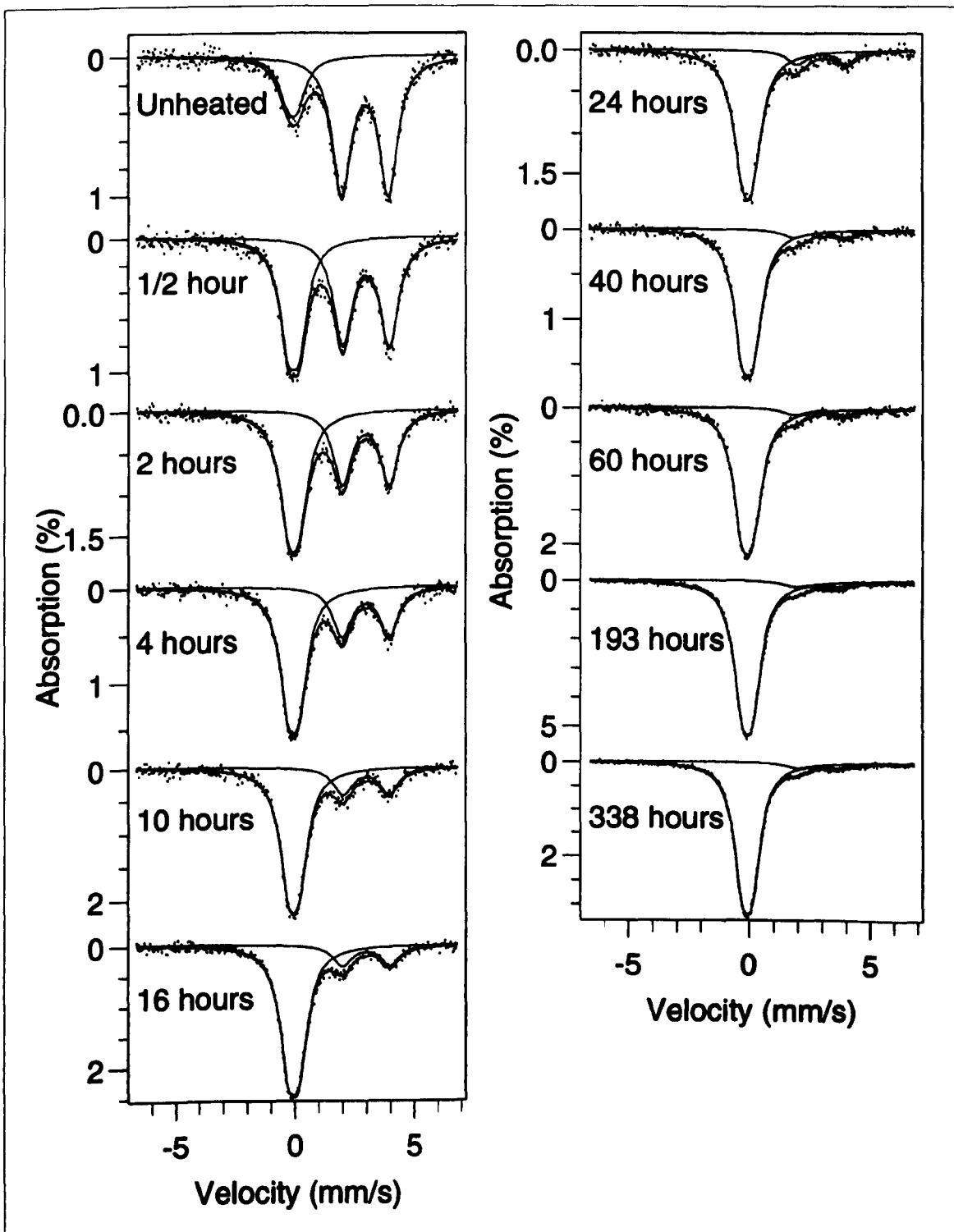

Figure 7.15 Mössbauer spectra at ~77 K of float glass heated at ~730°C for up to 345 hours.

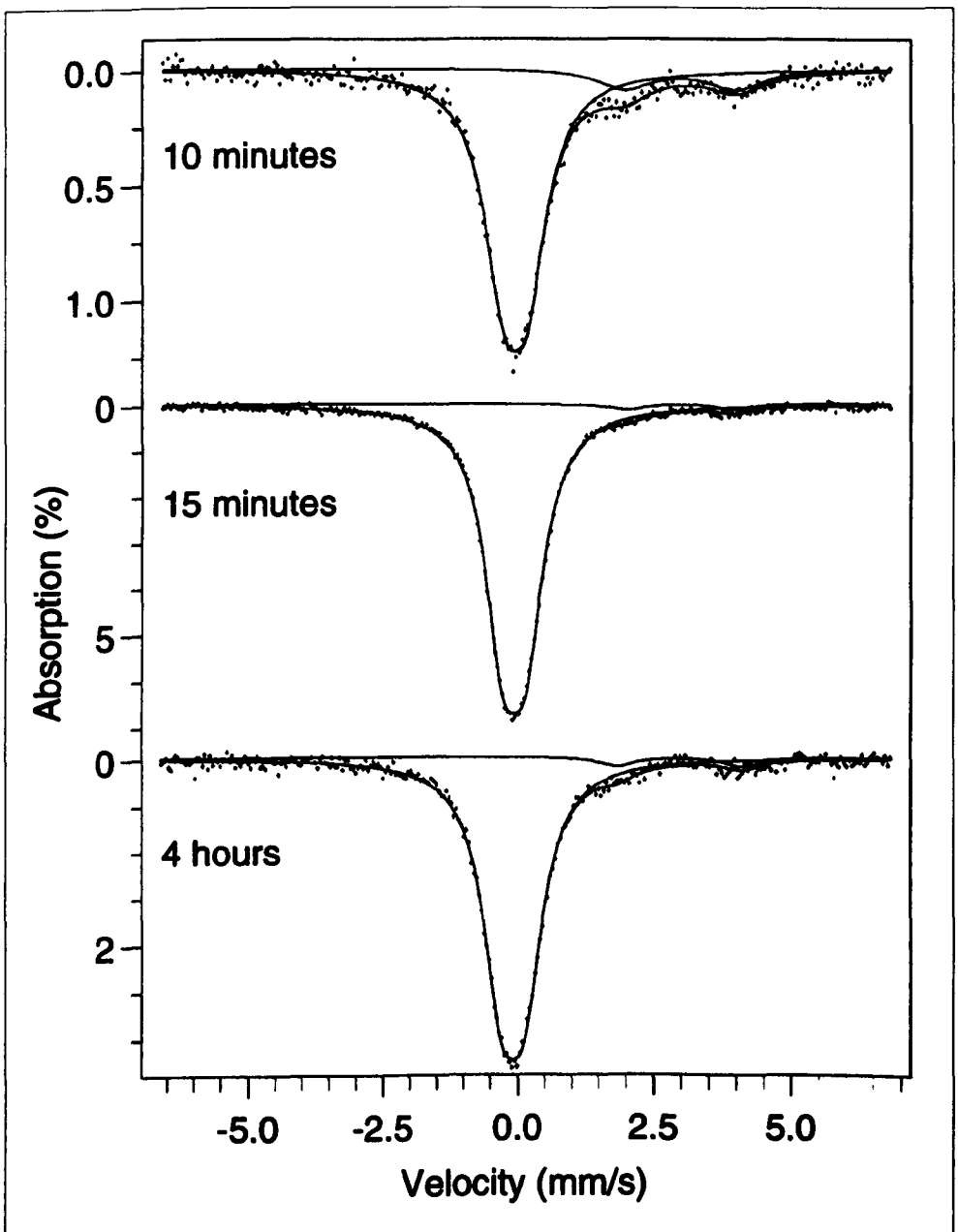

Figure 7.16 Mössbauer spectra at ~77 K of float glass heated at 1050°C for up to 4 hours.

7.4.3 Model of the Tin Oxidation and Estimation of Oxygen Diffusivity

To see how the oxidation of Sn^{2+} progressed with time and temperature, the percentage of Sn^{4+} in each of the samples was plotted against heating time. The

considerable increase in oxidation which occurred initially was not maintained as the amount of Sn^{2+} remaining became less. The points are shown in figure 7.17, together with the curves generated from a model of oxygen diffusivity and subsequent oxidation of Sn^{2+}.

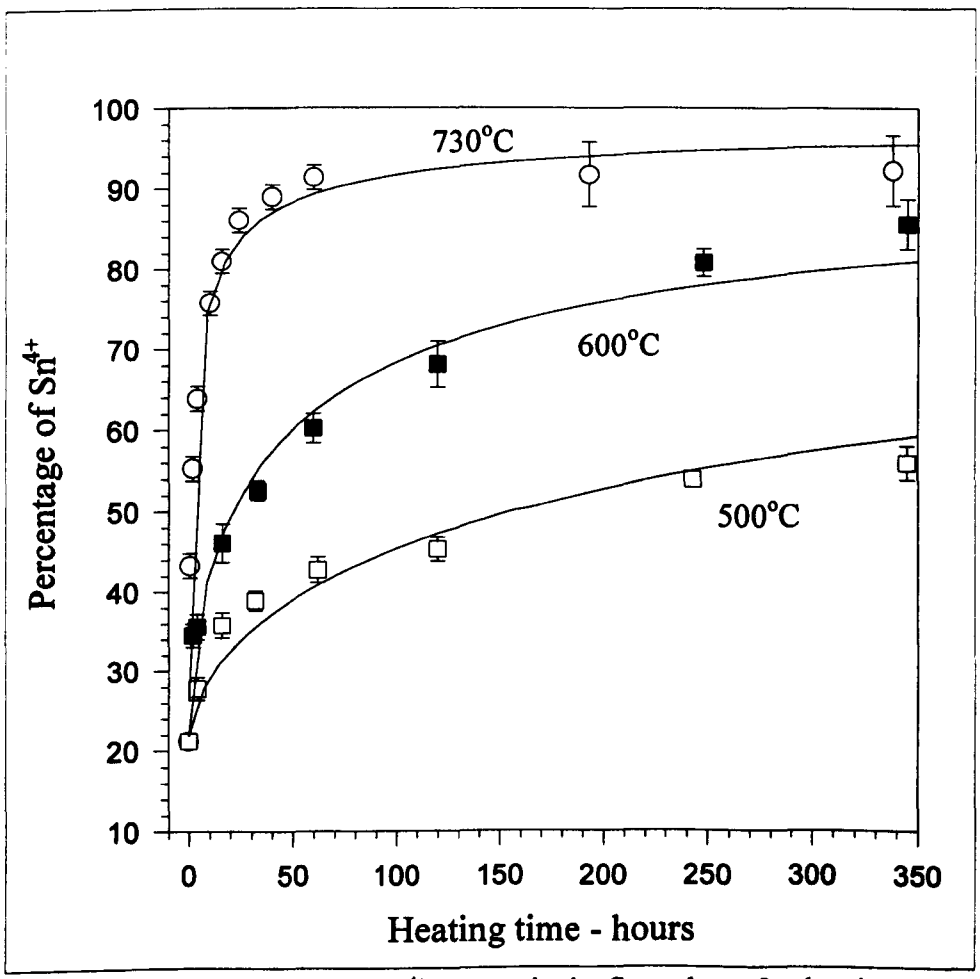

Figure 7.17 Percentage of Sn^{4+} present in the float glass after heating at the temperatures indicated and the curves fitted to the data.

The distribution of tin in the glass has been found from the EMPA tin profile, (figure 7.21). The concentration is greatest at the surface and it decreases with depth into the glass. In the simplest case the tin distribution would remain unchanged after the heat treatment (although the results of tin profile measurements show that it does not). If the

surface tin concentration is C_S then at some distance x into the glass, the tin concentration, C, may be written as $C = C_S\left(1 - \text{erf}\left(\frac{x}{x_0}\right)\right)$ where $\text{erf}(x/x_0)$ is the error function and x_0 would be the depth into the glass at which the tin concentration would have dropped to 0.84 of its surface value. This distance x_0 was estimated from the tin profile of the unheated glass and was taken to be 3.5×10^{-6} m. The error function, which may often be used in modelling diffusion, appears in the following equation which gives the amount of Sn^{4+} produced after a time t. This expression was suggested by Mr. D. Gelder from Pilkington Technology Centre and gives the proportion of tin present as Sn^{4+};

$$Sn^{4+}(t) = 0.20 + 0.80\frac{\int_0^\infty C_S\left(1 - \text{erf}\left(\frac{x}{x_0}\right)\right)\left(1 - \text{erf}\left(\frac{x}{2\sqrt{Dt}}\right)\right)dx}{\int_0^\infty C_S\left(1 - \text{erf}\left(\frac{x}{x_0}\right)\right)dx} \qquad (7.1)$$

This assumes that oxygen diffused into the glass as it was heated for a time, t. The equation may be re-written expressing the time in hours, and x/x_0 as a new variable y, so that the equation becomes;

$$Sn^{4+}(t) = 0.20 + 0.80\frac{\int_0^\infty C_S\left(1 - \text{erf}(y)\right)\left(1 - \text{erf}\left(\frac{x_0 y}{120\sqrt{Dt}}\right)\right)dy}{\int_0^\infty C_S\left(1 - \text{erf}(y)\right)dy} \qquad (7.2)$$

20 % of the tin was already present in the glass as Sn^{4+} before it was heated and this is accounted for by the 0.20 at the front of the equation.

The best fit to the data was achieved by varying the value of the diffusivity, D, until the lowest χ^2 was produced. This provided an estimate of the oxygen diffusivity under

the assumptions stated above. The results are shown in table 7.6 and are similar to results obtained for diffusivity measurements at Pilkington Technology Centre. The above assumption for this model that the tin distribution remains constant is not strictly valid, as the XPS profile results show. The tin profiles for some of the heat treated glass are shown in figure 7.18.

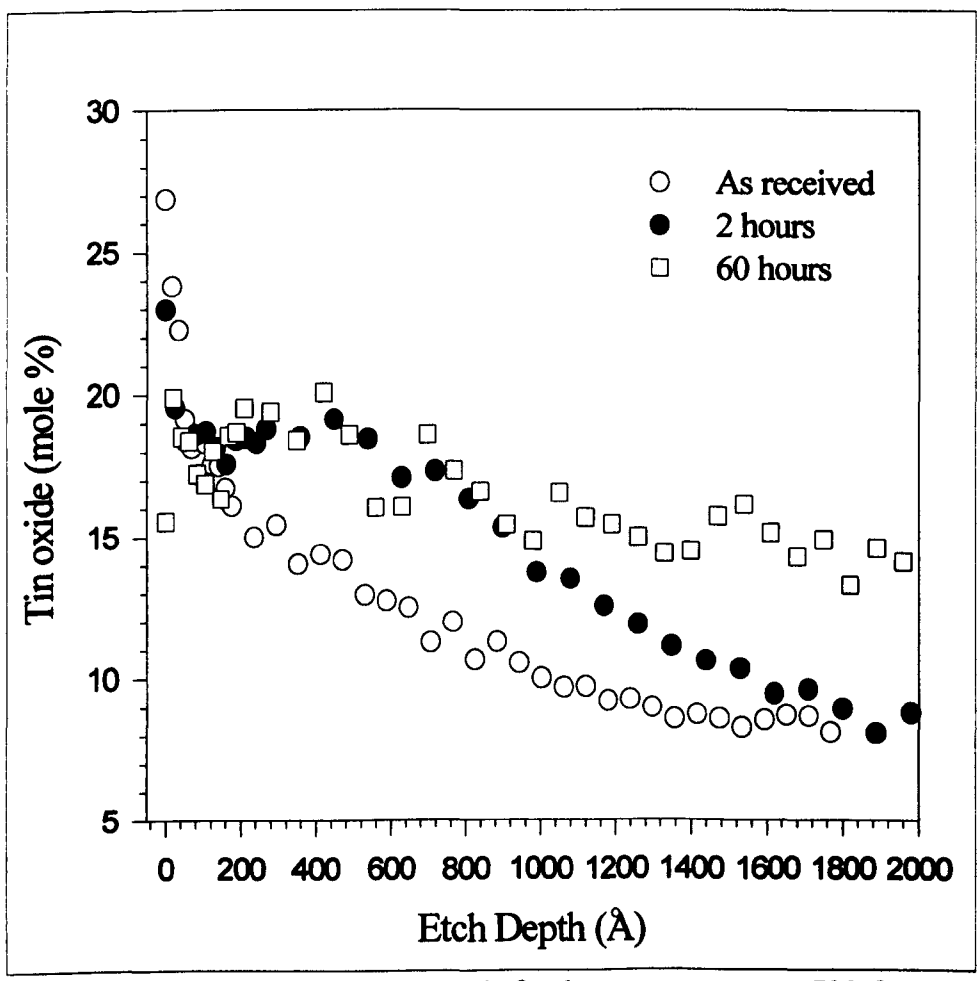

Figure 7.18 Tin profiles before and after heat treatments at ~730°C.

Table 7.6

Temperature - °C	Oxygen Diffusivity (D) - m^2s^{-1}
500	1.285×10^{-18}
600	9.598×10^{-18}
730	1.92×10^{-16}

Assuming that the oxygen diffusion depends upon the collision frequency and the proportion of molecules with energy greater than the activation energy or barrier height, Δ, then the oxygen diffusivity, D, may be expressed as

$$D = D_0 \, e^{-\frac{\Delta}{kT}} \tag{7.3}$$

where k is Boltzmann's constant. From the results shown in table 7.6, estimates of D_0 and Δ may be obtained from the intercept and slope of a plot of ln(D) versus 1/T respectively, (figure 7.19). These are found to be $D_0 = 3.3 \times 10^{-9}$ m^2s^{-1} and Δ = 1.45 eV. These results are similar to those obtained for the diffusion of oxygen into fused silica and also into soda-lime silicate glass.[61] In these studies, D_0 was found to be 1.3×10^{-8} m^2s^{-1} and 1.41×10^{-11} m^2s^{-1} for the silica and the silicate glass respectively, and the barrier height was found to be 1.085 eV for oxygen diffusion into silica at 1000°C, and 2.3 eV for diffusion into the glass at 400°C.

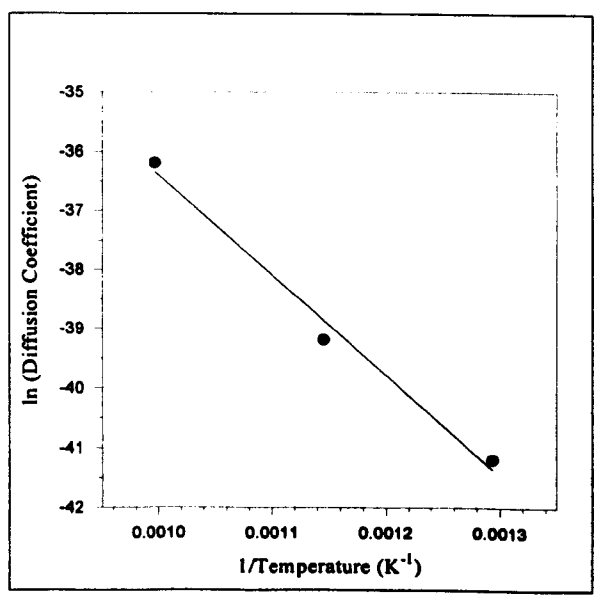

Figure 7.19 Variation of ln(D) with 1/T.

Examination of the float glass surfaces after they had been heated showed that the wrinkling only occurred after heating at about 730°C and not at 500°C or 600°C. A further sample, heated at about 720°C for 2 hours in nitrogen did not show the surface wrinkling, although its Mössbauer spectrum did show that some oxidation of Sn^{2+} to Sn^{4+} had occurred. There was an increase of 21% compared with 34% for the glass heated in air at

the same temperature for the same time.

These results suggest that the appearance of bloom is dependent upon the temperature at which the glass is heated even though oxidation of the tin ions occurs at the lower temperatures. It is possible that the oxidation which takes place when the glass is heated in nitrogen does so from within the glass. If this is so, then it may explain the absence of bloom in this case, i.e. if the oxidation occurs at a greater depth and not in the usual region nearer the surface where the wrinkling is seen.

A difference in viscosity during heat treatment between the glass regions containing tin and those which do not has been suggested as the cause of bloom because of stresses created in the glass surface. [58] This implies that the oxidation process is not predominant in the formation of bloom. However, that should mean that even glass heated above 700°C without the presence of oxygen should show wrinkling. As it does not, it suggests that oxidation is significant, perhaps because Sn^{2+} and Sn^{4+} ions have a different effect on viscosity.

7.5 Preliminary Tin Oxidation State Depth Profile of Float Glass

To try to establish how the tin oxidation state varied with depth into the glass surface, Mössbauer spectra of polished samples were recorded. The polishing technique aimed to remove just a few microns from the bottom surface. Discs of the glass ribbon were prepared and small indentations to different depths were made in the underside of each disc as a means of establishing how much glass would be removed. Different weights were PJL ENTER LANGUAGE = PCL

used as an abrasive to polish away the glass as the board revolved. After variable times, the discs were removed and viewed under a microscope to discover which indentations were still visible. A check on the amount of glass which had been removed could be made by studying the measured XRF tin counts.

The remaining glass in each case was prepared as normal for Mössbauer analysis by removing the bulk glass backing. The average depths removed were calculated to be 1.5 μm, 3.5 μm and 7.5μm. The tin was found to extend to a total depth of 17 μm.

7.5.1 Results and Calculations from Mössbauer Spectra

The Mössbauer spectra of samples of different surface thicknesses produced by polishing float glass samples are shown in figure 7.20, i.e. these show the tin oxidation state ratios in the full 0-17 μm, between 1.5 and 17 μm, between 3.5 and 17 μm and from 7.5 to 17 μm. The tin counts were also measured in these samples. The regions of interest were those from the surface to 1.5 μm, from 1.5 to 3.5 μm, from 3.5 to 7.5μm and from 7.5 to 17μm, i.e. regions which could not be measured directly. However, it was possible to obtain information about these areas by calculating the differences between measured regions. The results obtained from the spectra are shown below in table 7.7.

Table 7.7

Region	Tin Count	Percentage Sn^{4+} (±≤ 1%)	Percentage Sn^{2+} (±≤ 1%)
0 - 17 μm	4638	20.6	79.4
17 less 1.5 μm	3528	24.3	75.7
17 less 3.5 μm	2266	34.6	65.4
17 less 7.5 μm	1412	36.4	63.6

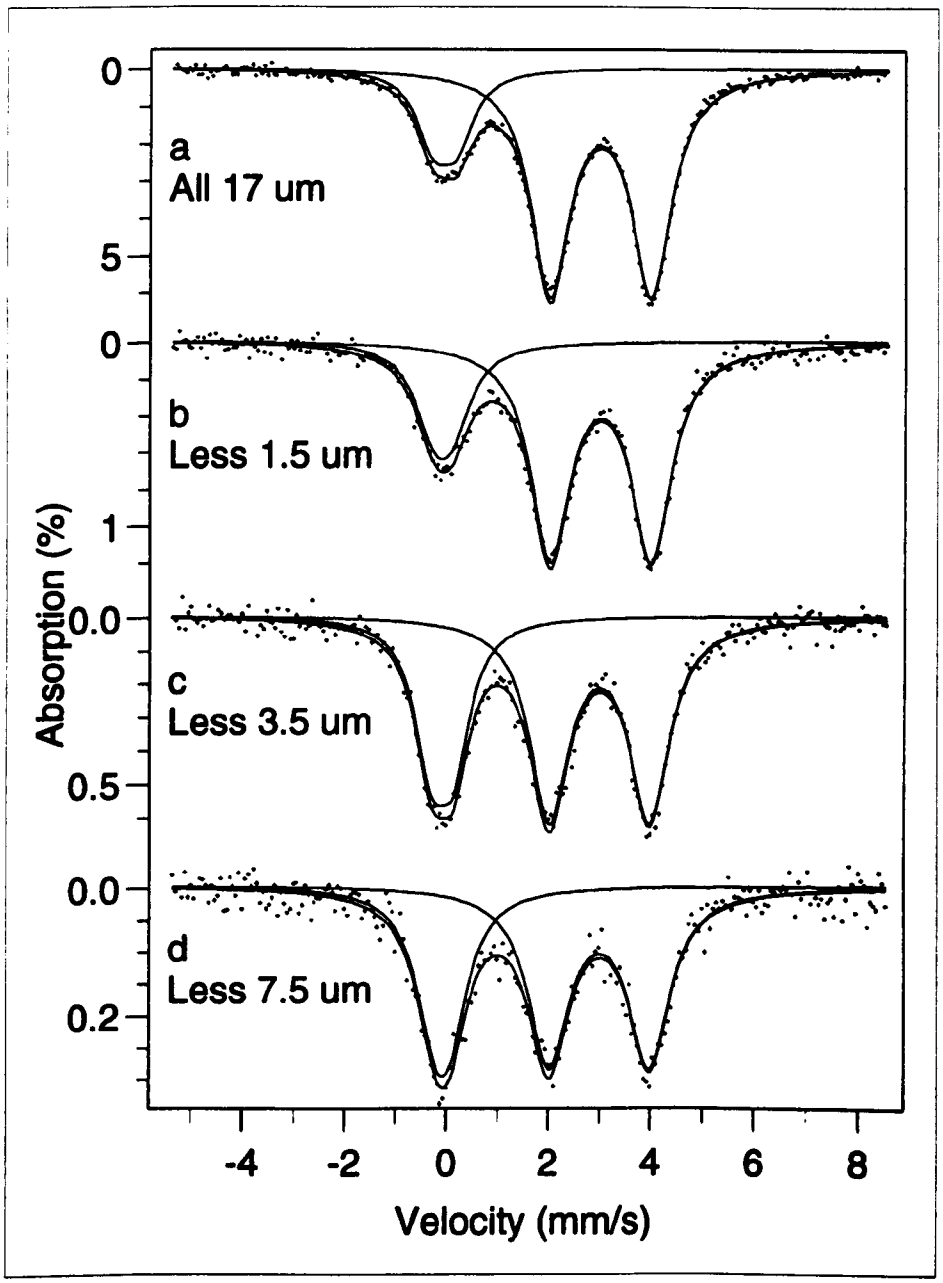

Figure 7.20 Mössbauer spectra at ~77 K of the surface of one float glass before and after removal of several microns by polishing.

As an example of the calculation performed; after removal of 1.5μm the fraction of tin remaining is (3528) / (4638) of some amount x, therefore $(0.7607 \times 0.757)x = 0.576x$ exists as Sn^{2+} in the remaining section, and $(0.7607 \times 0.243)x = 0.185x$ exists as Sn^{4+} in the remaining glass. Hence in the outer 1.5μm, the fraction of tin existing as Sn^{2+} is $(0.794 - 0.576)x = 0.218x$, and as Sn^{4+} is $(0.206 - 0.185)x = 0.021x$. The percentage of stannic ions

is therefore (0.021) / (0.021 + 0.218), i.e. 8.8%, and 91.2% of the tin is present as stannous ions. Similar calculations for the other regions give the results shown in table 7.8.

Table 7.8

Region	Tin Count	Percentage Sn^{4+} (±≤ 1%)	Percentage Sn^{2+} (±≤ 1%)
0 - 17 μm	4638	20.6	79.4
0 - 1.5 μm	1110	8.8	91.2
1.5 - 3.5 μm	1262	5.8	94.2
3.5 - 7.5 μm	854	31.0	69.0
7.5 - 17 μm	1412	36.3	63.7

These results show that the majority of the tin nearest the surface exists as Sn^{2+}, over half the Sn^{2+} occurs in the first 3.5μm and that more than 80% of the stannic tin is deeper than 3.5μm from the surface. These are perhaps consistent with the idea that it is the Sn^{2+} ions that are taken up into the glass from the tin bath, and the oxidation to Sn^{4+} occurs at greater depths within the glass. The proportions of the two tin oxidation states at the different depths are illustrated schematically in figure 7.21.

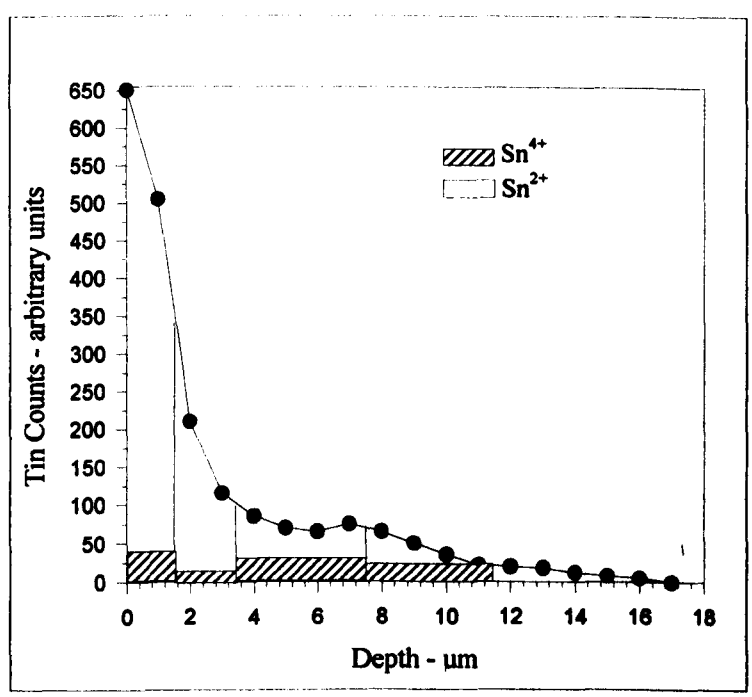

Figure 7.21 Schematic illustration of the proportion of Sn^{4+} and Sn^{2+} at different depths into the float glass surface.

7.6 The Determination of the Tin Recoilless Fraction in Float Glass

To compare the strength of binding of the diffused tin in float glass with that present in the glass samples discussed earlier, it was necessary to record the Mössbauer spectra over a temperature range. As the initial measurements at room temperature had produced spectra with a very poor signal to noise ratio, the float glass sample chosen was one with a relatively high tin count (~ 4700). In this case reasonable results were obtained between 10 K and 300 K, and the spectra are shown in figure 7.22. The same method of calculating the dependence of ln(f) on temperature discussed previously was used and the data and curve fitted according to the Debye model are plotted in figure 7.23.

The values of the Debye temperatures, θ_D, were found to be 185 K for Sn^{2+} and 260 K for Sn^{4+}, i.e. the result for the stannic component was less than that obtained for the tin in the re-melted doped-float glass.

To see if this result would be affected by the heat treatments discussed in 7.4.2, variable temperature measurements were also made on these samples, which came from the same piece of glass ribbon, i.e. had the same high tin count. The glasses which were heated for 2 hours above 700°C, for 120 hours at 500°C and for 15 minutes at 1050°C were analysed.

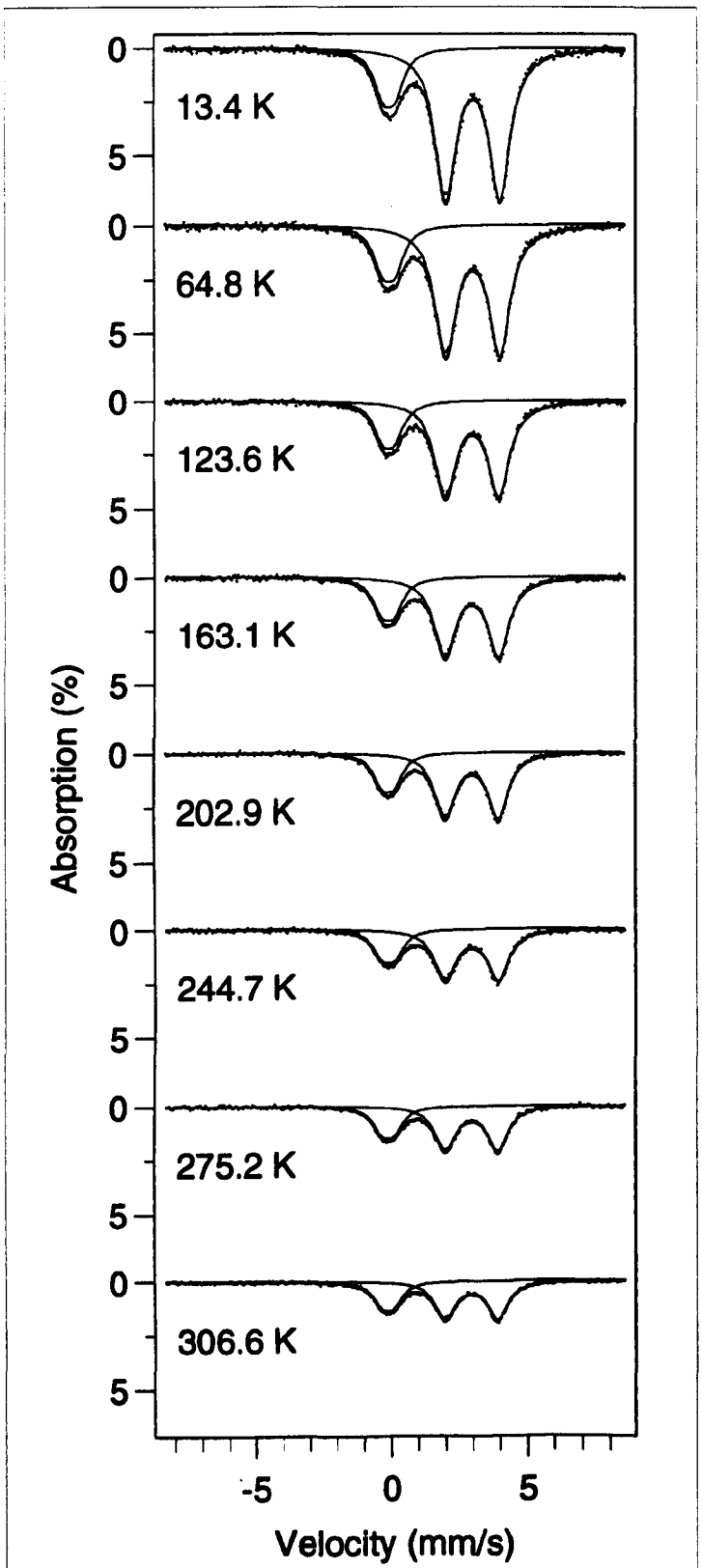

Figure 7.22 Variable temperature Mössbauer spectra of tin in float glass.

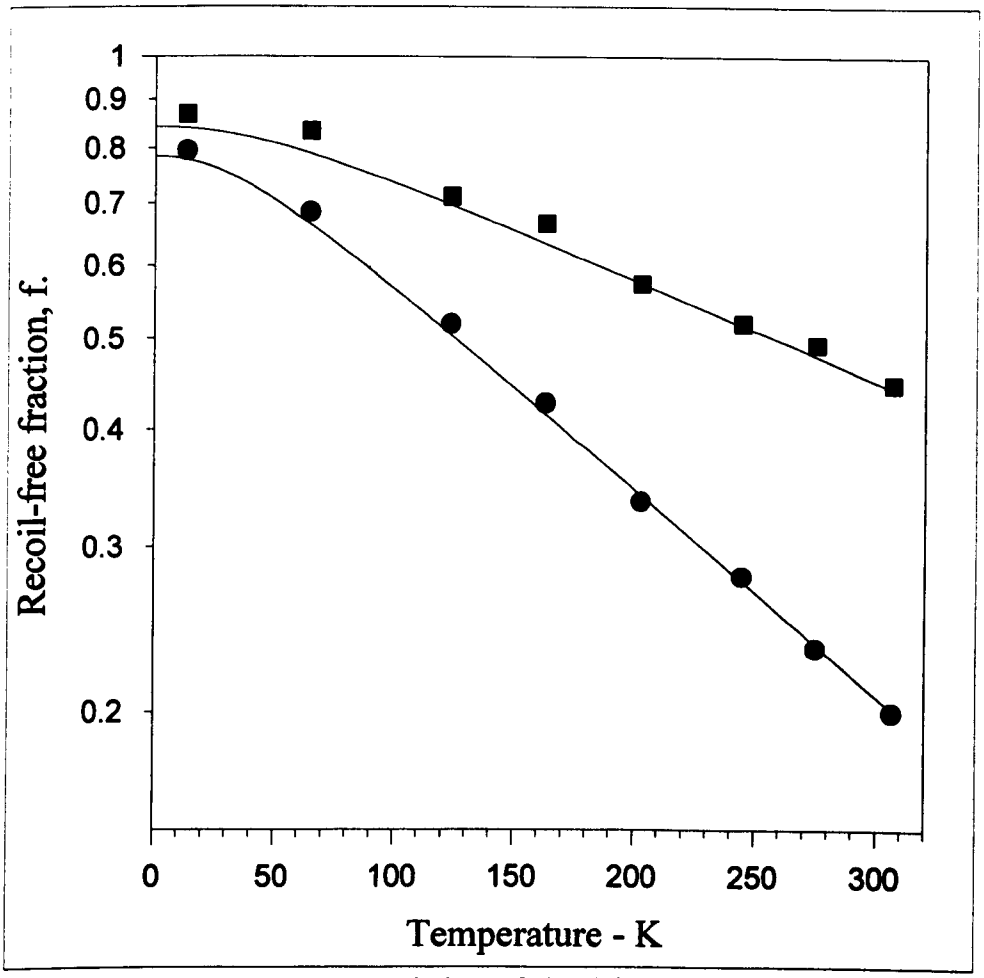

Figure 7.23 Temperature variation of the f-factor for tin in float glass, (■) Sn^{4+}, (●) Sn^{2+}.

The variable temperature Mössbauer spectra of the heat treated float glasses are shown in figures 7.24, 7.25 and 7.26 respectively. The graphs obtained of the temperature variation of f are plotted in figures 7.27 - 7.29 and the Debye temperatures calculated from these results are listed in table 7.9.

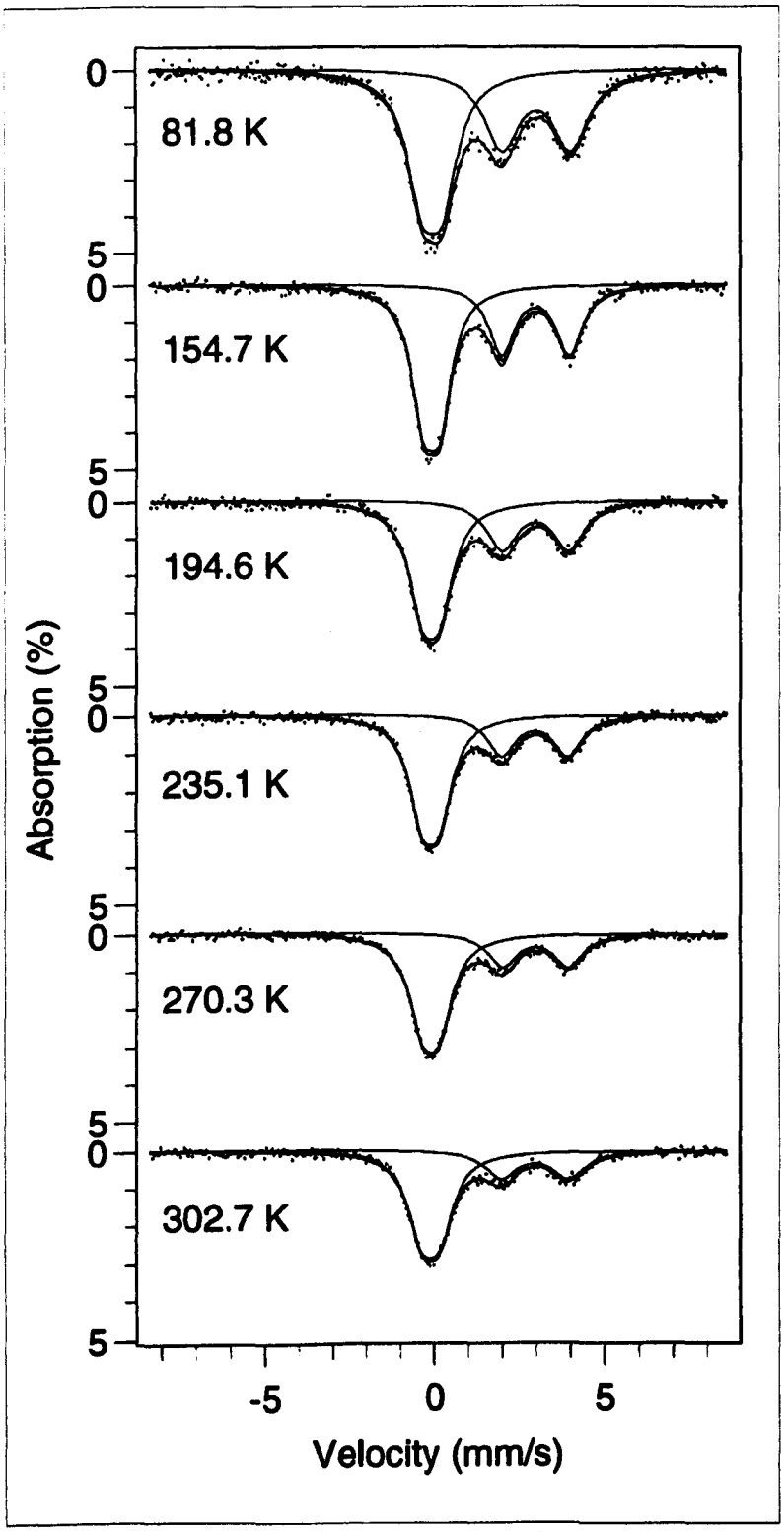

Figure 7.24 Variable temperature Mössbauer spectra of tin in float glass heated for 2 hours at ~730°C.

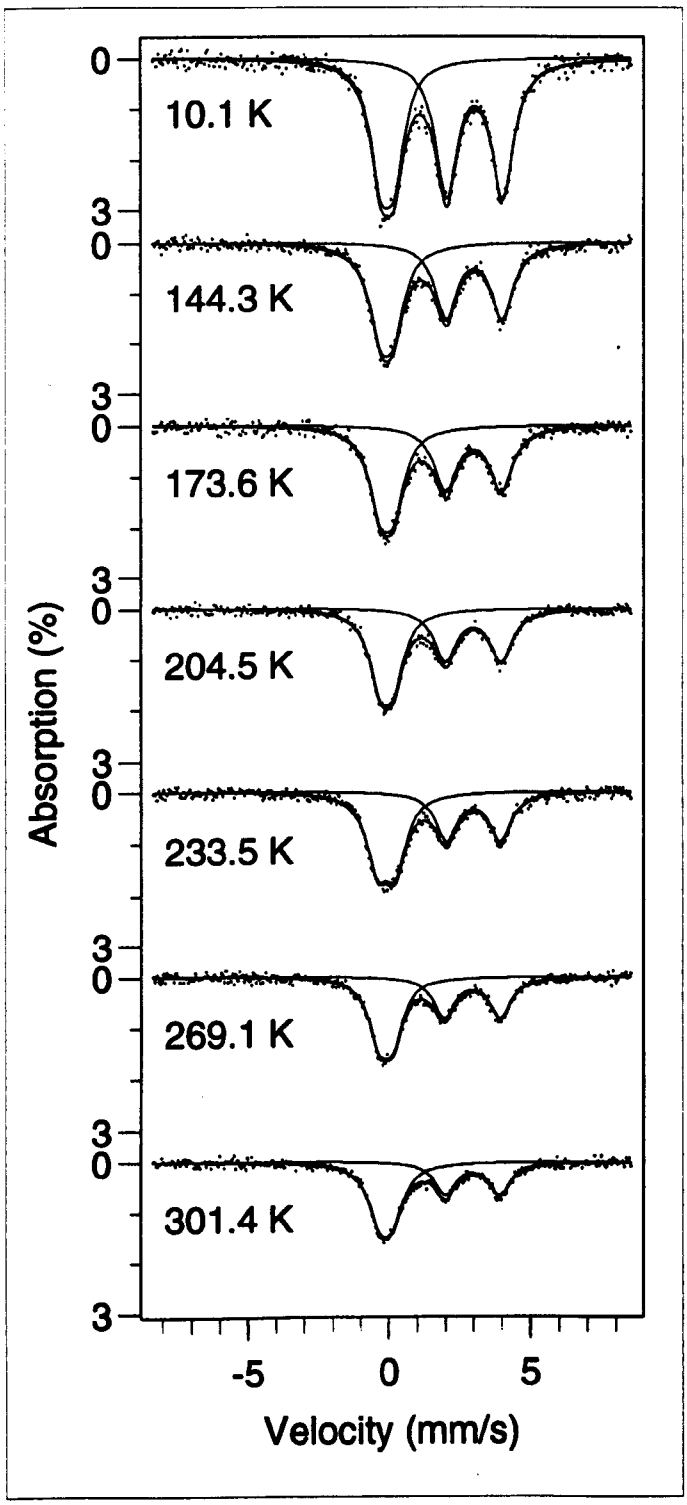

Figure 7.25 Variable temperature Mössbauer spectra of tin in float glass heated for 120 hours at 500°C.

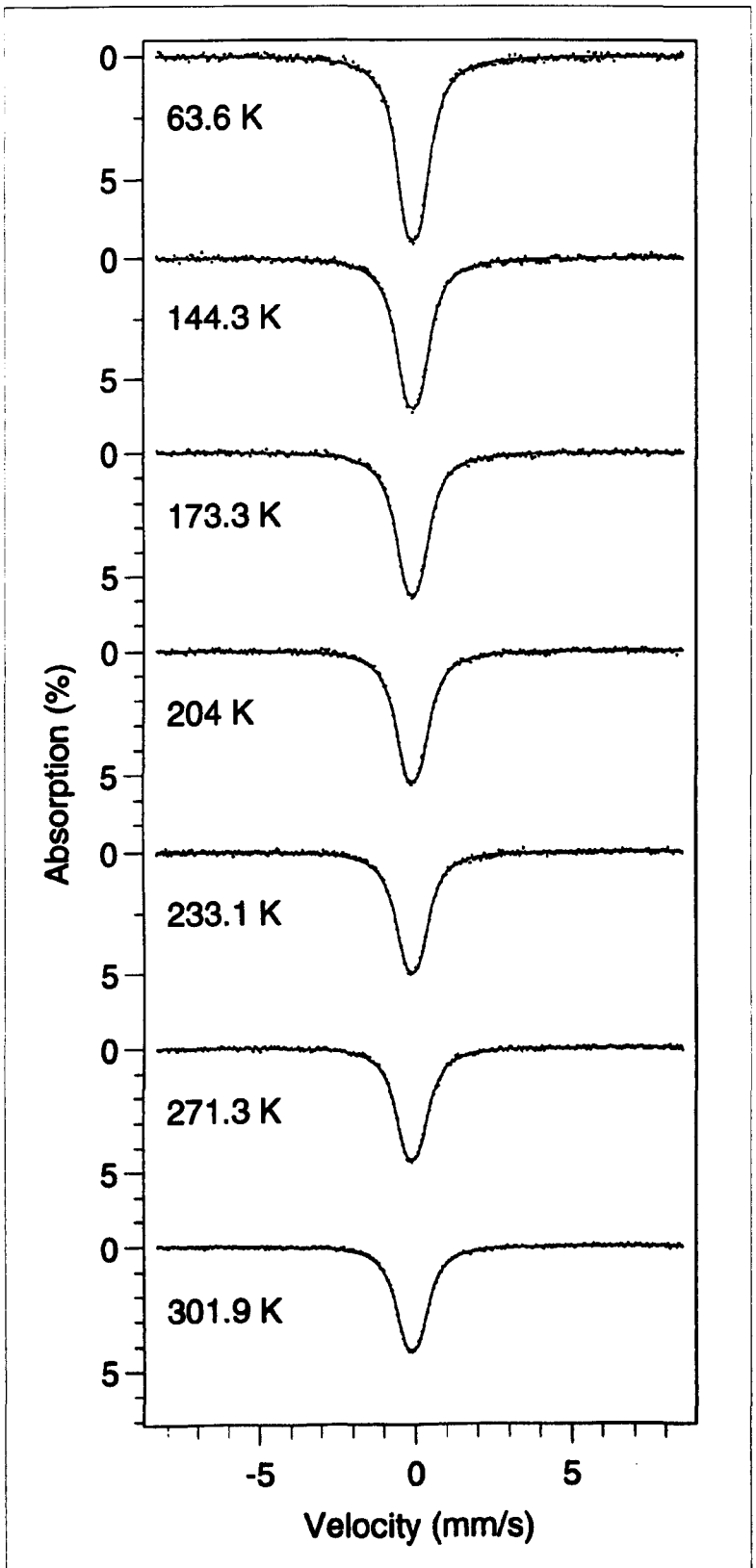

Figure 7.26 Variable temperature Mössbauer spectra of float glass after heating for 15 minutes at 1050°C.

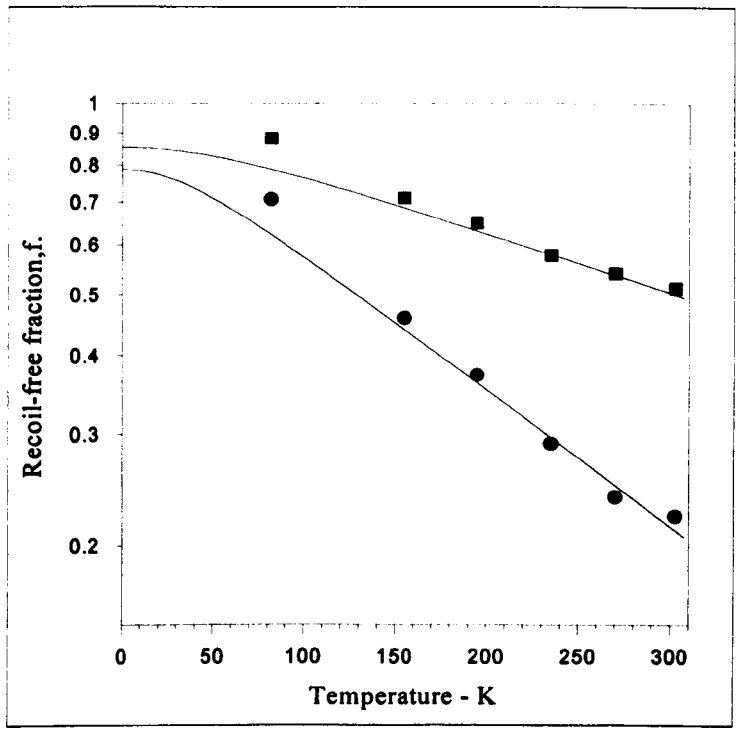

Figure 7.27 Temperature variation of the f-factor of tin in float glass heated for 2 hours at ~730°C. (■) Sn^{4+}, (●) Sn^{2+}.

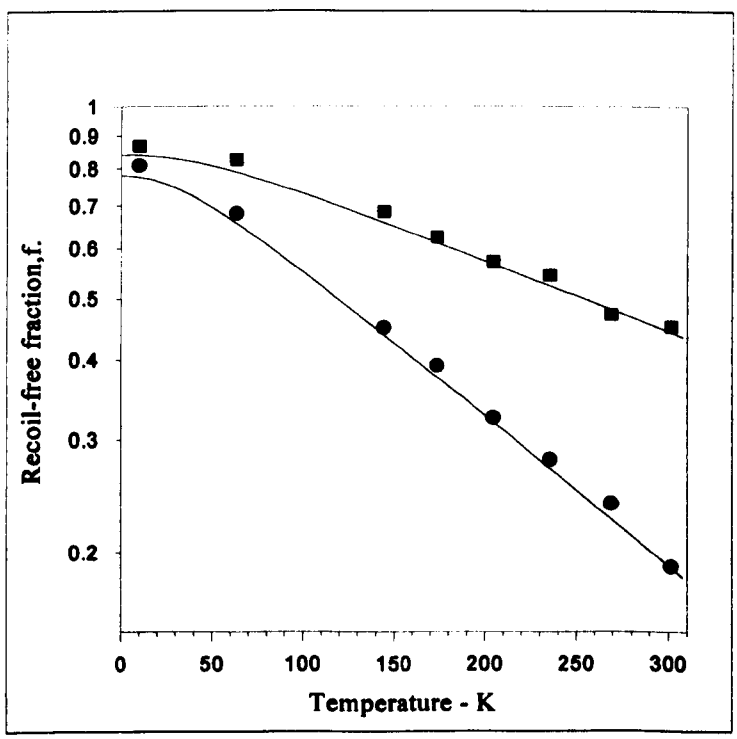

Figure 7.28 Temperature variation of the f-factor of tin in float glass heated for 120 hours at 500°C. (■) Sn^{4+}, (●) Sn^{2+}.

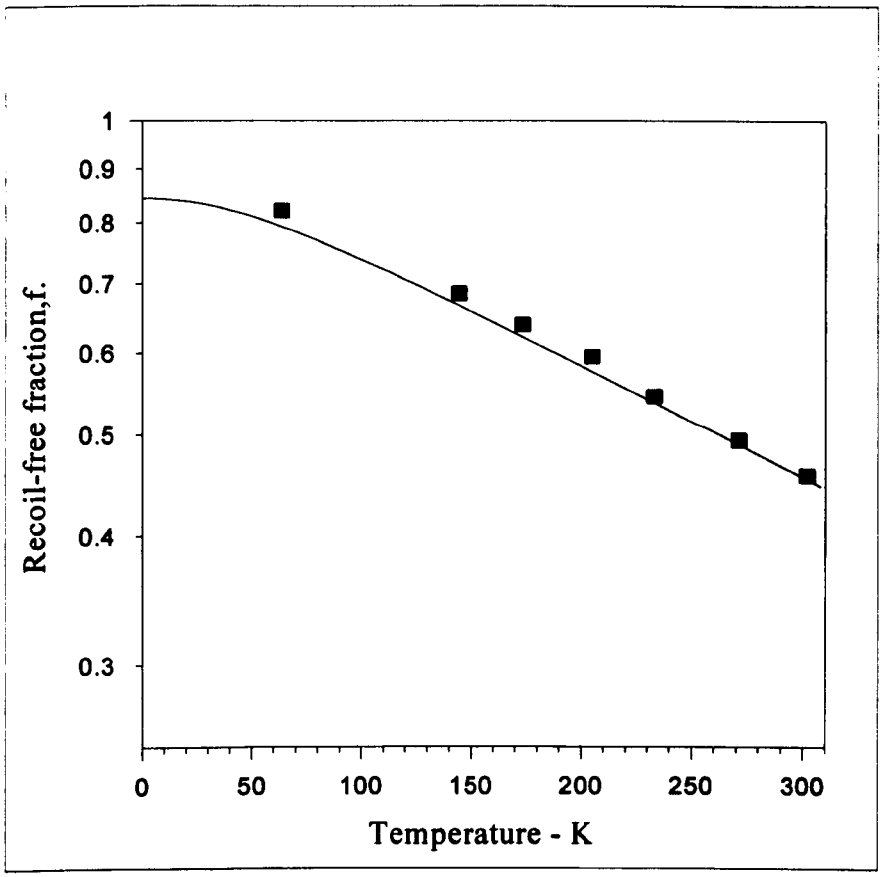

Figure 7.29 Temperature variation of the f-factor of tin in float glass heated for 15 minutes at 1050°C.

Table 7.9

Float Glass Sample	Percentage Sn^{4+}	θ_D (Sn^{4+}) - K	θ_D (Sn^{2+}) - K
Unheated	20.6 (±≤ 1%)	260 (±0.2)	185 (±0.1)
120 hours at 500°C	45.2 (±≤ 1%)	258 (±0.4)	180 (±0.2)
2 hours at 730°C	55.3 (±≤ 1%)	282 (±0.6)	187 (±0.4)
10 minutes at 1050°C	100 (±≤ 1%)	263 (±0.5)	-

These results suggest that there has been little change in the strength of binding of the Sn^{2+} ions. There is not much change in the Debye temperature of Sn^{4+} for the glass heated at only 500°C which is reasonable considering that this is below the glass transition temperature (about 580°C for float glass). The increase in the Debye temperature of Sn^{4+}

after heating above 700°C does suggest that there was some increase in the strength of binding of the Sn^{4+} ions. The 1050°C result is more unexpected however, as even after the glass was heated above the liquidus temperature, there was little change in the Debye temperature, although all the Sn^{2+} was converted to Sn^{4+}. Although 1050°C is a reasonably high temperature, it is similar to the temperature in the float bath during manufacture and is not as high as that used in the preparation of the tin-doped float glass samples. The other difference with this sample is that it was quenched in water immediately after being removed from the muffle. This was unlike the other heated float glass samples which were quenched in air and was very different to the doped float-composition glass which was cooled slowly.

7.7 Coated Glasses

Pilkington 'K' glass is one product which results from float glass which has been coated with tin oxide. Mössbauer spectra of a few coated samples were recorded to see if any of the coatings contained stannous oxide as this was what the members of the coatings group at Pilkington Technology Centre were looking for. Samples of various thicknesses (up to 15 000Å) and with different amounts of fluorine doping were compared. All results showed the presence of only Sn^{4+} ions, and from the chemical shifts of about 0.012 mms^{-1}, the tin environment seemed to be more like that of the tin in the oxide SnO_2 (δ ~ 0.017 mms^{-1}), than of Sn^{4+} ions in float glass (δ ~ -0.17 mms^{-1}). An example of the spectra obtained is shown in figure 7.30, and may be compared with that of crystalline SnO_2 shown in figure 8.1(b). Some asymmetry in the absorption line of the coating can be seen. This

suggests that there is some difference between the Sn^{4+} in the coating to that in the crystalline oxide where no asymmetry is observed. More results from a wider range of samples should be obtained before any further conclusions can be drawn.

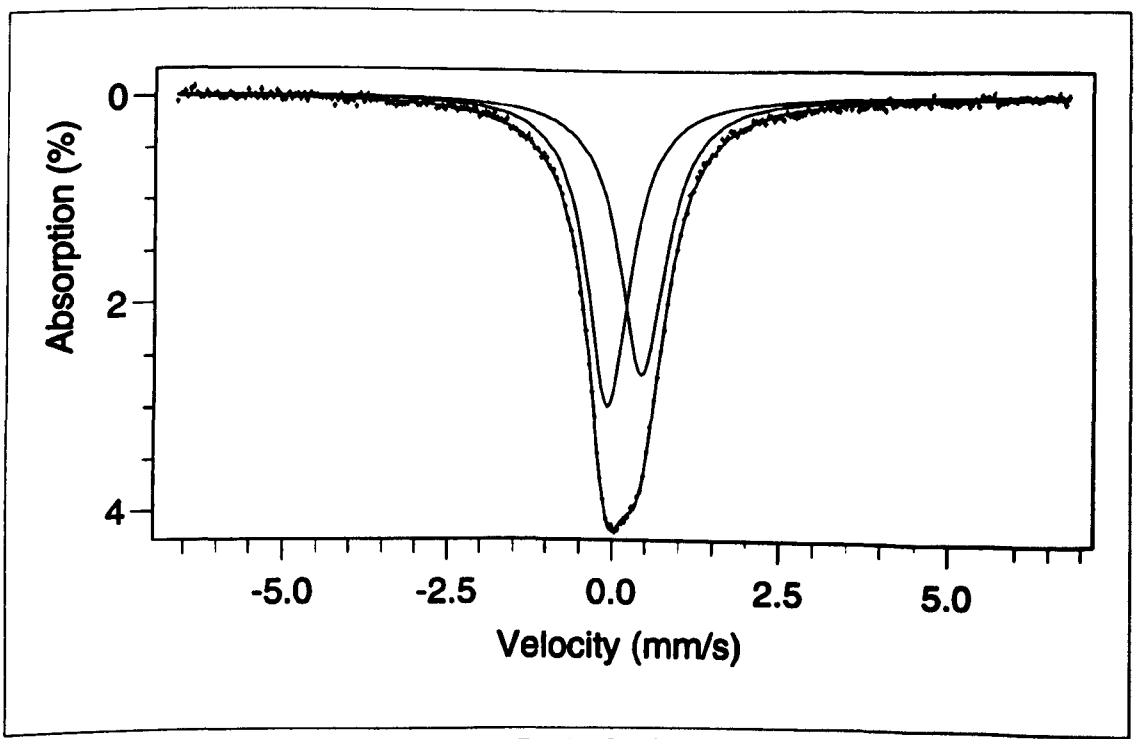

Figure 7.30 Mössbauer spectrum at ~77 K of a tin oxide coating on float glass.

7.8 Discussion and Conclusions

The results obtained show that many float glass samples can be studied using transmission Mössbauer spectroscopy if the samples are suitably prepared and the spectra are recorded at low temperatures. They show that both oxidation states of tin are present in float glass.

In combination with other experimental techniques, the Mössbauer spectra of the

polished float glass provided the first results showing how the tin oxidation state varies with depth into the glass surface. In particular, the results showed that most of the tin near the surface is present as Sn^{2+} ions.

The results obtained for the heat treated samples showed not only the way the tin oxidation progressed, but also that some change in binding of the Sn^{4+} could be produced. The effect of bloom appears to depend upon temperature of treatment. Although it is accompanied by the oxidation of Sn^{2+} to Sn^{4+}, oxidation may still occur without surface wrinkling resulting at lower temperatures.

The heat treatment experiments suggest that as the time for which the glass is heated increases, the oxygen diffuses in to greater depths and more Sn^{2+} is oxidised to Sn^{4+}. The Debye temperature of stannic tin in float glass was found to be lower than that of stannic tin which is present in re-melted tin-doped float glass. This indicates that it is less tightly bound. The increase in the Debye temperature of stannic tin after the glass was heated above 700°C, (i.e. above T_g), suggests that at these temperatures some structural reorganisation has taken place. However this did not occur at the higher temperature of 1050°C in 15 minutes.

Further discussion and conclusions about the tin in the float glass surface will be given in chapter 8.

Chapter 8 Discussion of Tin in Glass and in Tin Oxide

8.1 Introduction

The three different types of tin-containing glasses which were studied provided a range of possible environments in which the tin could exist. The measured Mössbauer parameters (chemical shift, quadrupole splitting and linewidth) were found to be considerably different from those obtained for the crystalline tin oxides. The tin oxide Mössbauer spectra are discussed in 8.2 so that a full comparison may be made.

A complete table of measured Debye temperatures and Mössbauer chemical shifts for most of the different tin-containing materials studied will be presented in this chapter. The intention is to provide an overview of the comparable results so that possible conclusions may be drawn.

Measurements of the Debye temperature and the chemical shift are useful for providing information about the nature and strength of binding of the Mössbauer atoms and of their surrounding environment. A high value of θ_D is indicative of strong binding, i.e. covalent bonding, and suggests possible tetrahedral coordination of the ions. The chemical shift will be lowered for Sn^{2+} ions when there is covalent bonding, but raised for Sn^{4+} ions as the covalency of the bonding increases. In glass, covalent bonding generally occurs with a network forming oxide, while ionic bonding (and therefore possibly octahedral coordination) usually occurs with a network modifier.

8.2 Sn^{2+} and Sn^{4+} in Crystalline Tin Oxides

Several samples of stannous oxide, SnO, and stannic oxide, SnO_2, were prepared. Spectra of each oxide were recorded separately and then a sample consisting of a mixture

of both SnO and SnO_2 was prepared for the variable temperature measurements. The conditions were therefore identical for both the Sn^{2+} in SnO and the Sn^{4+} in SnO_2 whilst the spectra which were used to determine the Debye temperature were recorded.

8.2.1 Mössbauer Spectra of the Tin Oxides

Crystalline stannous and stannic oxides were obtained separately from chemical suppliers Aldrich and from Fisons respectively. The purity was quoted to be greater than 99%. Mössbauer spectra of each of the oxides are shown in figure 8.1.

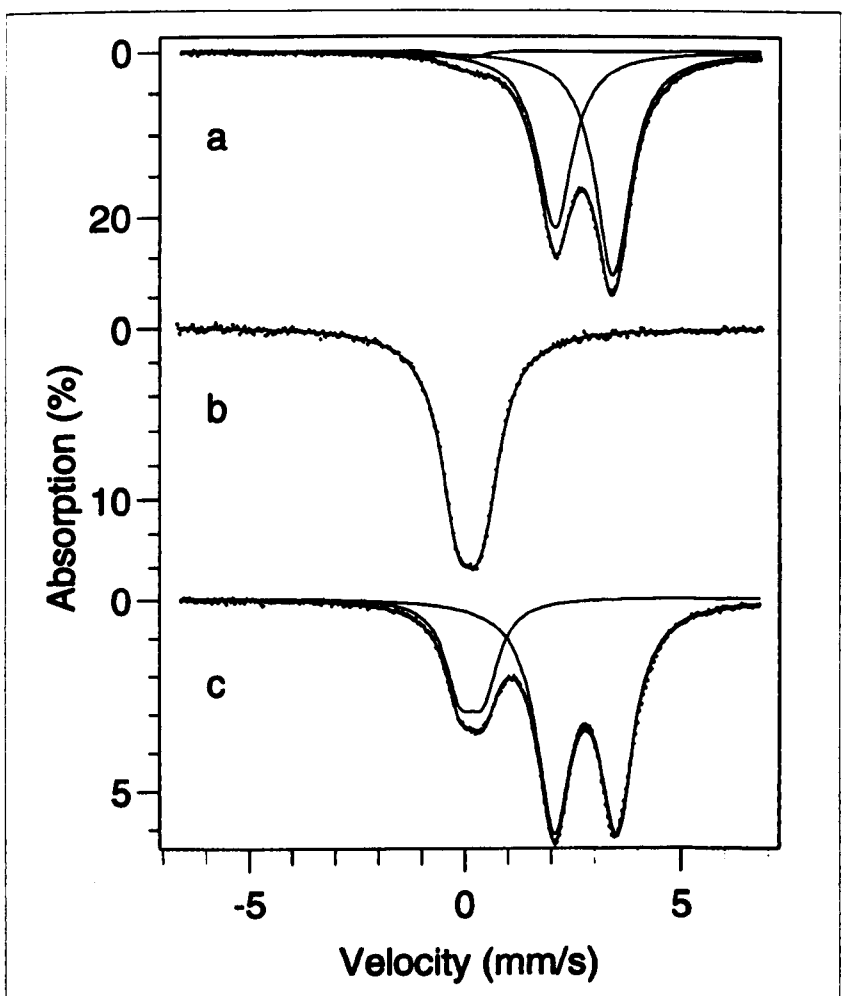

Figure 8.1 Mössbauer spectra at ~77 K of (a) SnO, (b) SnO_2 and (c) SnO after milling for 2 minutes in a mechanical grinder.

The SnO doublet was found to have a large asymmetry in line intensity when the black crystallites were just mixed with boron nitride, so several further samples were prepared by grinding the crystallites. The finest powder was obtained by using the mechanical grinder for two minutes although this spectrum, figure 8.1(c), showed that some oxidation had occurred during the grinding and a small amount of stannic oxide (~ 18% at ~77 K) was present. The fact that it was possible to eliminate the asymmetry in the two lines of the doublet by grinding showed that it was caused by a preferential orientation of the crystallites in the sample holder. The chemical shift of the Sn^{2+} in any of the glass samples was noticeably greater than the shift of stannous oxide (~2.9 mms^{-1} compared to ~2.67 mms^{-1}). That of Sn^{4+} in the glass was less than the shift of stannic oxide, (~ -0.17 mms^{-1} compared to ~ -0.02 mms^{-1}).

8.2.2 Determination of the Debye Temperature

The sample was prepared from similar quantities of each oxide and mixed with boron nitride. Once again the spectra were recorded between 10 K and 300 K and they are shown in figure 8.2. The resulting curves of the temperature dependence of the f-factor of each valence state are shown in figure 8.3.

The Debye temperatures were calculated to be 306 K for Sn^{4+} in SnO_2 and 204 K for Sn^{2+} in SnO. Both results were higher than those obtained for the corresponding tin state in glass, and were consistent with the values found by Collins et al. [32] (313 ± 6 K for SnO_2 and 203 ± 1 K for SnO). The measured shifts are also similar to those quoted by Collins, i.e. 2.67 mms^{-1} (at 77 K) compared with 2.678 mms^{-1} (at room

temperature)[32], and 0.05 mms^{-1} (at 77 K) compared with 0.004 mms^{-1} (at room temperature).

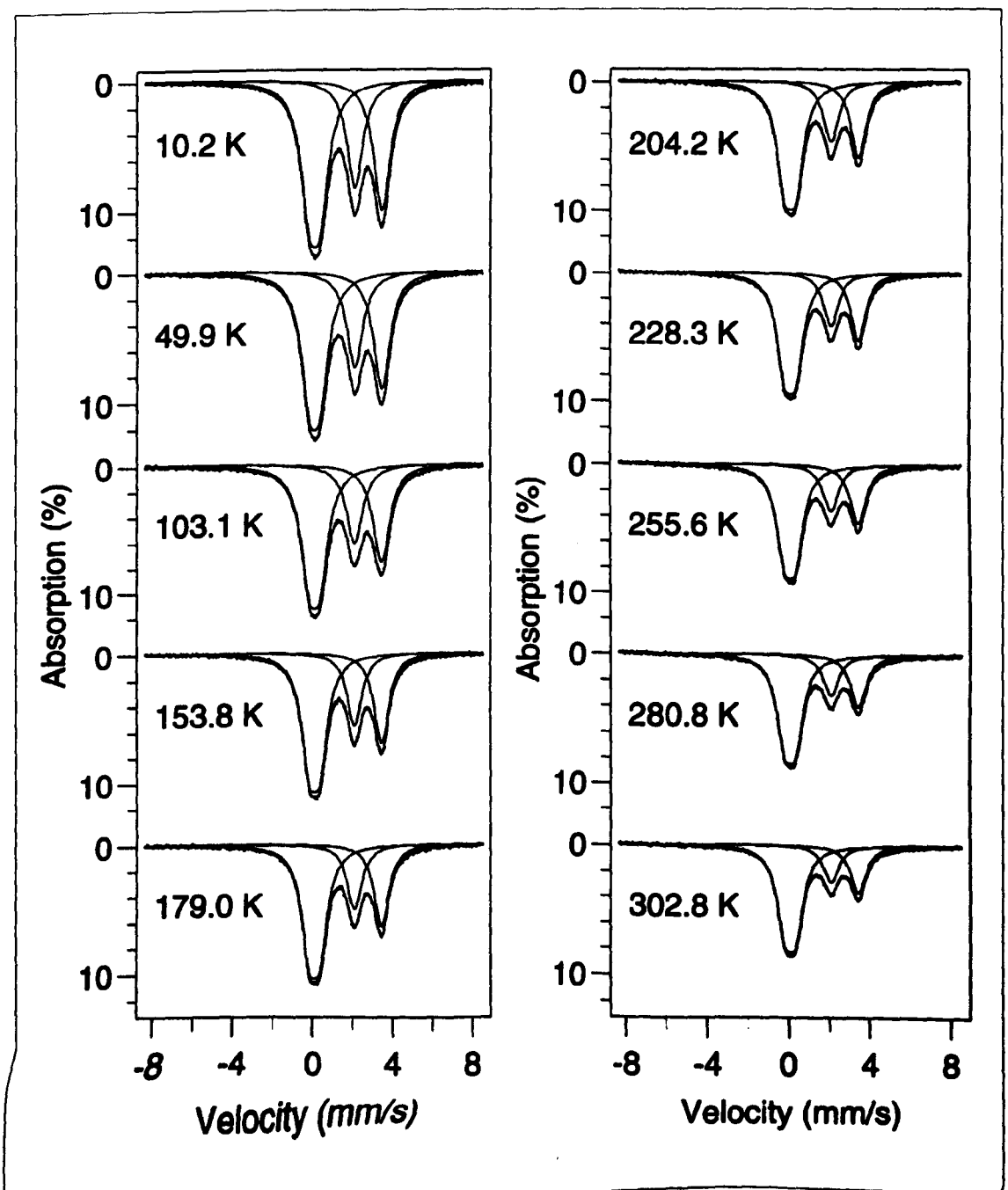

Figure 8.2 Mössbauer spectra of SnO and SnO_2 recorded between *10.2 K and* 302.6 K.

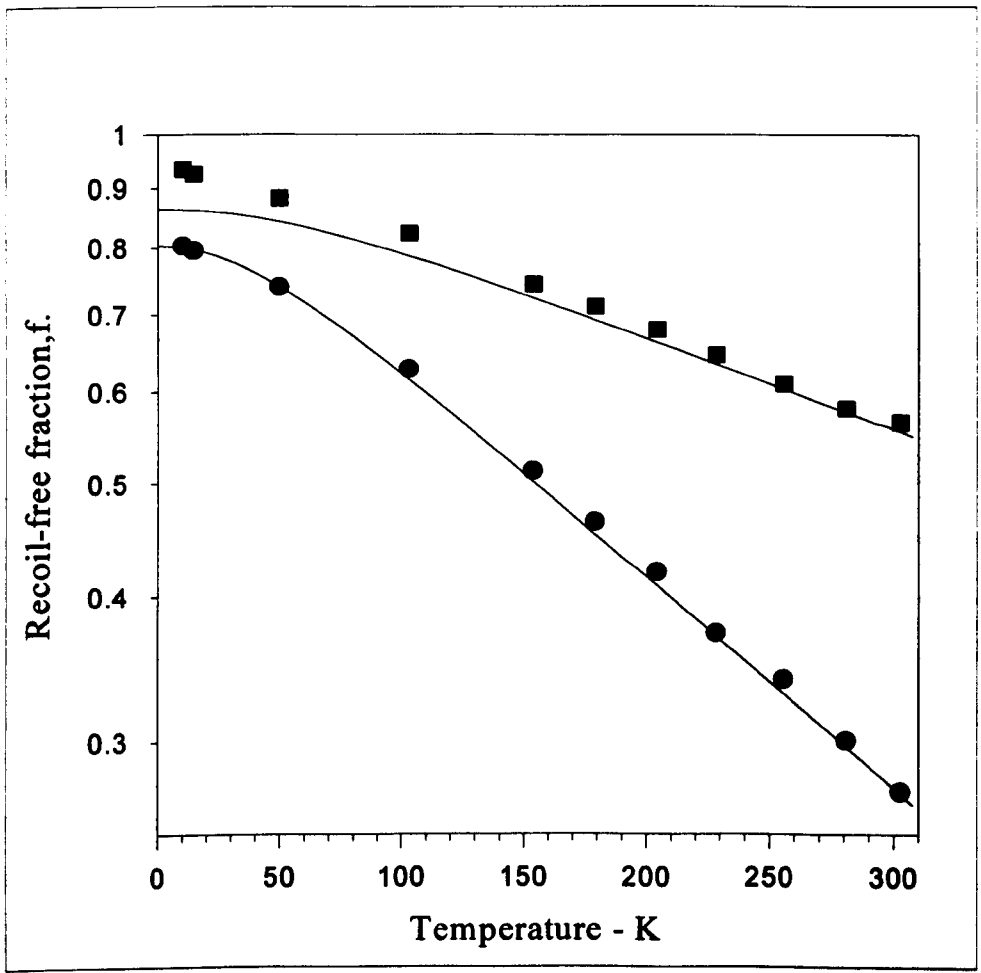

Figure 8.3 Temperature variation of the f-factor of Sn^{4+} (■) in SnO_2 and Sn^{2+} (●) in SnO.

8.3 Comparison of Tin in the Materials Studied

Whilst the results obtained for both tin oxides have been seen to be similar to those measured by Collins [32], the value obtained for the Debye temperature of each glass sample is slightly different to that found for Sn^{4+} in the amorphous oxides [32]. This was (243 ± 3)K compared to a minimum of 258 K in float glass.

The samples studied consisted of the yellow-orange binary tin oxide-silicate glasses containing considerable quantities of tin, the re-melted tin-doped float composition glasses, various commercial float glass samples with low quantities of tin

and the crystalline tin oxides for comparison.

8.3.1 The Debye Temperature and Chemical Shift of Tin

The most significant results are listed in table 8.1 below. The chemical shifts at 77 K are compared as this was the usual temperature at which the Mössbauer spectra were recorded.

Table 8.1

Glass or Oxide	θ_D - K		Chemical Shift δ - mms^{-1}	
	Sn^{4+}	Sn^{2+}	Sn^{4+}	Sn^{2+}
Binary 33 mol.% SnO in SiO_2	-	191	-0.138 (01)	3.060 (04)
Binary 53 mol.% SnO in SiO_2	-	181	-	2.991 (07)
Re-melted tin-doped float glass	319	200	-0.186 (02)	2.862 (03)
Re-melted tin-doped float glass containing aluminium oxide	318	192	-0.107 (03)	2.838 (07)
Float glass	260	185	-0.203 (17)	2.862 (07)
Float glass after heat treatment for 2 hours above 700°C	282	187	-0.174 (05)	2.862 (07)
Float glass after heat treatment for 120 hours at 500°C	258	180	-0.227 (68)	2.829 (10)
Float glass after heat treatment for 15 minutes at 1050°C	263	-	-0.176 (01)	-
Crystalline tin oxide SnO_2/SnO	306	204	-0.027 (03)	2.672 (03)

These results show that there is a wider variation in the Debye temperature, i.e. in the strength of binding, of the Sn^{4+} ions than of the Sn^{2+} ions. Tin in float glass has the lowest Debye temperature, although for the binary glass containing the higher proportion

of SnO these results also imply a low strength of binding of the stannous ions. This is reasonable considering that as the tin concentration increases, the number of non-bridging oxygen ions will increase and the glass network is weakened. The Debye temperature of Sn^{2+} in any of the glasses was lower than that of the crystalline oxides. The shift of Sn^{2+} in glass or the amorphous oxide is greater than that of Sn^{2+} in stannous oxide, SnO. The greater shift indicates less covalency of the tin-oxygen bonding in the glass compared to the oxide. This is consistent with the higher Debye temperature of the SnO and with the Sn^{2+} being 4-coordinate in the crystal.

The strongest binding of the Sn^{4+} ions appears to occur in the re-melted tin-doped float composition glasses as these have the highest Debye temperature by more than 10 K. The measured chemical shift for any glass is lower than that of Sn^{4+} in stannic oxide, SnO_2.

8.4 Conclusions

The results obtained suggest the following conclusions for Sn^{2+} and Sn^{4+} ions in glass.

(i) Tin 2+

Sn^{2+} in the binary glasses is acting as a NWM. The result obtained showing that the Debye temperature was lower for the 53 mol.% SnO glass than the 33 mol.% SnO glass, and that the volume corrected chemical shift increases as the concentration increases is consistent with the glass network weakening as tin oxide is added.

In float glass and re-melted tin-doped float-composition glass the similar values

of θ_D and δ which were obtained suggest little difference in the role of Sn^{2+}. However, for the tin-doped glasses, θ_D is slightly higher, therefore there may be closer packing of the whole network in these glasses.

(ii) Tin 4+

The Debye temperature of Sn^{4+} in float glass is consistently lower than that in the re-melted tin-doped float-composition glasses. The chemical shifts are, however, very similar. This shows that although the electronic distributions in the Sn-O bonds are similar in the two glass systems, the bond strength is weaker in the float glass. It is important to consider the differences between these two types of glass, in particular that the tin enters the surface of the float glass during the short time that the glass ribbon travels down the tin bath and at relatively low temperatures between 1100°C and 600°C. The temperature of the bath is only ~600°C at the end before the formed ribbon leaves the bath. In contrast, although the constituent oxides of the re-melted tin-doped float-composition glass are effectively the same as those in float glass, the doped glass was re-melted to temperatures of about 1500°C and the tin was present as the glass network formed.

It may be concluded that Sn^{4+} in the tin-doped float-composition glass may be acting as a NWF, but that Sn^{4+} could not enter an NWF site in the float glass ribbon. As much of the glass network would have already formed before the tin diffuses into it, the Sn^{4+} may more easily occupy interstitial sites where the resulting bond strengths would be lower. This is consistent with the fact that Sn^{4+} favours octahedral coordination.

The above conclusions do not show whether the bath tin enters the ribbon as Sn^{4+}

or if it is mainly formed because of oxidation occurring within the glass. However the oxidation state depth profile measurements showed that a higher proportion of tin exists as Sn^{4+} at depths greater than ~ 3.5 μm from the bottom surface, suggesting that the Sn^{4+} forms later after diffusion of predominantly Sn^{2+} from the bath. In either case the results imply that Sn^{4+} is 6-coordinate, i.e. in a site similar to that occupied by a NWM.

No change in θ_D for the float glass heated to 1050°C (and quenched in water) was measured. This suggests that a higher temperature alone or both a higher temperature and a greater length of time, e.g. several hours, would be necessary for a structural re-organisation to occur that would allow the Sn^{4+} ions to achieve a closer packed site, like that occupied by a NWF. It would therefore be useful to obtain further results for float glass after heat treatments at higher temperatures.

Appendix I

The absorption area, A, of each component is proportional to the concentration, c, of that oxidation state and its recoil-free fraction, f, i.e. $A = \lambda cf$, where λ is a constant. As the straight line region of the curve of f should extrapolate back to zero, f or ln(f) may be obtained by subtracting the intercepts of the ln(A) versus temperature curve. i.e.

$$\ln f = \ln A - \ln(\lambda c)$$

The concentration relative to the other component is obtained from the intercept of the straight line region of the ln(A) curve with the axis at T=0.

$$\textit{Relative concentration} = \frac{\lambda c_1}{\lambda(c_1 + c_2)}$$

where λc_1 and λc_2 are the intercepts of two components.

References

[1] *Chemistry of the Elements*, N.N. Greenwood & A. Earnshaw, Pergammon Press.

[2] *'Glass'*, G.O. Jones, Chapman & Hall Ltd. 2nd ed.

[3] Zachiarason, W.H. *J. Amer. Chem. Soc.* **54**, 3841, (1932)

[4] *'Glass-Ceramics'*, P.W. M^{c}Millan.

[5] Greaves, G.N. (1985), *J. Non-Cryst. Solids*, **71**, 203.

[6] Pilkington, L.A.B. *Proc. Roy. Soc. Lond.* A, **314**, 1-25, (1969)

[7] Loukes, D.G., *Glass Technology* Vol. 32. No. 6, December 1991, p 187.

[8] M.M. Karim, *PhD thesis* 1995, University of Warwick.

[9] Keysselitz, B. & Kohlmeyer, E.J., (1933), *Metall Erz.* **30**, 172.

[10] Carbo-Nover, J. & Williamson, J. (1967), *Phys. Chem. Glasses*. **8(4)**, 164.

[11] Ishikawa, T. & Akagi, S. (1978), *Phys. Chem. Glasses*, **19(5)**, 108.

[12] *Chemistry of Tin*, ed. P.G. Harrison, Blackie, 1989.

[13] R.V. Parish, The Interpretation of ^{119}Sn Mössbauer Spectra, *Progress in Inorganic Chemistry*, **15**, 1972. Ed. S.J. Lippard.

[14] M. Cordey Hayes, *Chemical Applications of Mössbauer Spectroscopy*, ed. V.G. Goldanskii & R.H. Herber, Academic Press, 1968.

[15] Lees, J. & Flinn, P.A., *Phys. Lett*, **19**, 136, (1965).

[16] *Mössbauer Isomer Shifts*, ed. Shenoy & Wagner, North Holland Publishing Co.

[17] *Mössbauer Effect Data Index*, Stevens & Stevens, 1972.

[18] Hohenemser, C. *Phys. Rev.*, **139**, 185, (1965).

[19] Bryukhanov, V.A., Delyagin, N.N., Opalenko, A.A., & Shpinel, V.S., *Sov. Phys. J.E.T.P.*, **16**, 310, (1963).

[20] Goldanskii, V.I., Makarov, E.F., Stukun, R.A., Sumarokova, T.N.,Trukhtanev, V.A., Khrapov, V.V., *Proc. Acad. Sci., U.S.S.R.*, **156**, 474, (1964).

[21] *Mössbauer Spectroscopy*, N.N. Greenwood & T.C. Gibb, Chapman & Hall Ltd. 1971.

[22] *Coloured Glasses*, W.A. Weyl, Dawsons, 1959, p 343.

[23] Paul, A., Donaldson, J.D., Donoghue, M.T., & Thomas, M.J.K., (1977), *Phys. Chem. Glasses*, **18**, (**6**), 125.

[24] Eissa, N.A., Shaisha, E.E., & Hussiun, A.L. (1974), *J. Non. Cryst. Solids*, **16**, 206.

[25] Silver, J., White, E.A.D., & Donaldson, J.D., (1977), *J. Material Science*, **12**, 828.

[26] Xu, X.J. & Day, D.E., (1990), *Phys. Chem. Glasses*, **31**,(**5**), 183.

[27] Nishida, T., (1995), *Hyp. Int.*, **95**, 23.

[28] Mitrofanov, K.P., & Sidorov, T.A., *Sov. Phys. -Solid State*, (1967), **9**(**3**), 693.

[29] Bartenev, G.M., Magomedev, G.M., Tsyganov, A.D., Zelenev, Yu.V.

[30] Kurkjian, C.R., *J. Non-Cryst. Solids*, (1970), **3**, 157.

[31] Coey, J.M.D., J. Phys. (Paris), (1974), **35**, C6-89.

[32] Collins, G.S., Kachnowski, T., Benczer-Koller, N., & Pasternak, M., *Phys. Rev. B*, (1979), **19**, (**3**), 1369.

[33] Principi, G., Maddalena, A., Gupta, A., Giotti-Bianchini, F., Hreglich, S., Verità, M., *Nucl. Instr. & Methods in Phys. Research*, (1993), **B76**, 215.

[34] H.J.Lipkin, *Ann. Phys.* 1960, **9**, 332.

[35] H.Frauenfelder, *"The Mössbauer Effect"*, W.A. Benjamin Inc. N.Y. 1962.

[36] G.Breit & E.Wigner, *Phys. Rev.* 1936, **49**, 519.

[37] S.Margulies & J.R.Ehrman, *Nucl. Instr. Meth.* 1961, **108**, 131.

[38] Long, G.J. Cranshaw, T.E. & Longworth, G. *Möss. Effect Ref. Data J.* 1983, **6**, 42.

[39] J.K.Lees & P.A.Flinn, *J. Chem. Phys.* **48**, 882, 1968.

[40] G.Breit, *Rev. Mod. Phys.* **30**, 507, 1958.

[41] D.A.Shirley, *Rev. Mod. Phys.* 339, 1964.

[42] Pound, R.V. & Rebka, G.A. Jr. 1960, *Phys. Rev. Lett.* **4**, 274.

[43] Josephson, B.D., 1960, *Phys. Rev. Lett.* **4**, 342.

[44] R. Sternheimer, *Phys. Rev.* 102, **80**, 1950.

[45] R. Sternheimer, *Phys. Rev.* 244, **84**, 1957.

[46] Foley, Sternheimer and Tycko, *Phys. Rev.* 734, **93**, 1954.

[47] R.Sternheimer, H.Foley, *Phys. Rev.* 731, **102**, 1956.

[48] Stevens, J.G. & Stevens, V.E., 1971, *"Mössbauer Effect Data Index"* (New York; Plenum).

[49] Goldanskii, V.I, Gorodinskii, G.M, Karyagin, S.V, Karytico, L.A, Kryzhanskii, L.M., Markorov, E.F, Suzdalev, I.P, & Khrapov, V.V, 1962. *Dokl. Acad. Nauk. SSSR* , **147**, 127, [1963, *Sov. Phys. Dokl.* **147**, 766.]

[50] *Radiation Detection and Measurement*, G.F. Knoll, John Wiley & Sons Inc. 1989.

[51] *Mössbauer Effect Research Data Journal*, **3**, no. 4, April 1980.

[52] Collins, R.W. & Nebergall, W.H., *Analytical Chemistry*, **34 (11)**, 1962, 1511.

[53] *Concepts, Instrumentation and Techniques in Atomic Absorption Spectrophotometry,* R.D. Beaty, Perkian Elmer (manufactures).

[54] *The Physical Properties of Glass*, D.G. Holloway, Wykeham Publications Ltd. 1973, (London)

[55] M. Verita, F. Geotti-Bianchini, S. Hreglich, C.G. Pantano, & V. Bojan, *Boletin de la Sociedad Española de Ceramica y Vidru*, **6**, 415.

[56] C.G. Pantano, V. Bojan, M. Verita, F. Geotti-Bianchini, & S. Hreglich, *Fundamentals of Glass Science & Technology*, Vol. XXIII, (1993), 285.

[57] H. Charnock, *Physics Bulletin* (1970), **21**, 153.

[58] LaPuma, P.J., Snyder, R.L., Zdzieszynski, S., Brücker, R., *Glastech. Ber. Glass Sci.Technol.* 68, C1, (1995).

[59] *The Elements*, J. Emsley, Clarendon Press.

[60] *Crystal Structures, Vol. 1*, Wykoff, John Wiley & Sons Inc.

[61] *Glass Science*, R.H. Doremus, John Wiley & Sons Inc. 1973.